AD A021330

APPLIED RESEARCH LABORATORIES

ARL-TR-75-41
2 January 1976

Copy No.

ACOUSTIC BOTTOM INTERACTION EXPERIMENT DESCRIPTION

Loyd D. Hampton

Research Sponsored by
OFFICE OF NAVAL RESEARCH
Contract N00014-75-C-0429

Approved for public release;
distribution unlimited.

ARL-TR-75-41
2 Jan[redacted]76

ACOUSTIC BOTTOM INTERACTION EXPERIMENT DESCRIPTION

Loyd D. Hampton

127p.

Research Sponsored By
OFFICE OF NAVAL RESEARCH
Contract N00014-75-C-0429

404 434

APPLIED RESEARCH LABORATORIES
THE UNIVERSITY OF TEXAS AT AUSTIN
AUSTIN, TEXAS 78712

ABSTRACT

The purpose of the bottom interaction experiment is to examine the influence of the ocean bottom on low frequency acoustic propagation. This document describes the goals of the experiment, the design of the experiment, including site selection, and details of conducting the experiment, and includes the data analysis plan.

The bottom interaction experiment will use ACODAC recording systems to obtain a record of SUS signals in a bottom limited region. The geometry will be selected so that the number of bottom interactions and the bottom interaction angles will be known. Data will be collected at short ranges with a small number of bottom interactions to duplicate previous measurements. Data will also be collected out to maximum range permitted by SUS source level to ensure the maximum number of bottom interactions and small grazing angles.

TABLE OF CONTENTS

I. INTRODUCTION

The bottom interaction experiment will collect data to:

- Measure acoustic propagation loss
- Measure bottom interaction
- Measure bottom loss
- Measure noise field
- Measure bottom properties

in a bottom limited region.

Bottom loss versus grazing angle as a function of frequency will be determined and examined for consistency throughout the region selected for the experiment.

Impulsive (explosive) sources have been used extensively to measure propagation features. Analysis of received energy from such sources by means of digital signal processing allows a greater flexibility than do other techniques. With the ability to resolve and analyze (on a routine basis) the individual arrivals contained in the received signal, it becomes possible to take into consideration the differences in propagation paths of the individual arrivals. The experiment described here will take advantage of the available modeling techniques to describe individual arrival paths. For those paths interacting with the bottom it is then possible to measure the influence of the bottom.

The acoustic data will be recorded by means of the ACODAC (Acoustic Data Capsule) recording system with hydrophones at selected depths in the water column. Hydrophone depths and SUS locations will be selected to include single bottom bounce data and to include ranges out to the maximum at which signals can be detected. SUS runs will be made in four directions from the two ACODAC systems so that consistency of the bottom effects over a large area will be established.

Additional features of the experiment include use of a continuous wave (CW) source to obtain CW propagation loss data to supplement the explosive source data, and to allow comparison of the two measurements in a severely bottom limited region.

The particular site selected as appropriate for the bottom interaction measurements permits additional useful measurements. The location allows both SUS and CW data to be taken in a transition region which goes across a trough to a continental slope into shallow water. Data will be collected to describe propagation down this slope into a bottom limited region.

Also for this particular region, the highest density of shipping occurs in a single lane which is parallel to the coast and is in shallow water. The selection of ACODAC sites will permit some interpretation of the distribution of the noise field from these shallow water sources in a bottom limited region.

Supporting the direct acoustic measurements will be measurements of temperature profile, sound velocity profile, and wind, sea, and swell conditions. To aid in describing the bottom, bathymetry, wide angle reflection, and subbottom profiling data will be taken.

It is important to acknowledge the assistance of the Naval Oceanographic Office and Texas Instruments in preparing this document. Mr. R. S. Winokur, Code 6130, NAVOCEANO, supplied the details of the deconvolution processing of the SUS data. Mr. A. Kirst, TI, supplied details of the event sche[illegible] and environmental data schedules.

Although the future of the experiment as described in this document became uncertain in the LRAPP program, certain elements of the experiment are useful to report. The final recommendations of the Technical Advisory Group of the Bottom Interaction Experiment are included in Appendix G. These recommendations go into detail concerning the experiment as configured in this report and discuss necessary changes when different experiment design criteria prevail.

II. PURPOSE OF EXPERIMENT

The experiment described here has several measurement goals, all directed toward further understanding of the interaction of low frequency sound with the ocean bottom. The experimental design is such that relatively simple measurements will achieve the multiple goals. The experiment will be conducted in a region without a fully developed acoustic channel, the so-called bottom limited condition. While not essential to some elements of the experiment, all the measurements goals can best be accomplished in a bottom limited region. The purpose of this section is to describe the goals of the experiment and especially to call attention to the necessary interrelations between these measurement goals.

To understand and describe propagation under the conditions of bottom interaction, it is necessary with existing modeling techniques to know the acoustic bottom loss versus grazing angle as a function of frequency. The ACODAC's receiving hydrophones will be configured and the SUS runs designed so that bottom reflectivity data will be collected from very close range (single bounce) to the maximum range at which signals can be detected. For comparison purposes, data for up to three bottom interactions will be analyzed by processing total energy received for each shot. This method of analysis will be essentially a repeat of those used previously This experiment will expand the analysis techniques to include analysis of individual arrivals; i.e., acoustic arrivals from an explosive source which have traveled by different transmission paths. The experiment design requires selection of source depth, receiver depth, and range to ensure transmission paths which interact with the bottom, and which have delay times between transmission paths adequate to allow resolution of individual arrivals.

To plan the experiment, the following steps are necessary.

1. Estimation of propagation loss expected for the bottom area of interest. This step is necessary in order to make the best estimate of signal levels to be expected and the best prediction of ranges over which bottom loss can be measured. For prediction purposes, a range of bottom loss behavior is assumed. Resulting propagation loss (PL) prediction from the FACT model for several source and receiver geometries of interest are generated. FACT is a ray theory layered ocean propagation model suitable for this type problem. It includes caustic corrections, surface image interference effects, and low frequency cutoff, and treats bottom interaction by application of a suitable bottom loss coefficient to bottom interacting multipaths as a function of the eigenray bottom grazing angle.

2. Prediction of eigenrays for expected ranges and the source and receiver depths of interest. With an indication of expected signal levels at the ACODAC receivers and using the propagation loss predictions from FACT, a tabulation of eigenrays is obtained to show bottom interaction angles, number of bottom interactions, and delay times between individual arrivals. The ability to compute details of eigenrays is a recent development from a NAVELEX sponsored program at ARL/UT. Additional information is given in Appendix B.

The primary uncertainty in this experimental design procedure is the exact nature of the bottom where the experiment is to be conducted. Use has been made of the limited bottom loss data for nearby regions to select several types of bottom behavior for use in the FACT runs. In the experiment design, ranges have been selected to allow measurement of bottom loss within a span of values similar to those used in the prediction.

A second major aspect of the experiment is the use of a continuous wave (CW) source. Although these data do not contribute directly to measurement of bottom interaction, it is important to make a direct comparison of propagation loss measurements using CW and SUS data in a bottom limited region. The propagation loss measurements will extend from the smooth bottom, up slope into very shallow water, again allowing direct comparison of the two measurements results. Because of the limits on towing depth and source level, the range over which CW measurements can be made is limited.

Another feature of this particular site is the concentration of shipping in a well defined lane running close to the shore in shallow water. The locations of the ACODAC systems have been selected to allow collection of data to give information on the distribution of noise from these shallow sources into a bottom limited region.

Experience from other acoustic experiments using the ACODAC systems will be used to select density of temperature profile data (XBT), sound velocity profile data (SVP), bottom profile (bathymetry), and meteorology data (wind, wave, and swell).

Two additional measurements will be made to aid in understanding the bottom features. Subbottom profiling will be conducted along all tracks where acoustic propagation measurements will be made. The subbottom profile will supplement the routine bathymetry data by giving information on the details of acoustic layers below the bottom down to depths on the order of 200 m. To increase the usefulness of the subbottom profile data, wide angle reflection measurements will be made at appropriate intervals along the tracks. The wide angle reflection data allow calculation of the acoustic propagation velocity in the subbottom layers.

III. LOCATION

In choosing an experimental site, there were two categories of information to be considered: those features which were necessary and those which were desirable.

It was necessary in this early stage of experimentation to have minimum bottom topographic variation over the maximum range from which measurements were expected. First choice was a smooth flat bottom and second choice was a smooth sloping bottom; the contribution of more complex bottom features can better be examined in later experiments. It is highly desirable to conduct the measurements in a severely bottom limited region, although this is not necessary for some goals of the experiment. It is desirable to have some additional knowledge of the area including sound velocity profile and bottom type.

Initially, three areas in the Eastern-Central Pacific were examined. These areas are shown in Fig. III-1. The entire region is bottom limited and each area has a relatively smooth bottom with several hundred miles dimension; and, there is adequate knowledge to support the planning phase and to determine that the desired measurements can be made. Site I was selected because it had the most desirable bottom features.

The SVP shown in Fig. III-2 is representative of this area. It shows a condition of severe bottom limited acoustic propagation for shallow sources. Bottom data, although limited, indicates a uniform region of thin (<100 m) sediments with high bottom loss at low grazing angles. No bottom loss data were available at grazing angles between 0° and 5°.

A benefit of this location is the proximity of the coastline and its rapid slope. With small additional effort, data on slope coupling in a bottom limited region will be obtained. Another feature is the

HEIGHT OF OCEAN BOTTOM (IN FATHOMS) ABOVE CRITICAL DEPTH

0 – 500
500 – 1500
> 1500

FIGURE III-1

BOTTOM LIMITING EXTENT IN EASTERN PACIFIC SHOWING SITES CONSIDERED FOR EXPERIMENT (I, II, III)

ARL - UT
AS-75-1164
ALA - DR
8 - 14 - 75

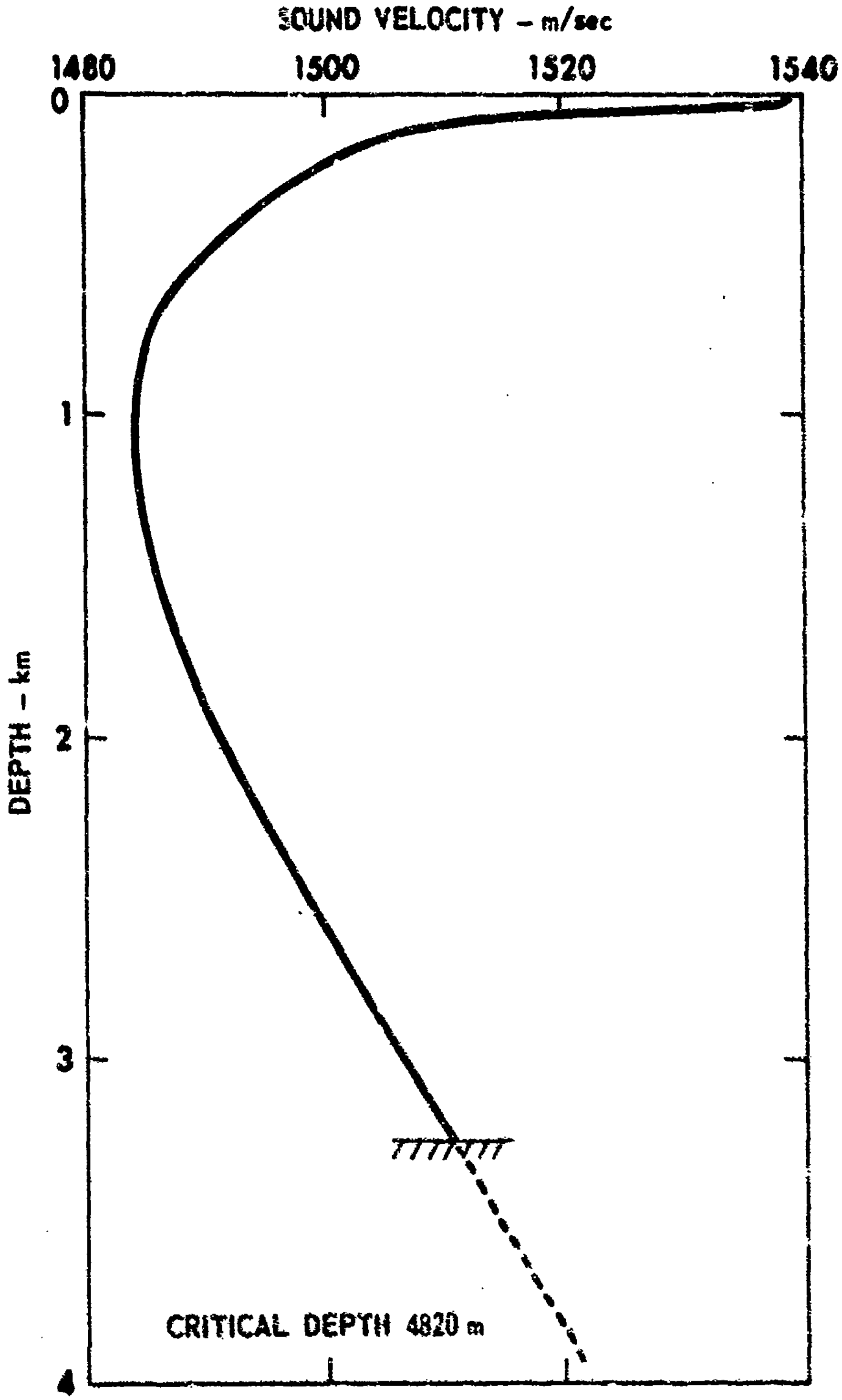

FIGURE III-2

SOUND VELOCITY PROFILE, TYPICAL OF REGION

AS-75-1165

concentration of shipping along the coastline. Useful data on the noise distribution from these concentrated, shallow water sources will also be obtained.

IV. EXPERIMENTAL DESIGN

With the purpose of the experiment established, and with a location selected, a range of expected acoustic behavior was then used to design the experiment. The first step consisted of using the available SVP, Fig. III-2, and available bottom loss data to obtain propagation loss predictions using FACT. Four SUS depths and four receiver depths are used. The resulting propagation loss runs for two expected extremes of bottom type (i.e., approximately 5 dB bottom loss at all grazing angles and a change of 0 to 5 dB between 0° and 5° grazing angle) are presented in Appendix A. For shallow sources and receivers, and high bottom loss, it is seen that extremely high propagation loss occurs and only short ranges can be expected. For less stringent conditions the predictions indicate the ACODAC systems will receive bottom interaction signals to several hundred miles. Tentative selection of ACODAC spacing and measurement distances were made based on those predictions.

For these ranges and for the available SVP data, families of eigenrays were examined to determine if the particular geometry allowed time resolution of individual arrivals and to determine the range of grazing angles for which data would be analyzed and the number of bottom interactions which would occur. Examples of specific eigenrays are shown in Figs. IV-1, IV-2, and IV-3. Summaries of the behavior of the eigenrays are tabulated in Appendix B.

The eigenray parameters are summarized in Fig. IV-4, which shows bottom reflection angle versus range, and Fig. IV-5, which shows arrival time (relative to first arrival) versus range for specific propagation paths.

These sample predictions are intended to illustrate the steps taken to determine hydrophone depths, source depths, density and spacing of

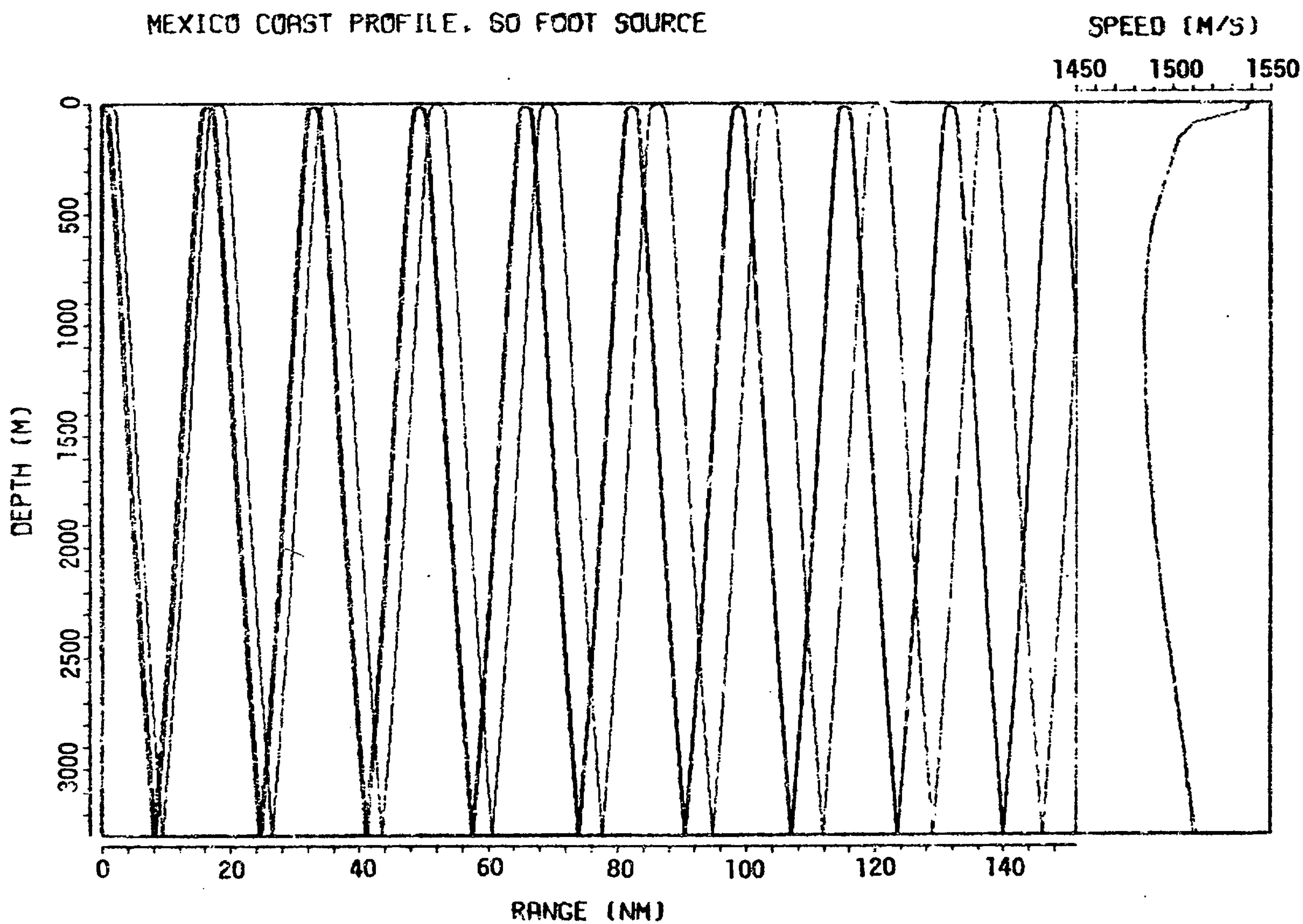

FIGURE IV-1

EIGENRAY DIAGRAM, MINIMUM DEEP TURNINGS

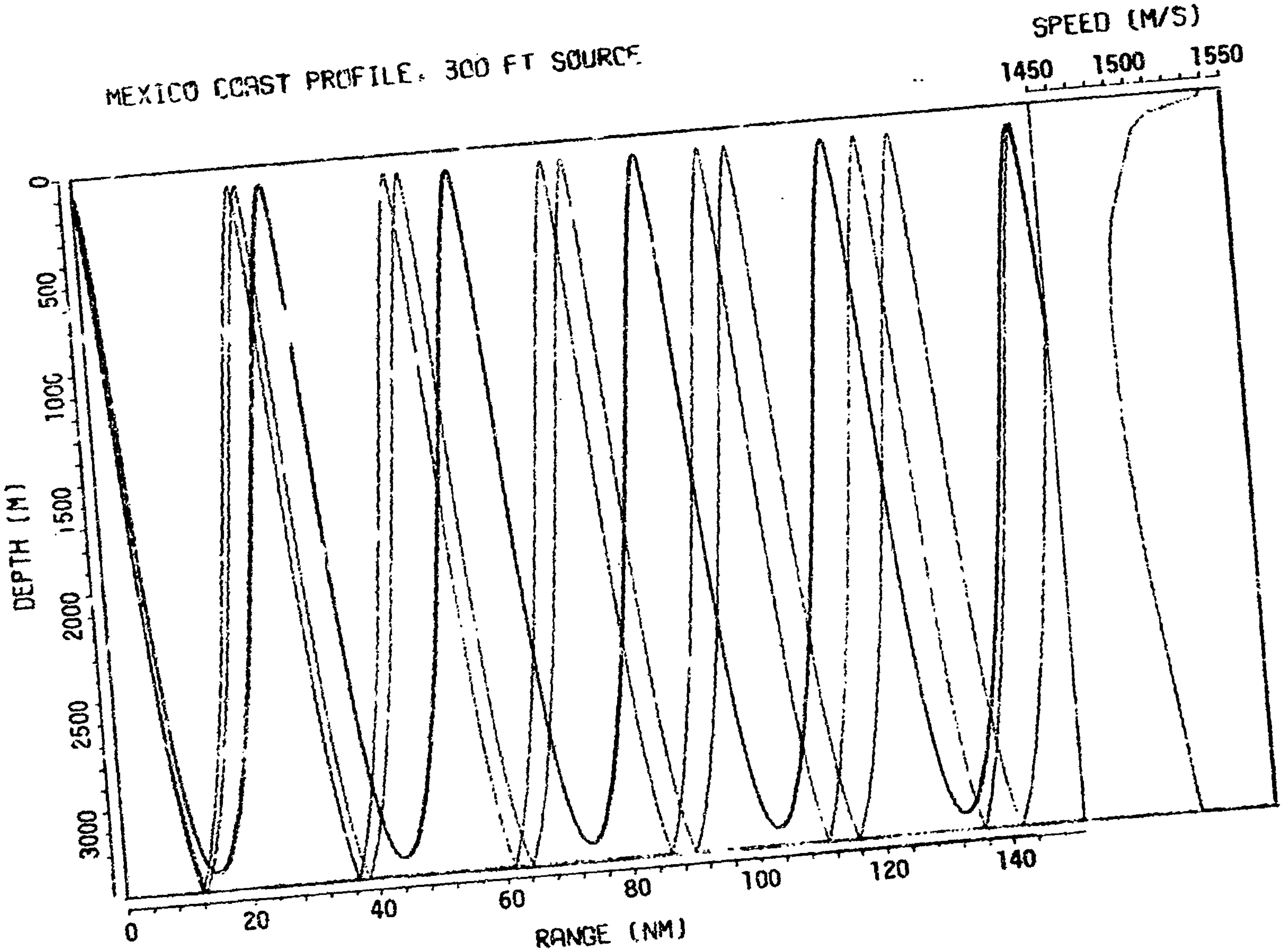

FIGURE IV-2
EIGENRAY DIAGRAM, DEEP REFRACTED AND BOTTOM REFLECTED RAYS

AS-75-2310

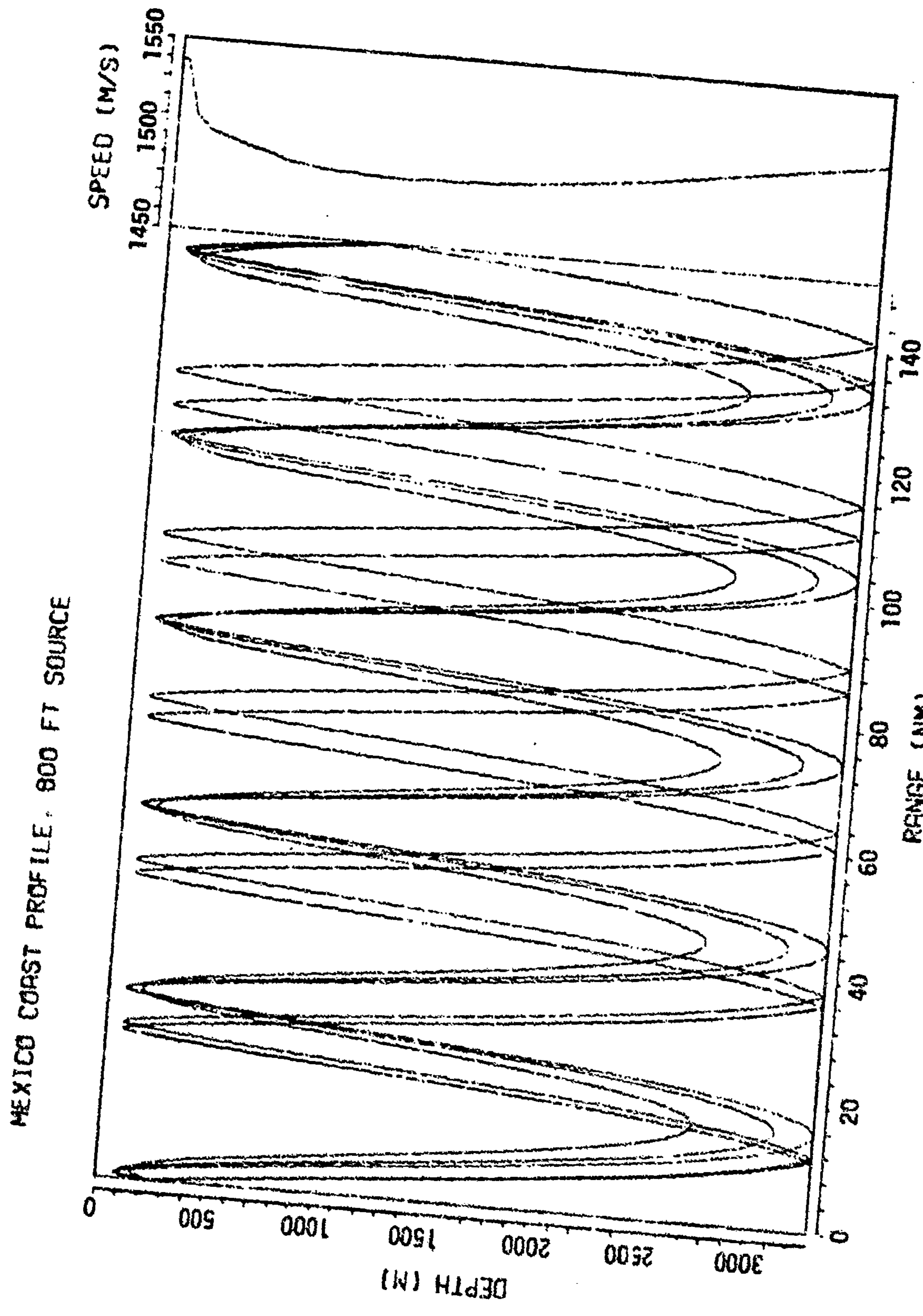

FIGURE IV-3
EIGENRAY DIAGRAM DEEP SOURCE

AS-75-2311

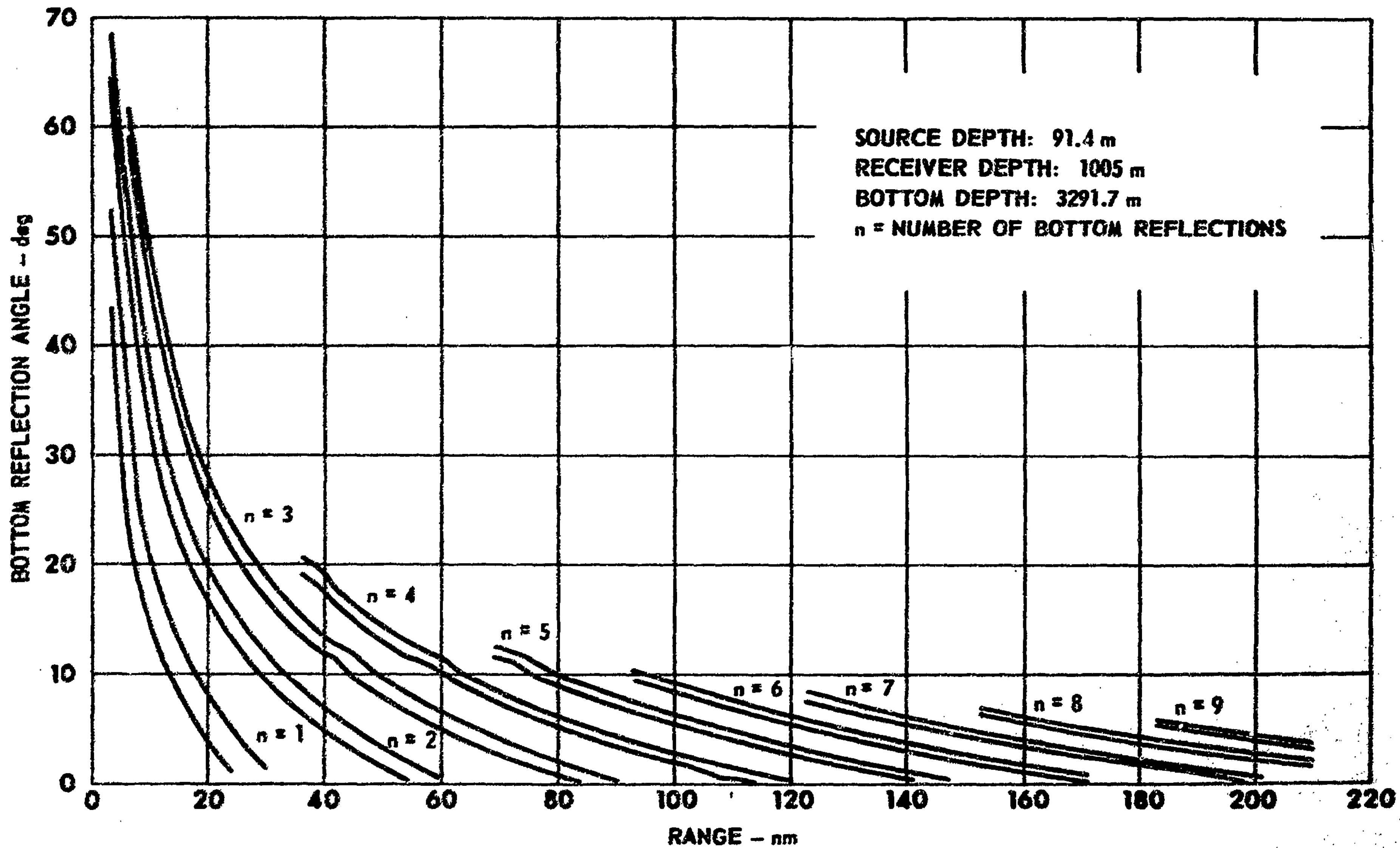

ARL - UT
AS-75-1162
ALA - DR
8 - 14 - 75

FIGURE IV-4
EIGENRAY BOTTOM REFLECTION ANGLE VERSUS RANGE

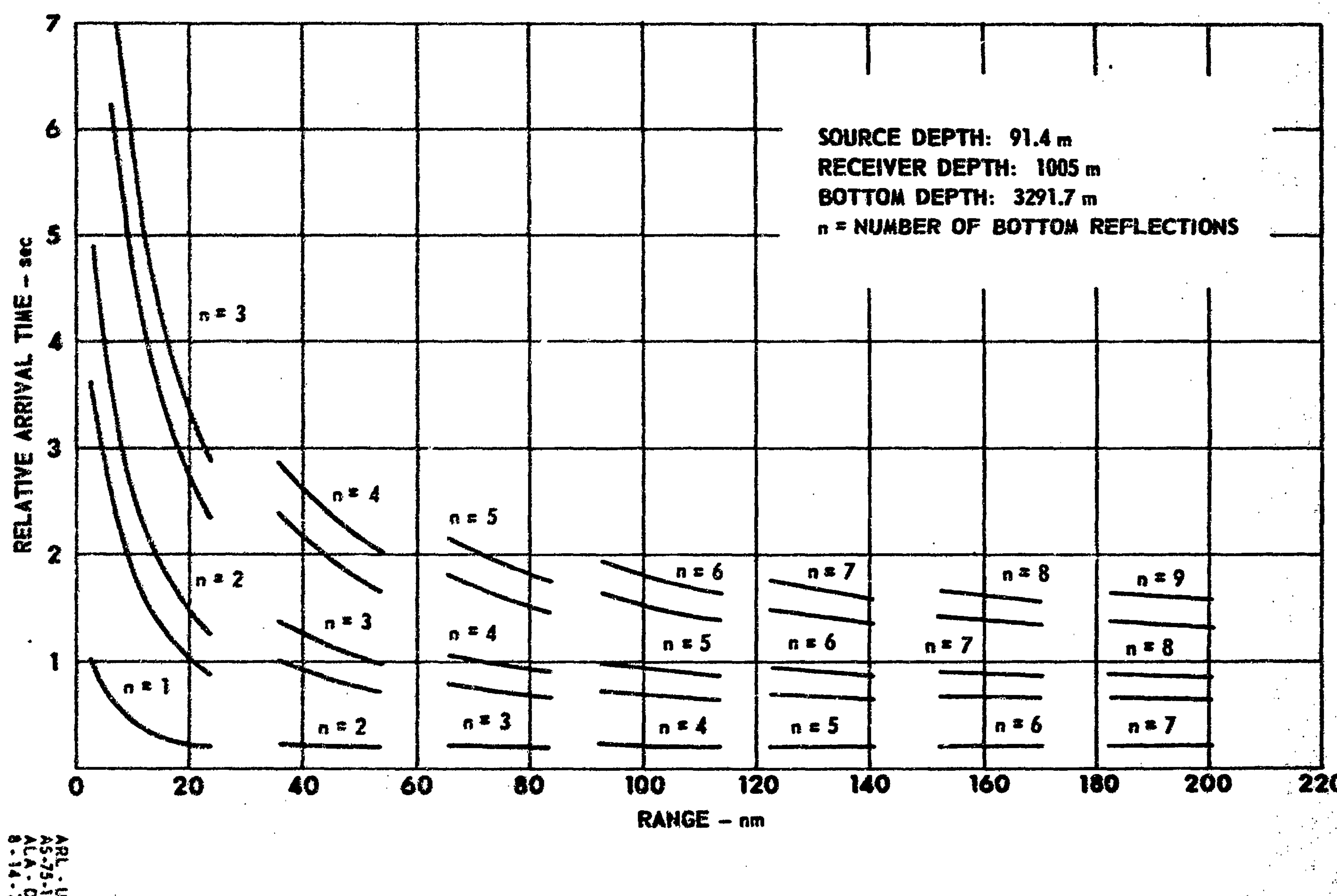

FIGURE IV-5
RELATIVE ARRIVAL TIME OF MULTIPATHS VERSUS RANGE

shots, separation of ACODAC systems, levels of signals to be received, and dynamic range required at the receiving system. The final experimental design described in the next section is a result of several repetitions of this design cycle.

V. EXPERIMENTAL DETAIL

Site and Track Detail

The experiment will use two ACODAC systems deployed as shown in Fig. V-1. The coordinates for ACODAC Site A are 11°31'N, 93°32'W and for Site B are 8°57'N, 95°49'W. A and B are separated by 206 miles.

The experiment will use two ship tracks. The first is the straight line track between the two sites extending up the slope to the 100 fathom contour. The second track crosses the first track at approximately 60° at Site A and turns to recross at approximately the same angle at Site B. The track from 1 to 2 (Fig. V-1) is approximately 480 miles. The track from 3 to 4 via P is 525 miles.

The purpose of making two runs is to collect data on as many bottom interactions as source level and receiver sensitivity will permit for this bottom area, and also to ensure reasonable duplication in the data. For example, the run ending at 2 is near the expected maximum range for System B and outside the expected range for System A. However, if the bottom loss is less than expected, then the range from 2 to System A will allow maximum number of bottom interactions to be measured. Also, there are useful results for system comparisons and analysis when energy from one source is received on both systems (i.e., those portions of the runs between A and B). For all the deep shots (244 m, 610 m) and portions of the shallow shots (18 m, 91 m) both ACODACs will record the events. In the unlikely event one ACODAC fails, most of the ship track and SUS sources will still contribute to the experiment.

SUS Deployment

Several factors influence the shot deployment pattern. To define the bottom loss versus grazing angle curve with reasonably fine resolution,

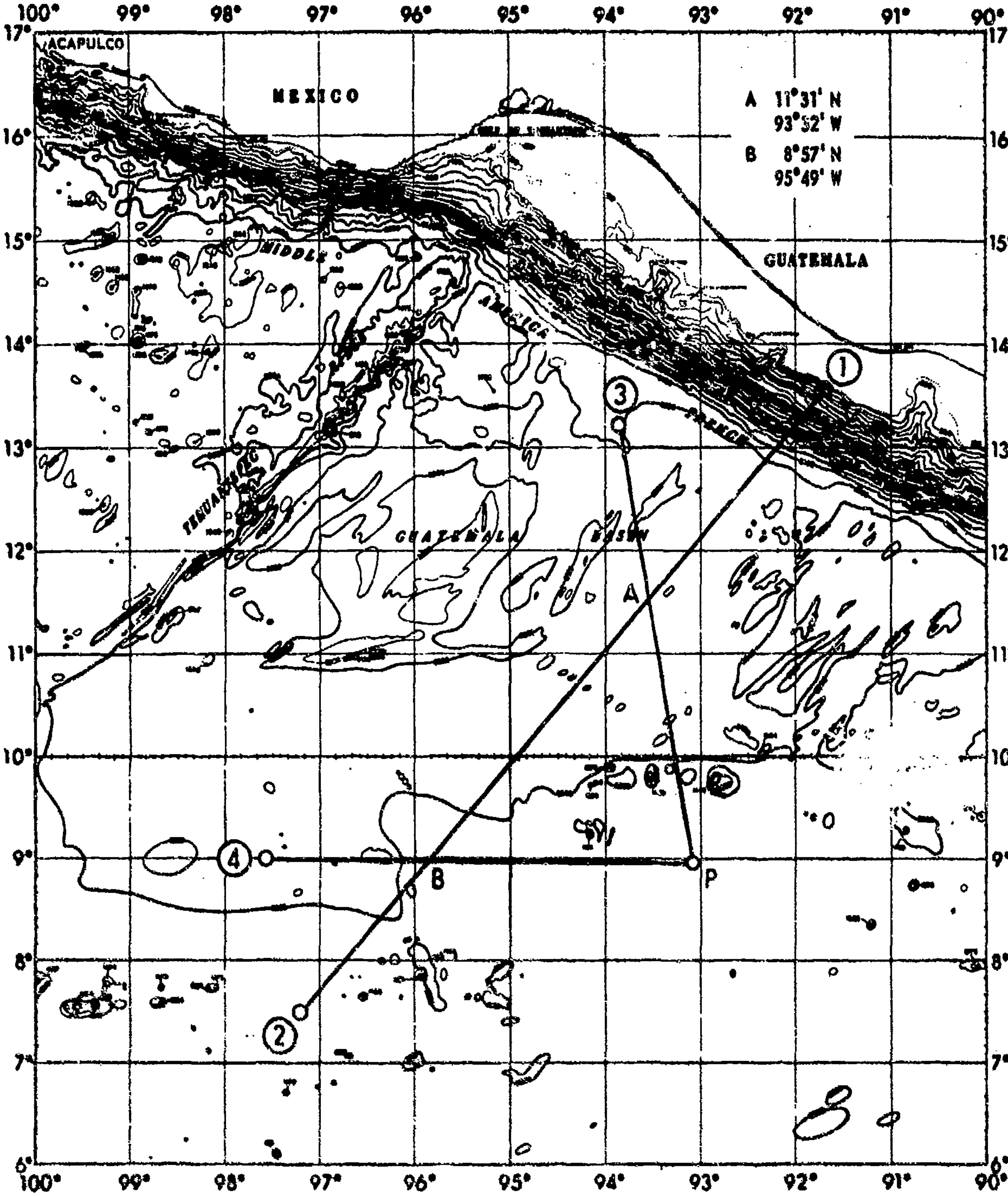

FIGURE V-1
TRACK CHART AND ACODAC LOCATIONS
BOTTOM INTERACTION EXPERIMENT

ARL - UT
AS-75-2299
LDH - DR
11 - 13 - 75

a high density of shots (small spacing between shots) is desirable, especially at short ranges. However, to keep the total number of shots used within reasonable bounds and to minimize the chance of reverberation from one shot interfering with reception of the next in a sequence, a minimum shot spacing had to be established.

A geometry frequently used for bottom loss measurement positions a receiver at 152 m (500 ft) depth and sources at 244 m (800 ft) depth deployed at ranges from near the receiver to 30 or 40 nm. Although the present bottom interaction experiment is designed to use several source depths and several receiver depths, to comply with this geometry one of the ACODAC hydrophones is to be at 152 m depth and one of the source depths is to be 244 m. Figure V-2 shows the bottom interaction angle versus range (out to 40 nm) for the first three bottom interacting multipaths. The relative arrival times shown in Fig. V-3 demonstrate that the various arrival orders will be separable in time during data processing. From the model results used to produce Fig. V-2, a shot separation of 1 nm for the 244 m depth sources results in an angular separation of measurements less than 3° beyond 8 nm range (bottom interaction angles below 25°) for the single deep turning multipath. For shorter ranges, angular separation of measurements increases to about 7° at 4 nm range. The shot deployment pattern to be used provides for a high density of 244 m depth shots for the first 15 nm range either side of an ACODAC, a medium density of 244 m depth shots on out to 35 nm range, and a lower but acceptable density for greater ranges. The two shallowest depth shots (18 m and 91 m) are to be deployed at the greater spacing (~3.3 nm) for all range segments. The deepest shots, which provide calibration information for reduction of the other data, will be detonated at 3.3 nm range increments for some range segments and at 10 nm increments for other range segments. Figure V-4 illustrates the four shot deployment patterns to be used and Fig. V-5 shows the range segment for which each pattern is to be used. Although the shots for all depths are shown at the same times in Fig. V-4, the actual deployment sequence is controlled by the various times between deployment and detonation for the different

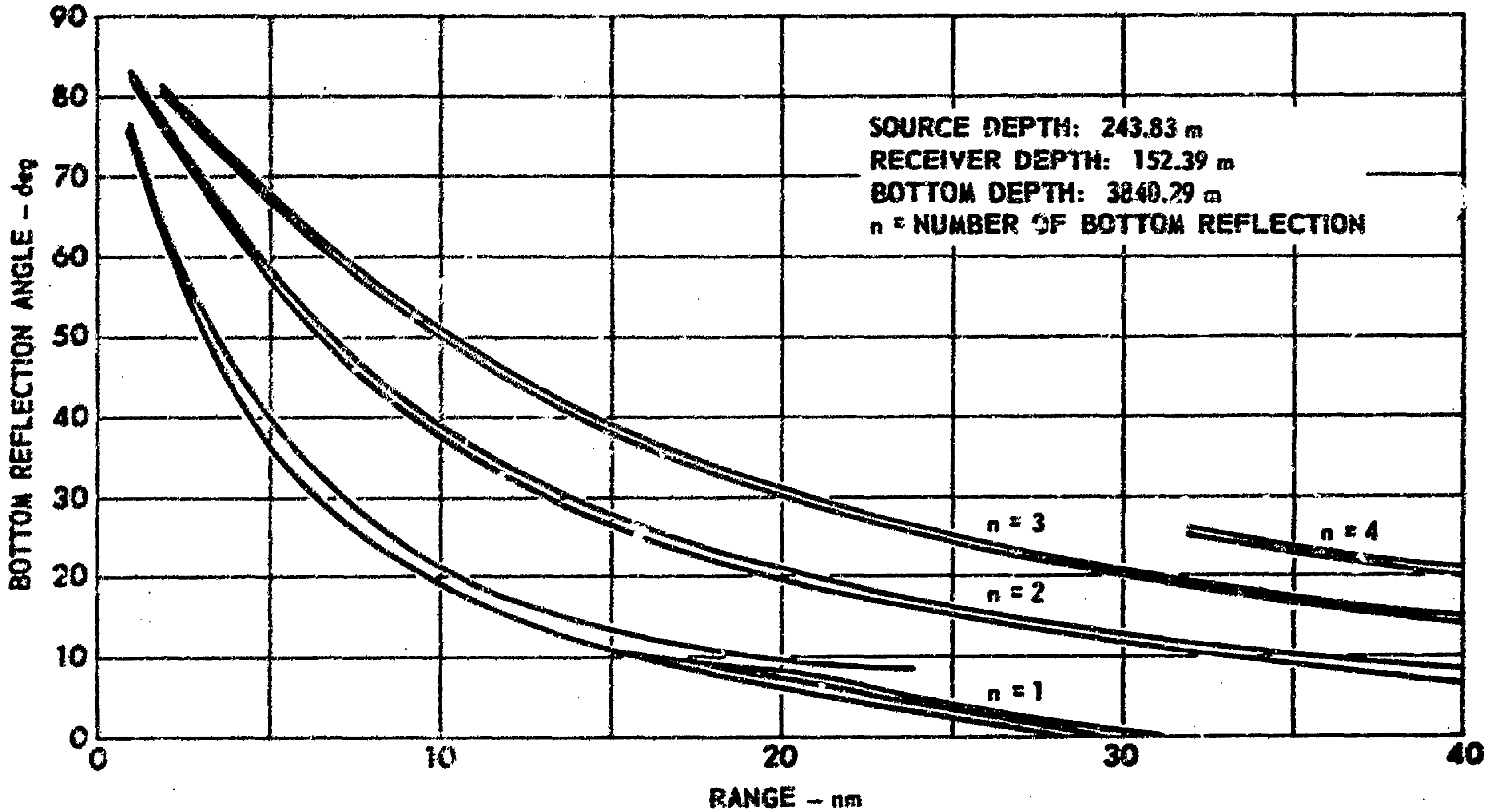

FIGURE V-2
EIGENRAY BOTTOM REFLECTION ANGLE VERSUS RANGE
(EXPANDED SHORT RANGE)

ARL - UT
AS-75-2300
LDH - DR
11-12-75

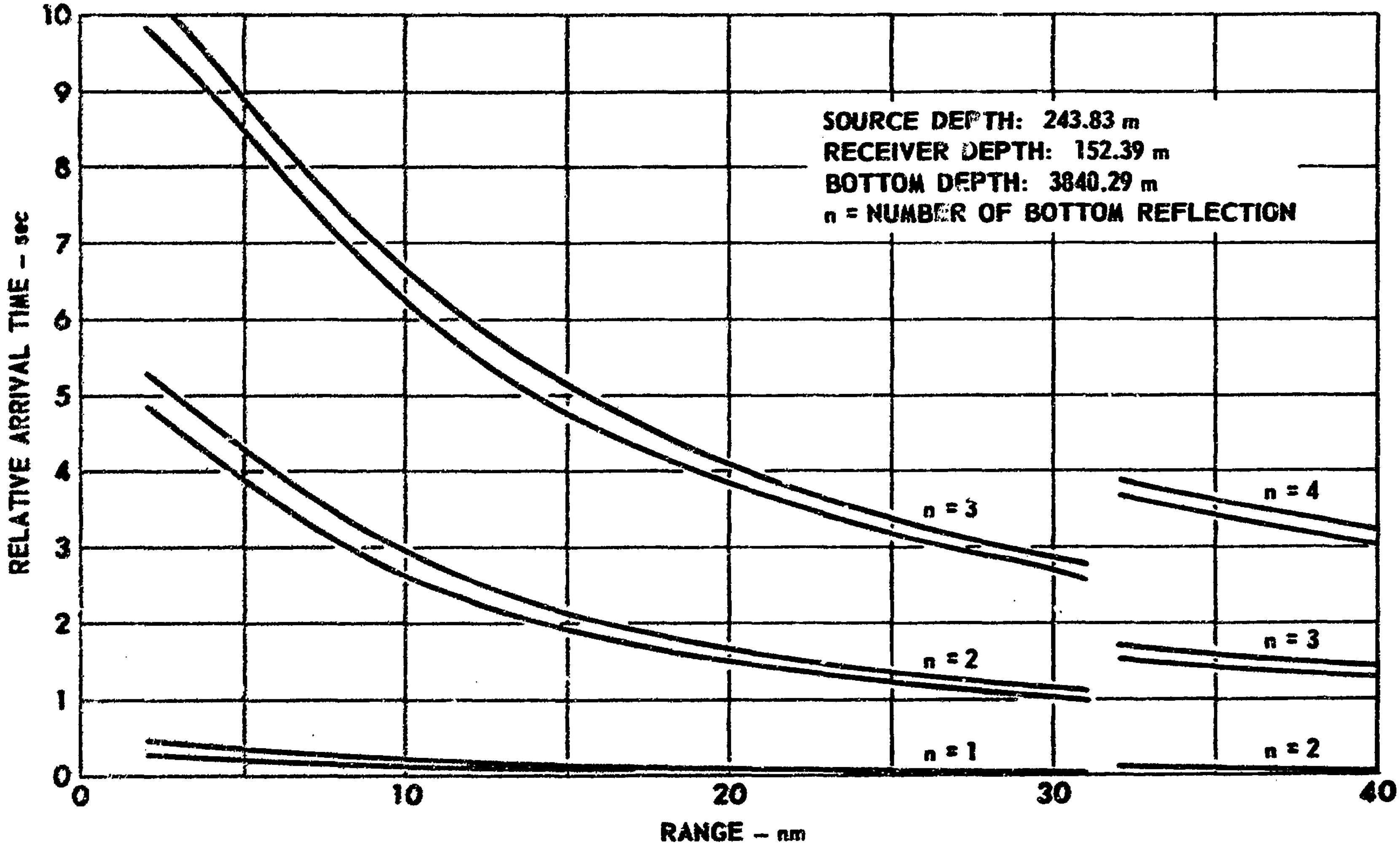

FIGURE V-3
RELATIVE ARRIVAL TIME OF MULTIPATHS VERSUS RANGE
(EXPANDED SHORT RANGE)

ARL - UT
AS-75-2301
LDH - DR
11 - 12 - 75

Density Pattern	Depth (m)	0	5	10	15	20	25	30	35	40	45	50	55	60	Shots/h
							Time (min)								
1	18	X				X				X				X	3
	91	X				X				X				X	3
	244	X				X				X				X	3
	610	X				X				X				X	3
2	18	X				X				X				X	3
	91	X				X				X				X	3
	244	X				X				X				X	3
	610	X												X	1
3	18	X				X				X				X	3
	91	X				X				X				X	3
	244	X		X		X		X		X		X		X	6
	610	X				X				X				X	3
4	18	X				X				X				X	3
	91	X				X				X				X	3
	244	X	X	X	X	X	X	X	X	X	X	X	X	X	12
	610	X				X				X				X	3

FIGURE V-4

SHOT DENSITIES

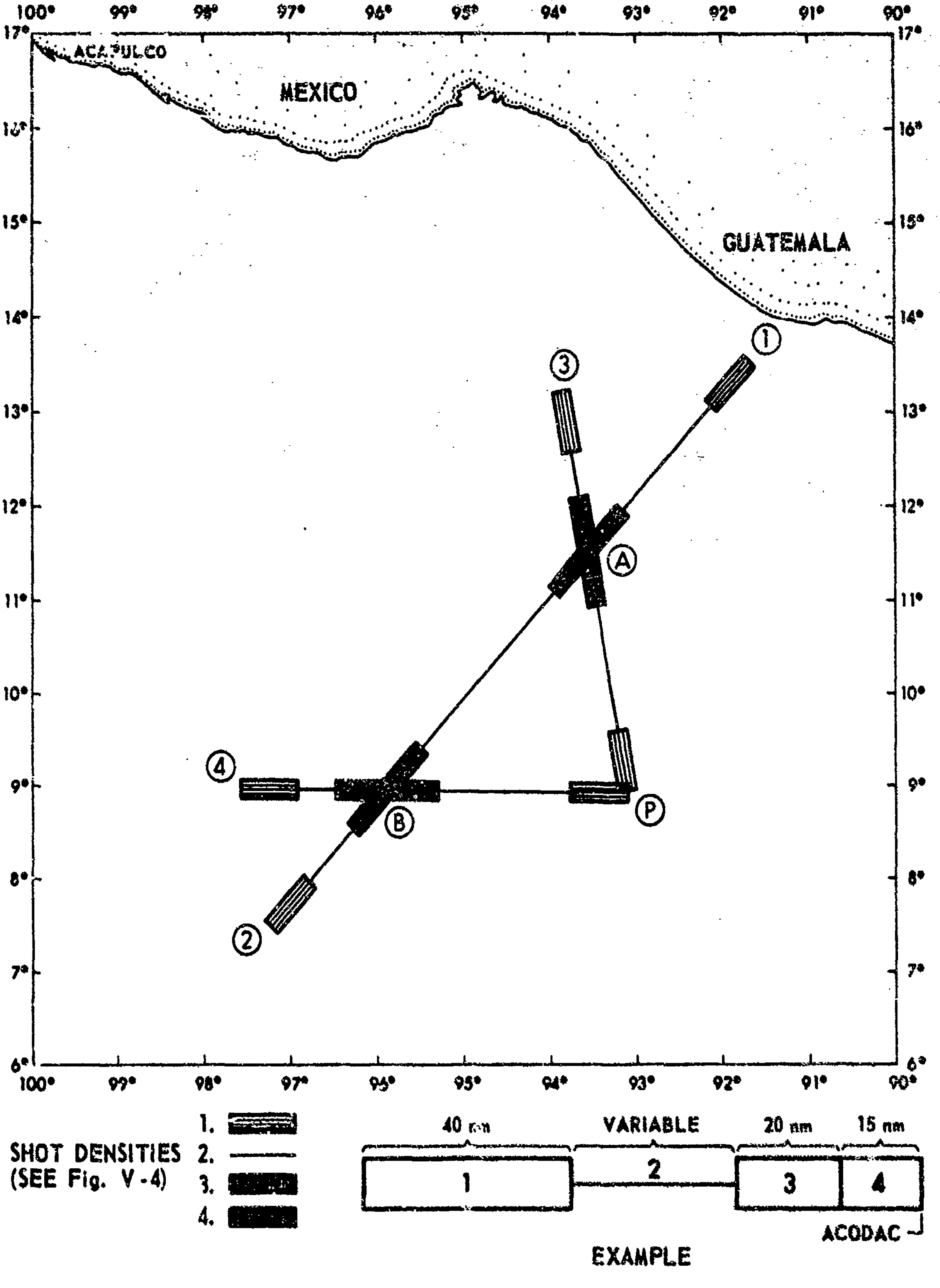

ARL - UT
AS-75-2303
LDH - DR
11-12-75

FIGURE V-5
SUS DEPLOYMENT SCHEDULE TRACK DETAIL

detonation depths. The sink rates and detonation depths result in the time delays shown in Table V-1. In order to minimize the probability of overlap of shot signals, the deployment schedule to be used is a 60 ft (18 m) SUS followed 60 sec later by a 300 ft (91 m) SUS followed 60 sec later by a simultaneous deployment of an 800 ft (244 m) and a 2000 ft (610 m) SUS. This basic pattern is modified to allow for the four different deployment patterns to be used, as shown in Tables V-2 through V-5. The total SUS requirements are as follows: 60 ft, 350; 300 ft, 350; 800 ft, 500; and 2000 ft, 250.

CW Deployment

The CW tow will be conducted along the track from point 1 to point 2 (see Fig. V-1) and will pass over ACODACs at Site A and Site B. Towing speed will be 5 kt, requiring 98 h to complete the tow. The Vibroseis system allows towing two sources simultaneously at two different depths. Each source can transmit two frequencies simultaneously; thus a total of four frequencies can be transmitted. During the CW tow for this experiment, four different frequencies over the band from 10 to 300 Hz will be transmitted with a schedule of 50 min on and 10 min off each hour. A high and a low frequency, in the stated band, will be selected for both tow depths. The shallow tow depth will be 60 ft while the deeper tow depth will be 300 ft, allowing comparison of propagation measured during the tow with that measured during the SUS runs. Frequencies for the CW source will be chosen to facilitate this comparison.

ACODAC Configuration

Figure V-6 is a schematic of the ACODAC configuration. The 13 receivers are clustered in four groups of three hydrophones with the remaining hydrophone located adjacent to the bottom.

TABLE V-1

Time Between Deployment and Detonation

for Various SUS Depths

Shot Detonation Depth (ft)/(m)	Relative Detonation Time (after deployment) (sec)
60/18	4 sec through the water (to 6 sec with spoiler plate)
300/91	26
800/244	46
2000/610	120

TABLE V-2

Shot Deployment Schedule for each Shot Density

Density 1:

Starting on the Hour Time	Deploy SUS, Depth (ft)	Starting on the Half Hour Time
0000	60	0030
0001	300	0031
0002	800 and 2000	0032
0020	60	0050
0021	300	0051
0022	800 and 2000	0052
0040	60	0110
0041	300	0111
0042	800 and 2000	0112

TABLE V-3

Shot Deployment Schedule for Each Shot Density

Density 2:

Starting on the Hour Time	Deploy SUS, Depth (ft)	Starting on the Half Hour Time
0000	60	0030
0001	300	0031
0002	800 and 2000	0032
0020	60	0050
0021	300	0051
0022	800 only	0052
0040	60	0110
0041	300	0111
0042	800 only	0112

TABLE V-4

Shot Deployment Schedule for Each Shot Density

Density 3:

Starting on the Hour Time	Deploy SUS, Depth (ft)	Starting on the Half Hour Time
0000	60	0030
0001	300	0031
0002	800 and 2000	0032
0012	800 only	0042
0020	60	0050
0021	300	0051
0022	800 and 2000	0052
0032	800 only	0102
0040	60	0110
0041	300	0111
0042	80C and 2000	0112
0052	800 only	0122

TABLE V-5

Shot Deployment Schedule for Each Shot Density

Density 4:

Starting on the Hour Time	Deploy SUS, Depth (ft)	Starting on the Half Hour Time
0000	60	0030
0001	300	0031
0002	800 and 2000	0032
0007	800 only	0037
0012	800 only	0042
0017	800 only	0047
0020	60	0050
0021	300	0051
0022	800 and 2000	0052
0027	800 only	0057
0032	800 only	0102
0037	800 only	0107
0040	60	0110
0041	300	0111
0042	800 and 2000	0112
0047	800 only	0117
0052	800 only	0122
0057	800 only	0127

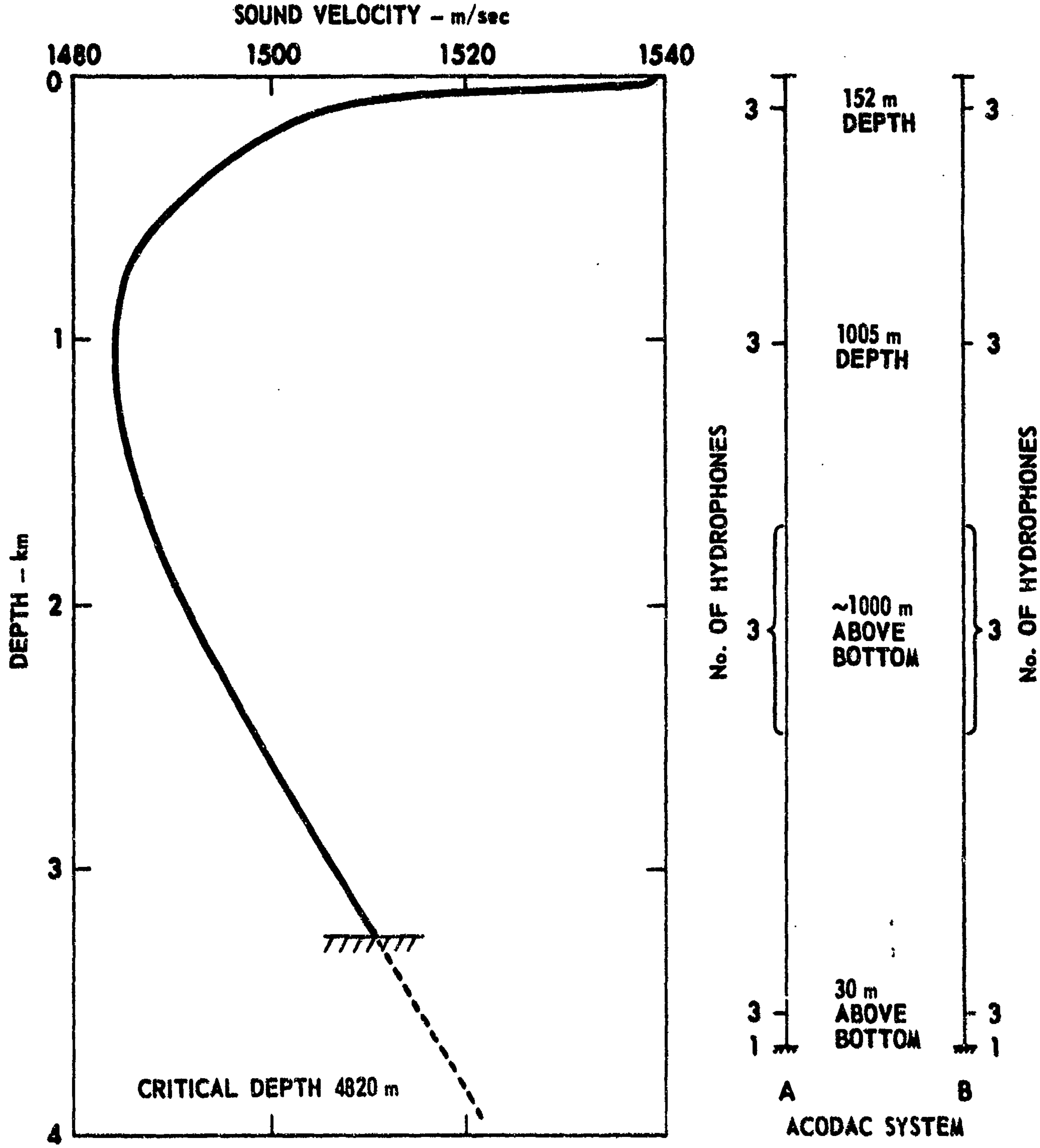

ARL - UT
AS-75-1159
ALA - DR
8 - 13 - 75

FIGURE V-6
ACODAC CONFIGURATION

In addition to the 152 m (500 ft) receiver depth, as shown in Fig. V-6 hydrophones will be placed at depths of 1005 m (near axis depth), 2840 m (about 1000 m above the bottom), and 3810 m (30 m above the bottom). This receiver configuration samples several important depths in the water column. It further ensures a variety of bottom interaction angles and arrival times from each shot, thus maximizing the range segments over which multipath separation and bottom loss analysis can be performed. The single bottom receiver will be configured to record bottom noise level.

Each of the three hydrophones at the four depths will be passed through a different preamplifier gain prior to recording, thus providing a large dynamic range for reception at each depth. The channel gains are adjusted to provide reception over the following sound pressure levels in the water at the hydrophone face:

Channel	SPL Range dB re μPa
Low Gain	198 - 168
Medium Gain	168 - 138
High Gain/	138 - 108/
(Ambient Noise)	(108 - 78)

As shown above, the low and medium channels are fixed gain, while the high gain (ambient noise) channel has two gain states and switches between the two in the usual manner of operation of the ACODACs. The low gain channels will allow reception of the SUS signals at ranges as short as 4 to 5 nm without overloading the recorder, while the other channels allow continuous definition of propagation details out to ranges experiencing much higher propagation loss.

All channels will use the maximum available bandwidth (10 Hz to 600 Hz) except the high gain/ambient noise channels which will be used to incorporate the necessary reference frequency and will have a useful bandwidth of 10 Hz to 300 Hz.

Event Schedule

Table V-6 is a Master Event Schedule for the bottom interaction experiment. The SUS vessel will conduct the experiment totally with the exception of the use of a CW vessel to provide the four day CW tow (Event 252).

Table V-7 is the SUS vessel event schedule and Table V-8 is the CW vessel schedule. Table V-9 gives details of the XBT and STD schedule. The locations are shown in Fig. V-7. The locations of the wide angle reflections measurements as a supplement to subbottom profiling are shown in Fig. V-8.

Appendix C gives a list of organizations, personnel, and major equipments participating in the experiment. Appendix D gives additional detail of operational plans including radio frequencies, acoustic source frequencies, and schedules, etc.

TABLE V-6. MASTER EVENT SCHEDULE SUMMARY

EXERCISE TIME	EVENT NUMBER	SUS VESSEL	CW VESSEL
0	10	Depart San Diego	
120	11		Depart San Diego
144	20	Arrive Acapulco	
166	30	Depart Acapulco for exercise area	
224	40	Wide angle reflection and subbottom profiling (Sites 2 to B)	
239	90	Deploy ACODAC B	
255	100	Wide angle reflection and subbottom profiling (Sites B to P to A)	
306	210	Deploy ACODAC A	
336	220	Wide angle reflection and subbottom profiling (Sites A to 1)	
348	251	ACODAC's turn on	
348	252		Begin CW Tow (Sites 2 to 1)
375	330	Wide angle reflection and subbottom profiling (Sites 3 to A)	
446	430	Begin SUS run (Sites 2 to 1)	End CW Tow
496	460	End SUS run	
513	490	Begin SUS run (Sites 3 to P to 4)	
521	491		Arrive Balboa, Panama
569	520	End SUS run	
570	530	Wide angle reflection and subbottom profiling (Sites 4 to B)	
590	610	Retrieve ACODAC B	

TABLE V-6, CONTINUED

EXERCISE TIME	EVENT NUMBER	SUS VESSEL	CW VESSEL
602	620	Wide angle reflection and subbottom profiling (Sites B to A)	
632	720	Retrieve ACODAC A	
694	740	Arrive Acapulco	
886	760	Arrive San Diego	

TABLE V-7. SUS VESSEL EVENT SCHEDULE

EVENT NUMBER	EXERCISE TIME HOURS	EVENT DESCRIPTION	COURSE	SOA	POSITION	TIME ALLOWED	DISTANCE
10	0	Depart NUC Dock (San Diego) and transit to Acapulco	AR	10	San Diego 32°41'N - 117°14'W	144	1420
20	144	Arrive Acapulco - In port	-	-	Acapulco 16°50'N - 99°53'W	22	
30	166	Depart Acapulco and transit to Site 2	AR	10		58	580
40	224	Arrive Site 2 and rig air gun and streamer			7°27'N - 97°06'W	1	
50	225	Transit to WR1 and COMEX sub-bottom profiling	041	10		4	40
60	229	Arrive WR1 slow to 5 kt; deploy sonobuoy and COMEX WR run	041	5	7°57'N - 96°40'W	4	20
70	233	FINEX WR run and resume 10 kt SOA and transit to Site B	041	10	8°12'N - 96°27'W	6	60
80	239	Arrive Site B and retrieve air gun and streamer	-	-	8°57'N - 95°48'W	1	-
90	240	Begin site survey - Take STD and XBTs (T-5 and T-7); and deploy ACODAC				25	-
100	265	Rig air gun and streamer; transit to WR2 and COMEX subbottom profiling	090	10	-	5	47
110	270	Arrive WR2 and slow to 5 kt; deploy sonobuoy and COMEX WR run	090	5	8°57'N - 95°00'W	4	20

TABLE V-7. SUS VESSEL EVENT SCHEDULE

EVENT NUMBER	EXERCISE TIME HOURS	EVENT DESCRIPTION	COURSE	SOA	POSITION	TIME ALLOWED	DISTANCE
120	274	FINEX WR run and resume 10 kt SOA and transit to WR3	090	10		4	40
130	278	Arrive WR3 and slow to 5 kt; deploy sonobuoy and COMEX WR run	090	5	8°57'N - 94°00'W	4	20
140	282	FINEX WR run and resume 10 kt SOA and transit to Site P	090	10	8°57'N - 93°40'W	4	36
150	286	Arrive Site P - Change course to 350 and transit to WR4	350	-	8°57'N - 93°04'W	3	33
160	289	Arrive WR4 and slow to 5 kt; deploy sonobuoy and COMEX WR run	350	5	9°30'N - 93'10°W	4	20
170	293	FINEX WR run and resume 10 kt SOA and transit to WR5	350	10	9°50'N - 93°13'W	4	41
180	297	Arrive WR5 and slow to 5 kt; deploy sonobuoy and COMEX WR run	350	5	10°30'N - 93°20'W	4	20
190	301	FINEX WR run and resume 10 kt SOA and transit to Site A	350	10	10°50'N - 93°25'W	4	41
200	305	Arrive Site A - Retrieve air gun and streamer	-	-	11°31'N - 93°32'W	1	-
210	306	Begin Site Survey - Take STD and XBTs (T-5 and T-7) and deploy ACODAC	-	-	-	30	-
220	336	Rig air gun and streamer and transit to WR6 and COMEX sub-bottom profiling	041	10	-	3	30

TABLE V-7. SUS VESSEL EVENT SCHEDULE

EVENT NUMBER	EXERCISE TIME HOURS	EVENT DESCRIPTION	COURSE	SOA	POSITION	TIME ALLOWED	DISTANCE
230	339	Arrive WR6 and slow to 5 kt; deploy sonobuoy and COMEX WR run	041	5	11°53'N - 93°11'W	4	20
240	343	FINEX WR run and resume 10 kt SOA and transit to WR7	041	10	12°08'N - 92°58'W	2	20
250	345	Arrive WR7 and slow to 5 kt; deploy sonobuoy and COMEX WR run	041	5	12°22'N - 92°45'W	4	20
251	348	ACODAC turn "ON"					
260	349	FINEX WR run and resume 10 kt SOA and transit to WR8	041	10	12°37'N - 92°32'W	2	20
270	351	Arrive WR8 and slow to 5 kt; deploy sonobuoy and COMEX WR run	041	5	12°52'N 92°18'W	4	20
280	355	FINEX WR run and resume 10 kt SOA and transit to WR9	041	10	13°07'N - 92°05'W	2	20
290	357	Arrive WR9 and slow to 5 kt; deploy sonobuoy and COMEX WR run	041	5	13°22'N - 91°52'W	3	18
300	360	Arrive Site 1 and retrieve air gun and streamer			13°36'N - 91°39'W	1	
310	361	Take STD and XBT (T-7)				1	
320	362	Transit to Site 3	258	10		13	130
330	375	Arrive Site 3 and rig air gun and streamer; COMEX subbottom profiling from Site 3 to Site A	170	10	13°10'N - 93°48'W	8	80
340	383	Arrive Site A/WR10 and slow to 5 kt, deploy sonobuoy and COMEX WR run	170	5	11°51'N - 93°34'W	2	10

TABLE V-7. SUS VESSEL EVENT SCHEDULE

EVENT NUMBER	EXERCISE TIME HOURS	EVENT DESCRIPTION	COURSE	SOA	POSITION	TIME ALLOWED	DISTANCE
350	385	Arrive WR11 and deploy sonobuoy and COMEX WR run	170	5	11°41'N - 93°33'W	2	10
360	387	Arrive Site A/WR12 and change course to 221; deploy sonobuoy and COMEX WR run	221	5	11°31'N - 93°32'W	2	10
370	389	Arrive WR13 and deploy sonobuoy and COMEX WR run	221	5	11°23'N - 93°38'W	2	10
380	391	FINEX WR run and retrieve air gun and streamer	-	-	11°16'N - 93°45'W	1	
390	392	Transit to Site 4	239	10	11°16'N - 93°45'W	27	266
400	419	Arrive Site 4 and take STD and XBTs (T-5 and T-7)			8°57'N - 97°30'W	3	
410	422	Transit to Site 2	165	10		9	92
420	431	Arrive Site 2 and take STD and XBTs (T-5 and T-7)			7°27'N - 97°06'W	3	
421	434	DAFA				12	
430	446	Rig shot streamer and COMEX SUS run from Site 2 to Site C	041	10		22	222
440	468	Arrive Site C and COMEX 24 shots	-	-	10°14'N - 94°39'W	1	-
450	469	COMEX SUS run from Site C to Site 1	041	10		27	269

TABLE V-7. SUS VESSEL EVENT SCHEDULE

EVENT NUMBER	EXERCISE TIME HOURS	EVENT DESCRIPTION	COURSE	SOA	POSITION	TIME ALLOWED	DISTANCE
460	496	Arrive Site 1 FINEX SUS run and retrieve streamer			13°36'N - 91°39'W	1	
470	497	Transit to Site 3	258	10		13	130
480	510	Arrive Site 3 and take STD and XBTs (T-5 and T-7)			13°10'N - 93°48'W	3	
490	513	Rig shot streamer COMEX SUS run from Site 3 to Site P	170	10		26	257
500	539	Arrive Site P and take STD and XBTs (T-5 and T-7)			8°57'N - 93°04'W	3	
510	542	COMEX SUS run to Site 4	270	10		27	266
520	569	Arrive Site 4 and retrieve shot streamer; rig air gun and streamer			8°57'N - 97°30'W	1	
530	570	COMEX subbottom profiling and transit to WR14	090	10		3	30
540	573	Arrive WR14 and slow to 5 kt; deploy sonobuoy and COMEX WR run	090	5	8°57'N - 97°00'W	4	20
550	577	FINEX WR run and resume 10 kt SOA and transit to WR15	090	10	8°57'N - 96°40'W	3	32
560	580	Arrive WR15 and slow to 5 kt; deploy sonobuoy and COMEX WR run	090	5	8°57'N - 96°07'W	2	10
570	582	Arrive WR16 and deploy sonobuoy and COMEX CW run	090	5	8°57'N - 95°57'W	2	10
580	584	Arrive Site B and WR17-Change course to 041 and deploy sonobuoy and COMEX CW run	041	5	8°57'N - 95°48'W	2	10

TABLE V-7. SUS VESSEL EVENT SCHEDULE

EVENT NUMBER	EXERCISE TIME HOURS	EVENT DESCRIPTION	COURSE	SOA	POSITION	TIME ALLOWED	DISTANCE
590	586	Arrive WR18 and deploy sonobuoy and COMEX CW run	041	5	9°05'N - 95°41'W	2	10
600	588	FINEX CW run and retrieve air gun and transit to Site B	221	10	9°12'N - 95°34'W	2	20
610	590	Arrive Site B and retrieve ACODAC			8°57'N - 95°48'W	12	
620	602	Rig air gun and streamer and COMEX subbottom profiling to WR19	041	10		3	30
630	605	Arrive WR19 and slow to 5 kt; deploy sonobuoy COMEX WR run	041	5	9°34'N - 95°14'W	4	20
640	609	FINEX WR run and resume 10 kt SOA and transit to WR20	041	10	9°49'N - 95°14'W	2	20
650	611	Arrive WR20 and slow to 5 kt; deploy sonobuoy and COMEX WR run	041	5	9°49'N - 95°01'W	4	20
660	615	FINEX WR run and resume to 10 kt SOA and transit to WR21	041	10	10°05'N - 95°48'W	2	20
670	617	Arrive WR21 and slow to 5 kt; deploy sonobuoy COMEX WR run	041	5	10°19'N - 94°35'W	4	20
680	621	FINEX WR run and resume 10 kt SOA and transit to WR22	041	10	10°34'N - 94°22'W	2	20
690	623	Arrive WR22 and slow to 5 kt; deploy sonobuoy and COMEX WR run	041	5	10°49'N - 94°09'W	4	20
700	627	FINEX WR run and resume 10 kt and transit to Site A	041	10	11°04'N - 93°56'W	4	37

TABLE V-7. SUS VESSEL EVENT SCHEDULE

EVENT NUMBER	EXEPCISE TIME HOURS	EVENT DESCRIPTION	COURSE	SOA	POSITION	TIME ALLOWED	DISTANCE
710	631	Arrive Site A. Retrieve air gun and streamer			11°31'N - 93°32'W	1	
720	632	Retrieve ACODAC				12	
730	644	Transit to Acapulco	AR	10		50	500
740	694	Arrive Acapulco. In port				48	
750	742	Depart Acapulco and transit to San Diego	AR	10		144	1420
760	886	Arrive NUC dock - San Diego					

TABLE V-8. CW VESSEL EVENT SCHEDULE

EVENT NUMBER	EXERCISE TIME HOURS	EVENT DESCRIPTION	COURSE	SOA	POSITION	TIME ALLOWED	DISTANCE
11	120	Depart San Diego and transit to Site 2	AR	10		204	2040
211	324	Arrive Site 2 and rig sources				24	
252	348	COMEX CW TOW from Site 2 to Site 1	041	5	07°27'N - 97°6'W	98	491
431	446	FINEX CW TOW at Site 1 and retrieve sources	-	-	13°36'N - 91°39'W	6	
451	452	Transit to Balboa, Panama	AR	10		69	690
491	521	Arrive Balboa, Panama					

TABLE V-8

XBT and STD Schedule

SITE	DISTANCE (nm)	COURSE	T-5	T-7	STD
2	0	----	✓		
	30	041	✓		
	50		✓		
	70		✓		
	100		✓		
2	120	041	✓	✓	✓
B	0				
B	20	090	✓		
	47		✓		
	62		✓		
	87		✓		
	112		✓		
	127		✓		
	157		✓		
B	163	090			
P	0				
	22	350	✓		
	43		✓		
	63		✓		
	94		✓		
	109		✓		
	134		✓		
P	155	350			
A	0				
A	0		✓	✓	✓
A	30	041	✓		
	45		✓		

TABLE V-9, cont.

SITE	DISTANCE (nm)	COURSE	T-5	T-7	STD
	70		✓		
	85		✓		
	110		✓		
	125		✓		
	150		✓		
A	168	041	✓		
1	0		✓	✓	✓
1	10	258	✓		
	40		✓		
	70		✓		
	100		✓		
1	130	258	✓		
3	0				
	30	170	✓		
	60		✓		
	85		✓		
3	100	170	✓		
A	0				
	15	221	✓		
A	20	221			
WR13	0				
WR13	10	239	✓		
	40		✓		
	70		✓		
	100		✓		
	130		✓		
	160		✓		
	190		✓		
	220		✓		
	250		✓		
WR13	266	239	✓		
4	0				

TABLE V-9, cont.

SITE	DISTANCE (nm)	COURSE	T-5	T-7	STD
4	0		✓	✓	✓
	10	165	✓		
	41		✓		
	72		✓		
4	92	165			
2	0				
2	0		✓	✓	✓
2	10	041	✓		
	40		✓		
	70		✓		
	100		✓		
	130		✓		
	160		✓		
	190		✓		
2	222	041	✓		
C	0				
	20		✓		
	50		✓		
	80		✓		
	110		✓		
	140		✓		
	170		✓		
	200		✓		
	230		✓		
	260		✓		
C	269	041	✓		
1	0				
1	10	258	✓		
	40		✓		

TABLE V-9, cont.

SITE	DISTANCE (nm)	COURSE	T-5	T-7	STD
	70		✓		
	100		✓		
1	130	258	✓	✓	✓
3	0				
3	30	170	✓		
	60		✓		
	90		✓		
	120		✓		
	150		✓		
	180		✓		
	210		✓		
	240		✓		
3	257	170			
P	0				
P	0		✓	✓	✓
P	10	270	✓		
	40		✓		
	70		✓		
	100		✓		
	130		✓		
	160		✓		
	190		✓		
	220		✓		
	250		✓		
P	266	270			
A	0				
	30	090	✓		
	45		✓		
	72		✓		
	92		✓		
	102	090			
B	0				

TABLE V-9, cont.

SITE	DISTANCE (nm)	COURSE	T-5	T-7	STD
	5	041	✓		
	20	041	✓		
B	0	221	✓		
	10	041	✓		
	35		✓		
	50		✓		
	75		✓		
	90		✓		
	115		✓		
	130		✓		
	155		✓		
	170		✓		
	200		✓		
B	207	041			
A	0				
A	0		✓		

Total -- T-5 -- 114
T-7 -- 7
STD -- 7

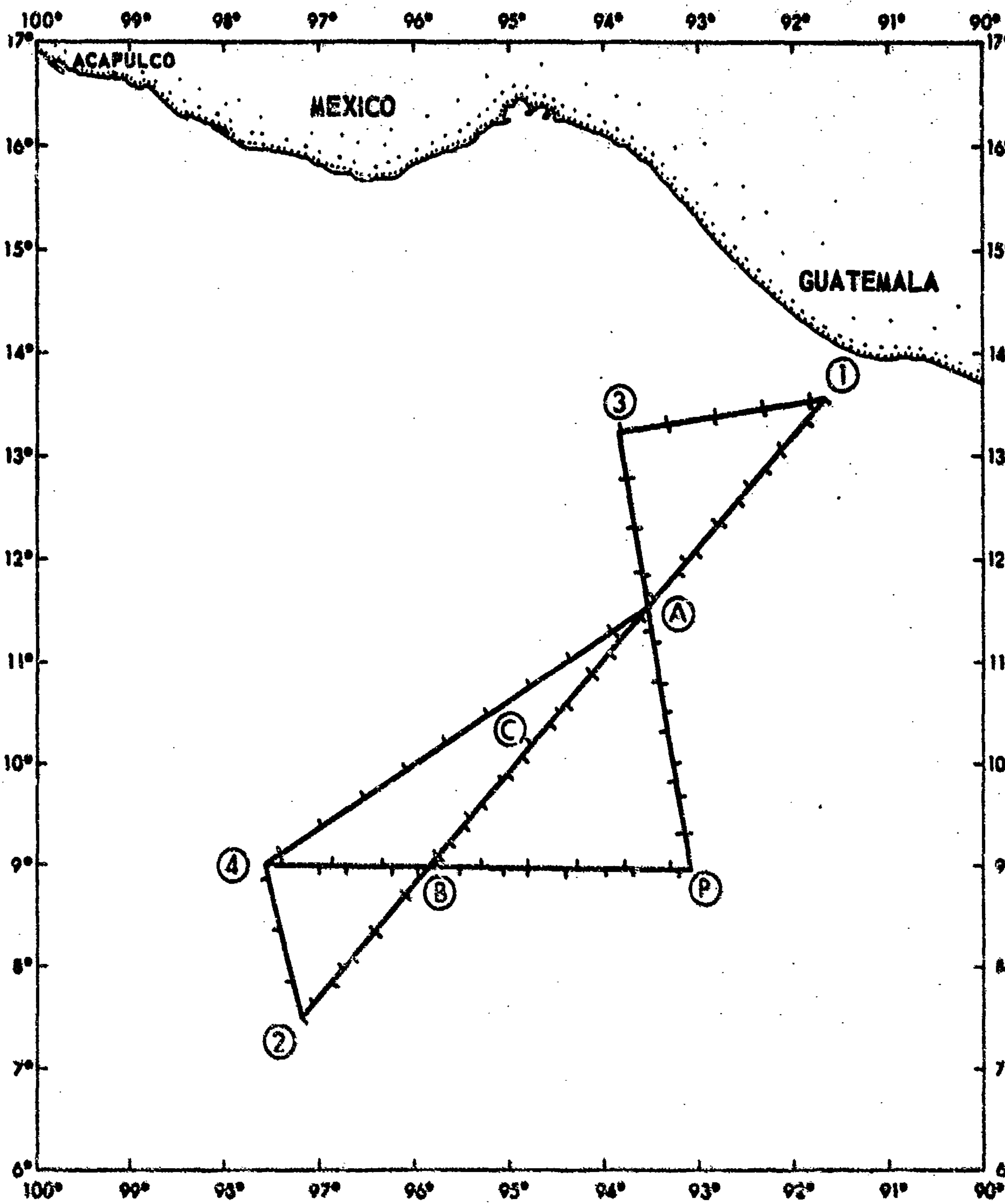

FIGURE V-7
XBT (T-5 AND T-7) AND STD TRACK DETAIL
BOTTOM INTERACTION EXPERIMENT

ARL - UT
AS-75-2302
LDH - DR
11-12-75

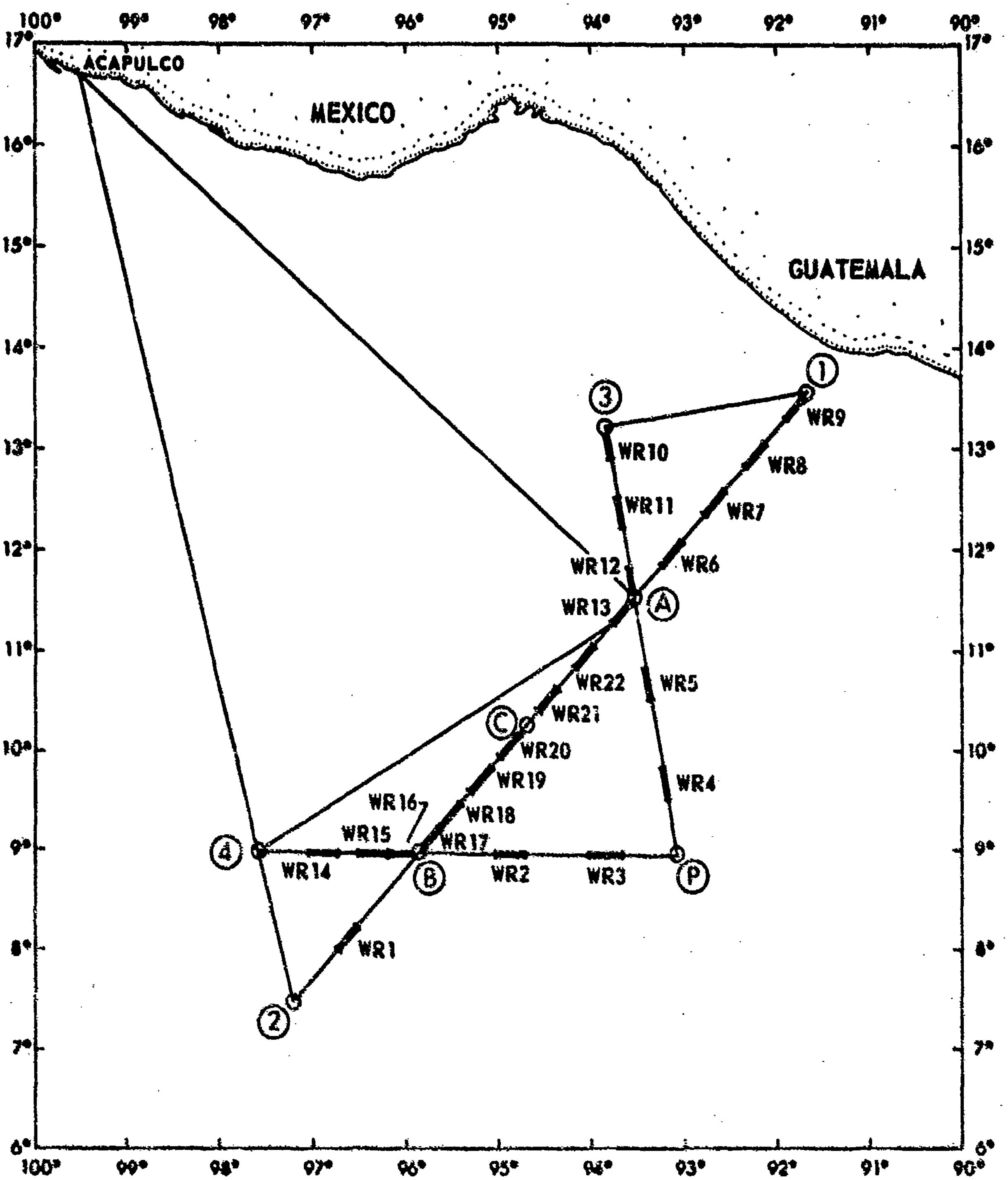

FIGURE V-8
WIDE ANGLE REFLECTION MEASUREMENTS TRACK DETAIL
BOTTOM INTERACTION EXPERIMENT

ARL - UT
AS-75-220
LDH - DR
11-12-75

VI. DATA ANALYSIS AND INTERPRETATION

The data acquired during this experiment will provide a base for studying the long range propagation of sound in a bottom limited environment. The primary objective of the data analysis and interpretation will be to understand and describe the effects of bottom interaction on the measured propagation characteristics.

Techniques developed by the Naval Oceanographic Office (NOO) to calculate bottom loss versus grazing angles for single bounce situations will be extended to study multiple bounce data. These techniques will be augmented by procedures developed at ARL/UT to extract basic information on the detailed propagation paths from source to receiver for the long range data. Together with the utilization of current propagation models, these data processing and analysis tools will provide the insight from the measurements to allow for a more applicable model of bottom interaction in propagation calculations. Analysis/interpretation of the seismic profiling data and the wide angle reflection data will be required to support the primary experiment objective.

To gain a full description of the environmental acoustics of the area, the CW data will be analyzed for propagation loss, the ambient noise data will be studied for the effects of the bottom limited conditions, bathymetry, and limited shipping distribution. The analysis of the environmental data will provide support to all of the interpretation.

<u>SUS Data Analysis</u>

The receiver location and tracks for the SUS deployments are shown in Fig. V-1. The track detail and deployment schedule for the SUS events are provided in Fig. V-5. Figure V-6 shows the sound velocity structure typical of the area and the receiver allocation in the water column.

Figure IV-4 shows the estimated bottom reflection angles versus range of several multipath arrivals for only one of the source/receiver combinations to be used. From these estimates, it is seen that as range increases the bottom reflection angles of the primary (first few) arrivals constituting the received signal are spread over a smaller range of angles. Beyond approximately 100 nm, most of the received signal will have encountered the bottom at angles less than 10°. Only at short ranges are the multipath arrivals reflected from the bottom at steep angles.

The SUS data received at short ranges (<50 nm) will be processed by NOO with the deconvolution procedures which consist of convolving the direct arrival (or proper replica) with the received signal structure to obtain the impulse response of each arrival. Each arrival is thus delineated in time to within the resolution of the convolution process and the energy associated with each arrival can be attributed to the proper mechanisms in terms of the physical structure of the bottom.

SUS data from all ranges will be processed by ARL/UT for propagation loss using the total energy of the received signal as well as the propagation loss and bottom loss determined from individual arrivals. Of particular importance will be the comparison between the bottom loss determined at the long ranges involving many reflections and the loss determined at short ranges from one or two reflections. The frequency and energy characteristics of the individual arrivals of the received signal will form the basic processing for this analysis. Details of the SUS data processing procedures are given in Appendix E.

Ambient Noise Data Analysis

Three features combine to make the study of the ambient noise field in the experiment area particularly interesting. First, from the bottom limited environmental condition, the shipping contribution to the ambient noise is expected to be low. Second, almost all shipping in the area is concentrated along a 6 nm limit off the coastline. Considering these two features together, the ambient noise level at Site B, approximately 100 nm further from the shipping lane, is expected to be less than at Site A. A third feature results from the shipping lane along the edge of the Middle American trench. Sound reflecting from the edge of the trench may couple into the sound channel and increase the ambient level above that expected for shallow sources in water of uniform depth.

ARL/UT will process the ambient noise data from both Sites A and B. Narrowband spectra will be used to produce the 1/3 octave estimates. The data will be analyzed for frequency, depth, and site dependence to gain insight into the governing mechanisms. Details of the noise data processing techniques are given in Appendix F.

CW Data Analysis

Event 252 is a CW tow using the Vibroseis source. The sources will be deployed at depths of 60 ft and 300 ft with four frequencies in the band from 10 to 300 Hz. The sources will transmit 50 min of each hour continuously at a constant level.

ARL/UT will process the CW data for propagation loss and signal excess along with the associated ambient noise levels. Using the measured bottom loss data, and environmental data, a meaningful comparison can be made between the CW propagation loss and predicted values. Details of the CW data processing technique are given in Appendix F.

Environmental Data Analysis

NOO will process the environmental data and reconstruct the source-to-receiver tracks/ranges. These data will be furnished to the participants in the acoustics data analysis and modeling.

Source Data Analysis

A reconstruction of the time history of the source level performance of the Vibroseis CW source will be carried out by ARL/UT.

The SUS deployment analysis will be performed by NOO and provided to the participants in the SUS analysis.

The source level correction calculations will be performed by USI from the on board recordings and provided to NOO and ARL/UT.

SUS Arrival Structure - ARL/UT

The task of measuring propagation loss, and bottom loss for individual arrivals from a large number of shots over a long range interval, requires expansion of the routine SUS processing. There will be three hydrophones at each receiver depth, to provide a large dynamic range for the recorded data; when required different portions of the same shot will be analyzed from different recording channels. Multipath arrival times, bottom angles, and propagation loss assuming perfectly reflecting bottoms will be computed and used to guide the signal processing. This will require good navigation, source, and environmental data prior to the time the acoustic data is processed. The ancillary data will be used by programs such as the eigenray program, described in Appendix B, and by propagation modeling programs such as FACT.

Figure VI-1 demonstrates the type of analysis which will be performed upon the shot arrivals. Also indicated are the bottom reflection angles for each arrival. If for example the spectral energy in the third arrival were integrated from 45 to 56 Hz, the results would be the energy in a 1/3 octave band centered at 50 Hz for signals bouncing ten times

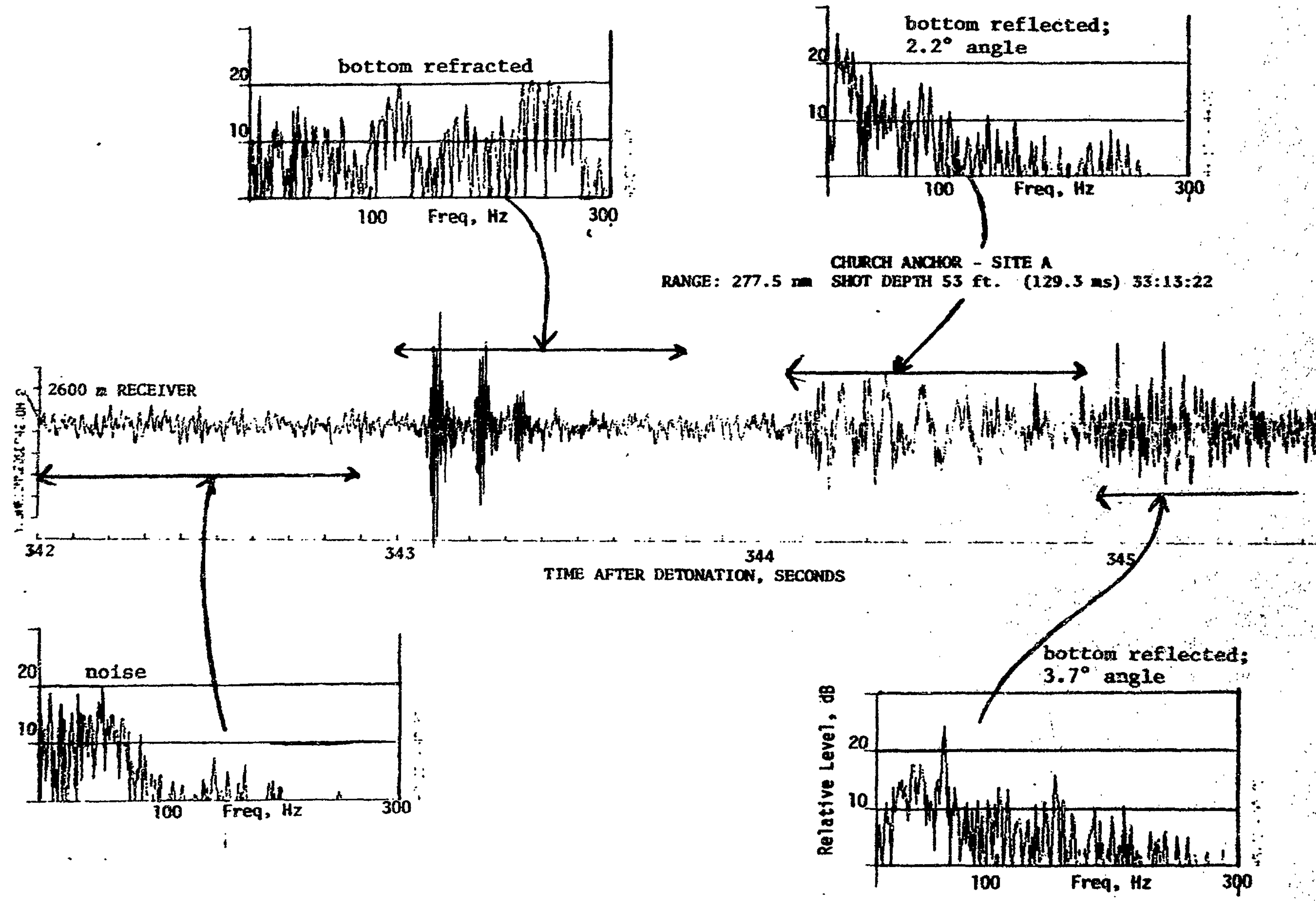

FIGURE VI-1
EXAMPLE OF INDIVIDUAL MULTIPATH STRUCTURE AND SPECTRA, SHALLOW SUS

AS-75-1164

from the bottom at 3.7° grazing angle. Subtracting the source energy in that same band yields the measured propagation loss for that path. Next, the propagation loss assuming perfectly reflecting bottom along that path is to be computed. The difference between these two values is then ten times the bottom loss at 50 Hz and 3.7° angle.

SUS Deconvolution - NOO

Acoustic bottom reflectivity data will be collected near ACODAC buoys along several tracks over a range sufficient to include up to three bottom bounces. The data will be digitized for digital deconvolution processing and 1/3 octave bottom loss computations. A geometry consisting of SUS charges at 244 m and hydrophones at 30 and 1000 m above the bottom and at 1000 m depth will be utilized. Over a relatively smooth bottom, this geometry permits the separation in time of a single bottom return from its surface reflections. As an aid to the deconvolution processing, direct signals will be recorded on the ACODAC hydrophones as well as the listening ship's 3.5 kHz profiler transducer. These direct signals permit precise measurement of bubble pulse periods and hence, through a synthetic deconvolution procedure, the source level spectrum is adjusted for the small but important variations in detonation depths. More importantly, the deconvolution removes bubble pulses from bottom reflected traces. The resulting impulse responses achieve near optimum resolution by pulse compression. It should also be possible by "deghosting" filtering to properly remove interference caused by water surface reflections overriding deeper bottom returns. This kind of processing permits direct interpretation in terms of the structure of the bottom, since reflections from individual sediment layers and refracted arrivals from sediment sound velocity gradients are easily identified. Measurement of pulse heights and positions from impulse responses leads to estimates of sediment parameters such as sound velocity and velocity gradient, density, and attenuation. These parameters integrated with geological knowledge of the bottom aid in understanding the acoustic - ocean bottom interaction. An example of a measured source signal is shown as the unprocessed trace in Fig. VI-2. The deconvolved trace shown in the figure is the effective source signal after processing and is a good representation of an ideal spike signal. Bottom returned signals corresponding to both of these source signals are also shown in Fig. VI-2.

The processing described above requires that fast Fourier transforms of the bottom return signal and a stored direct signal be computed. The frequency response function is then computed as the quotient of the two transforms with adjustments for the bubble pulse period and water column spreading and absorption losses. The impulse response is obtained by taking an inverse Fourier transform together with a filtering operation to minimize the effects of noise. The noise filtering is based on samples of the ambient noise background. Water column losses are determined from ray trace calculations based on sound velocity and bathymetry profiles measured over the bottom loss tracks.

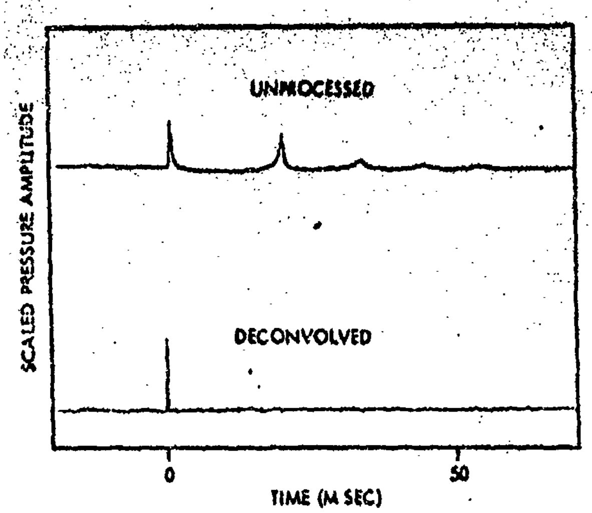

Acoustic Source Signal Before and
After Deconvolution Processing

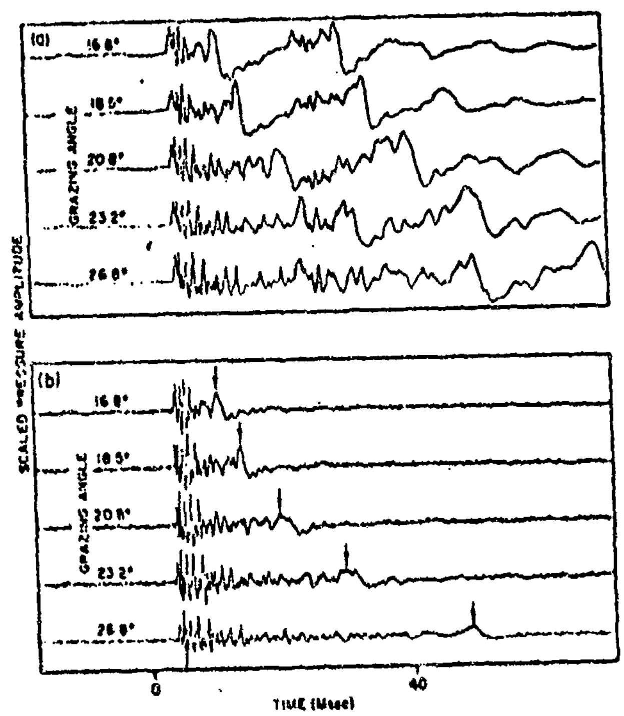

Ocean Bottom Returned Signals at Several Grazing Angles
(a) Before Processing and (b) After Deconvolution Processing.
Refracted Arrivals are Indicated by Vertical Arrows

FIGURE VI-2

APPENDIX A

PROPAGATION LOSS PREDICTIONS

This appendix presents propagation loss prediction from the FACT model for the expected range of bottom loss. Results from the two bottom loss types are given for four source depths and four receiver depths.

APPENDIX A

Bottom Loss Type 1: Approximately 5 dB for all grazing angles from 0° to 90°.

Bottom Loss Type 2: Same as A1, except that loss decreases linearly from 5 dB at 5° angle to 0 dB at 0° angle.

Figure Numbers for Bottom Loss Type 1

Source Depth ft/m	Receiver Depth ft/m			
	500/152.5	3297/1005	7520/2291.7	10702/3261.7
60/18.3	A1	A2	A3	A4
300/91.4	A5	A6	A7	A8
800/243.8	A9	A10	A11	A12
2000/609.6	A13	A14	A15	A16

Figure Numbers for Bottom Loss Type 2

Source Depth ft/m	Receiver Depth ft/m			
	500/152.4	3297/1005	7520/2291.7	10702/3261.7
60/18.3	A17	A18	A19	A20
300/91.4	A21	A22	A23	A24
800/243.8	A25	A26	A27	A28
2000/609.6	A29	A30	A31	A32

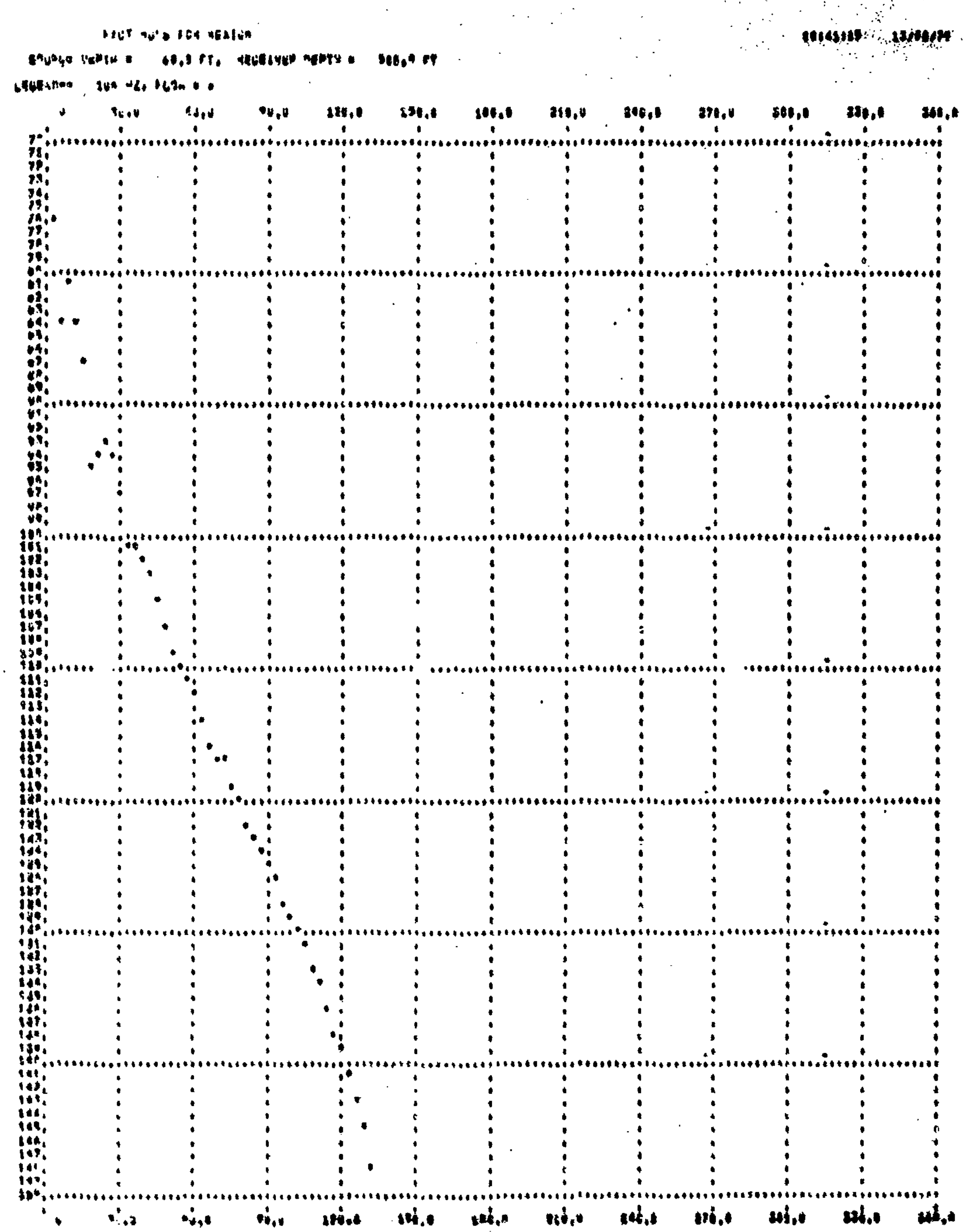

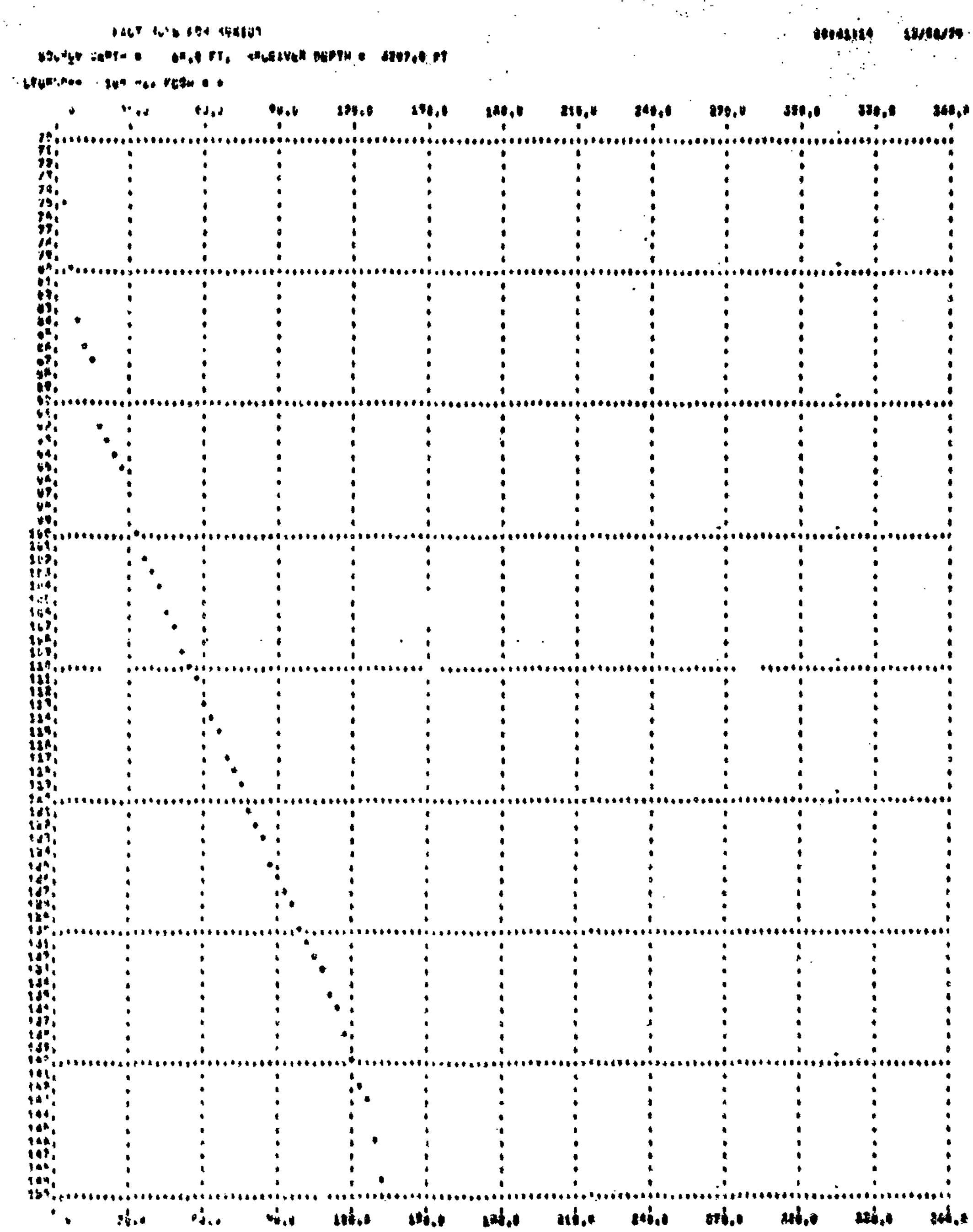

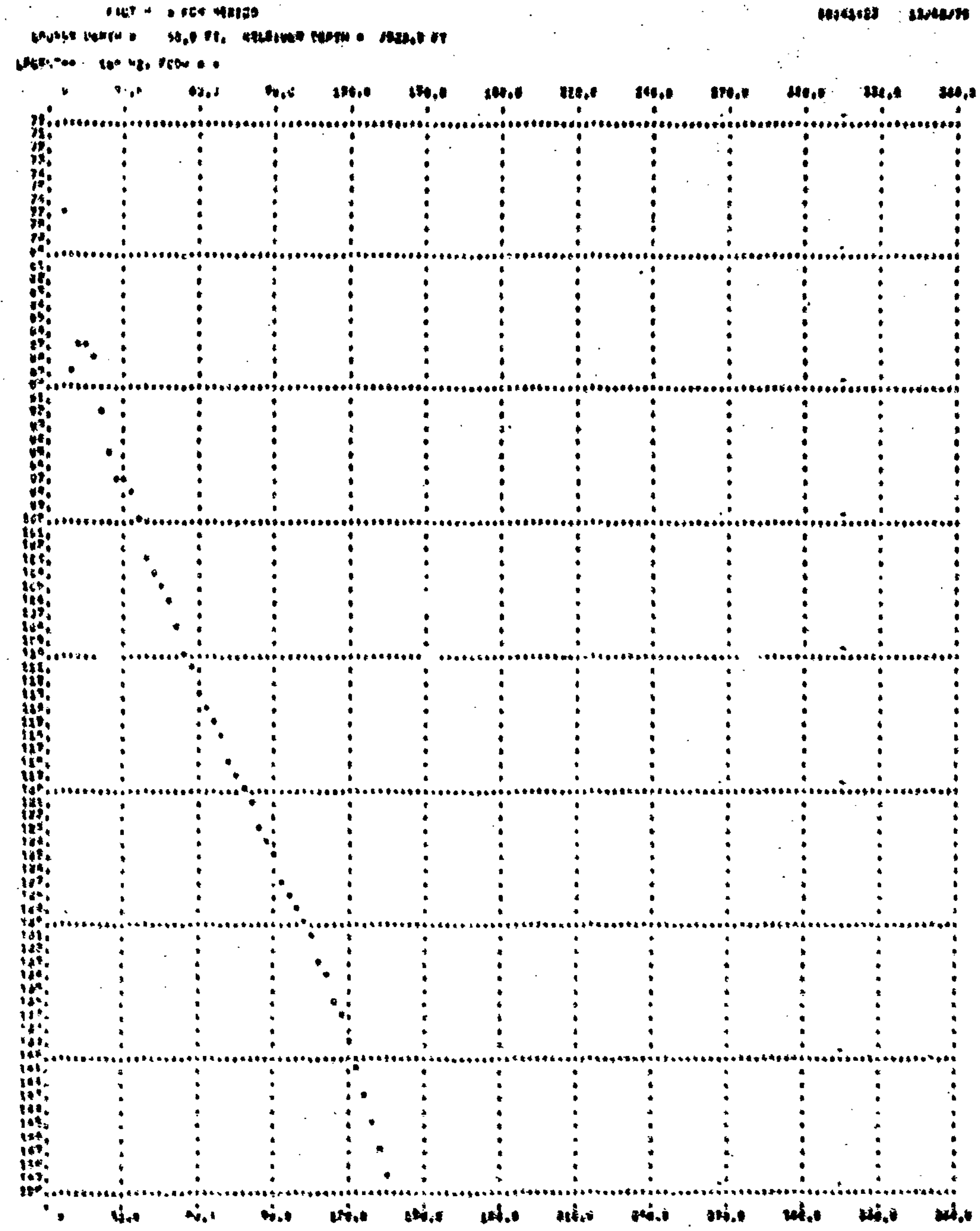

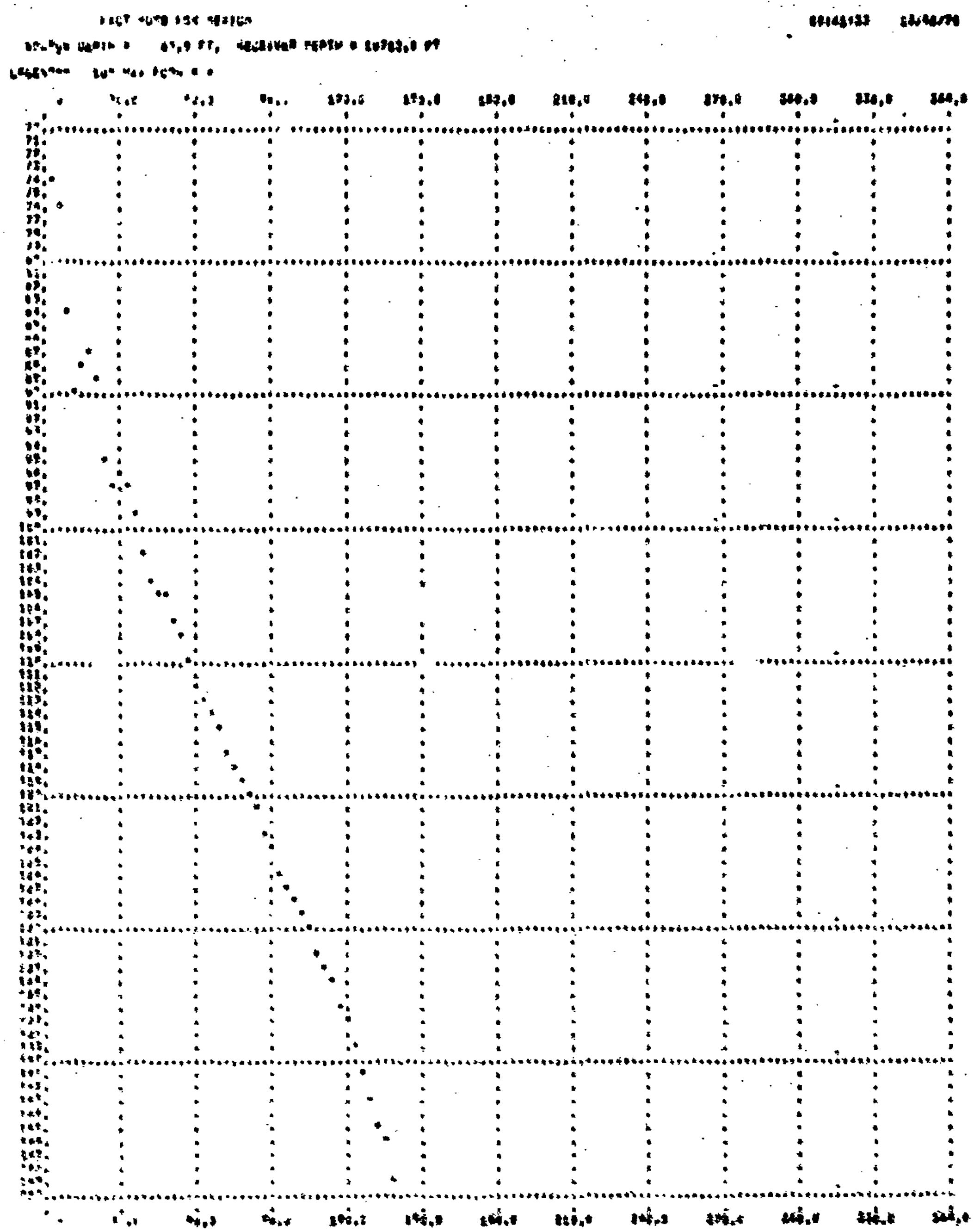

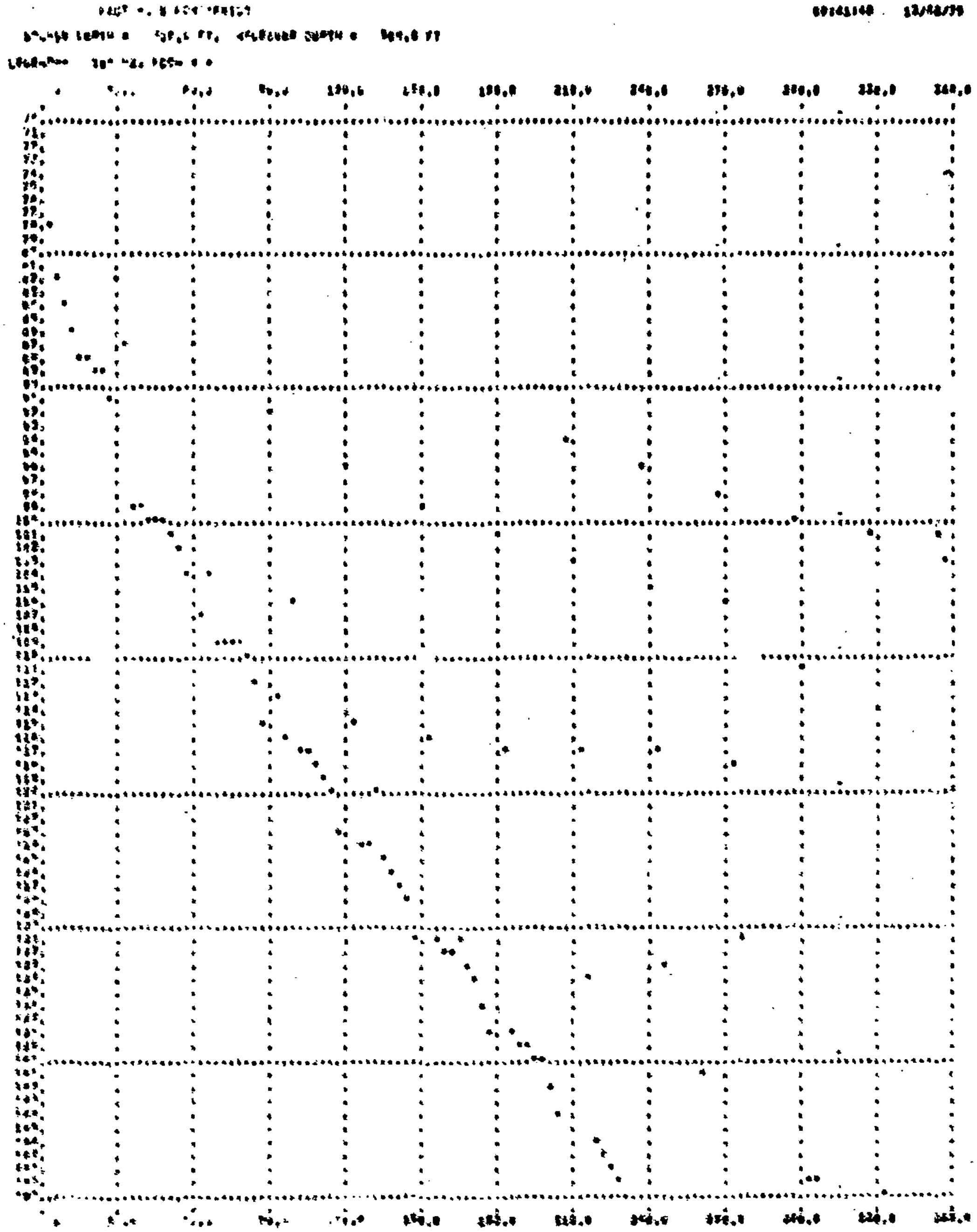

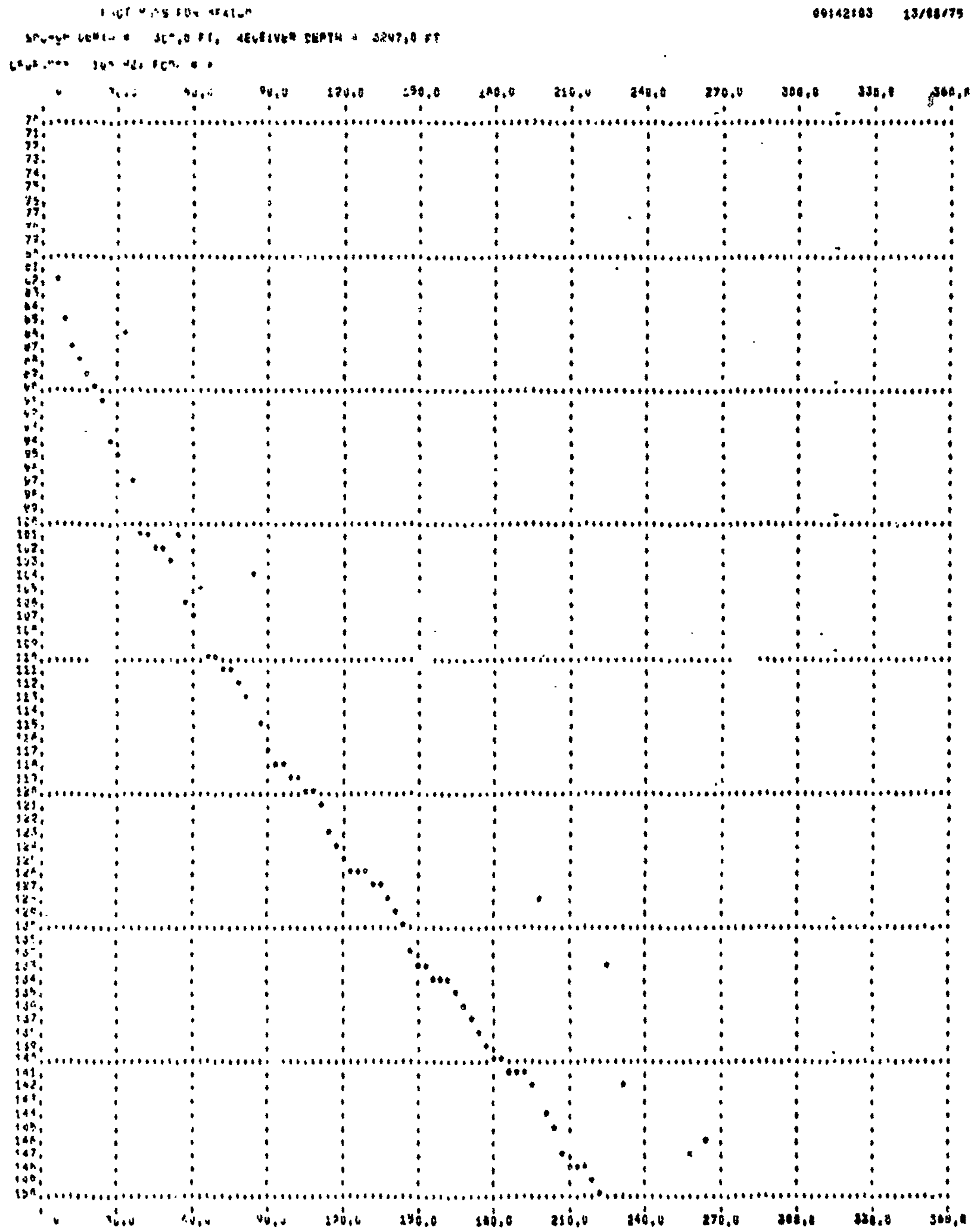
13/08/75
RECEIVER DEPTH
90.0
120.0
150.0
180.0
210.0
240.0
270.0
300.0
330.0
360.0

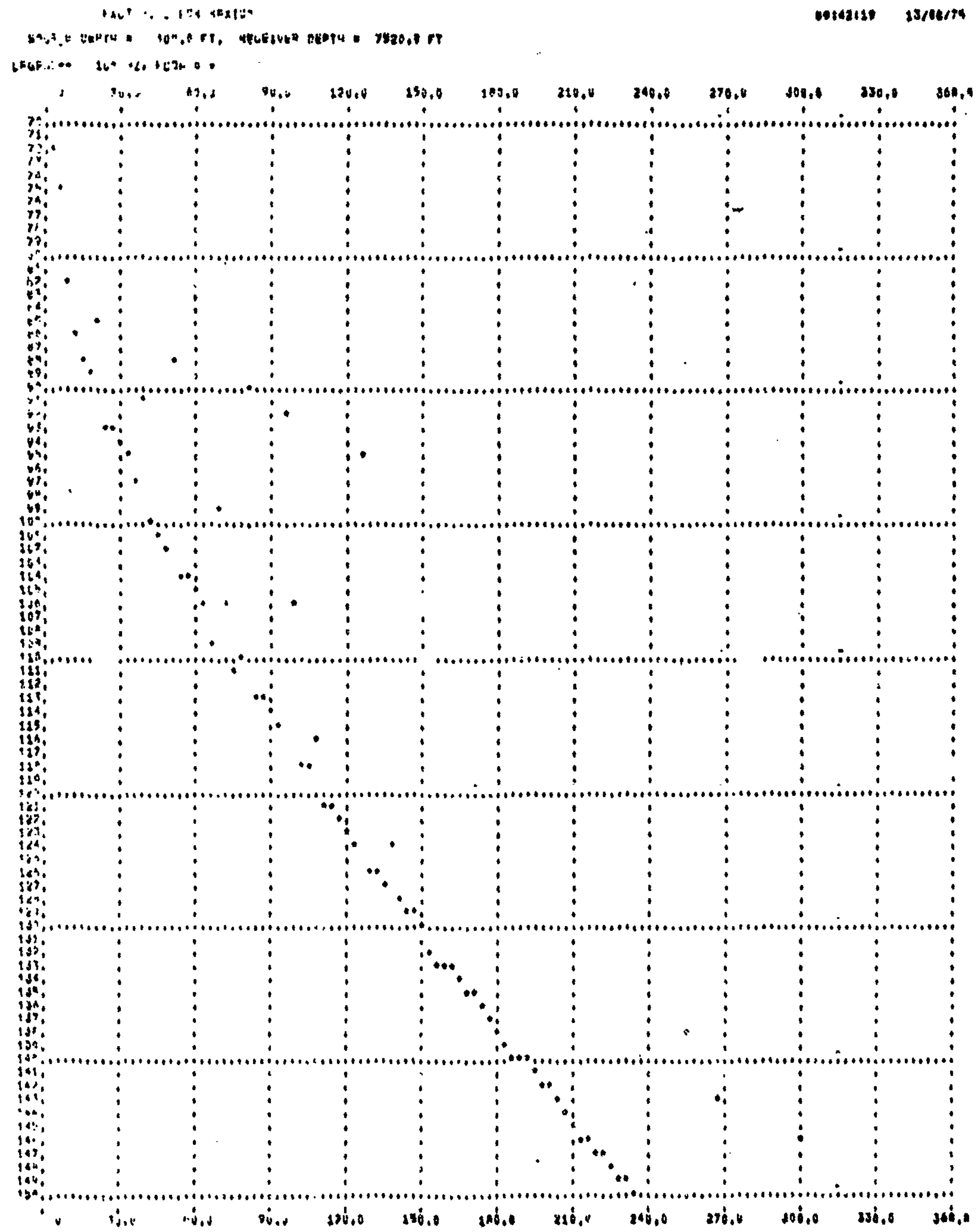
13/08/79
120,0
150,0
210,0
240,0
270,0
330,0

09142136 13/08/75

SOURCE DEPTH = 300.0 FT, RECEIVER DEPTH = 14702.0 FT

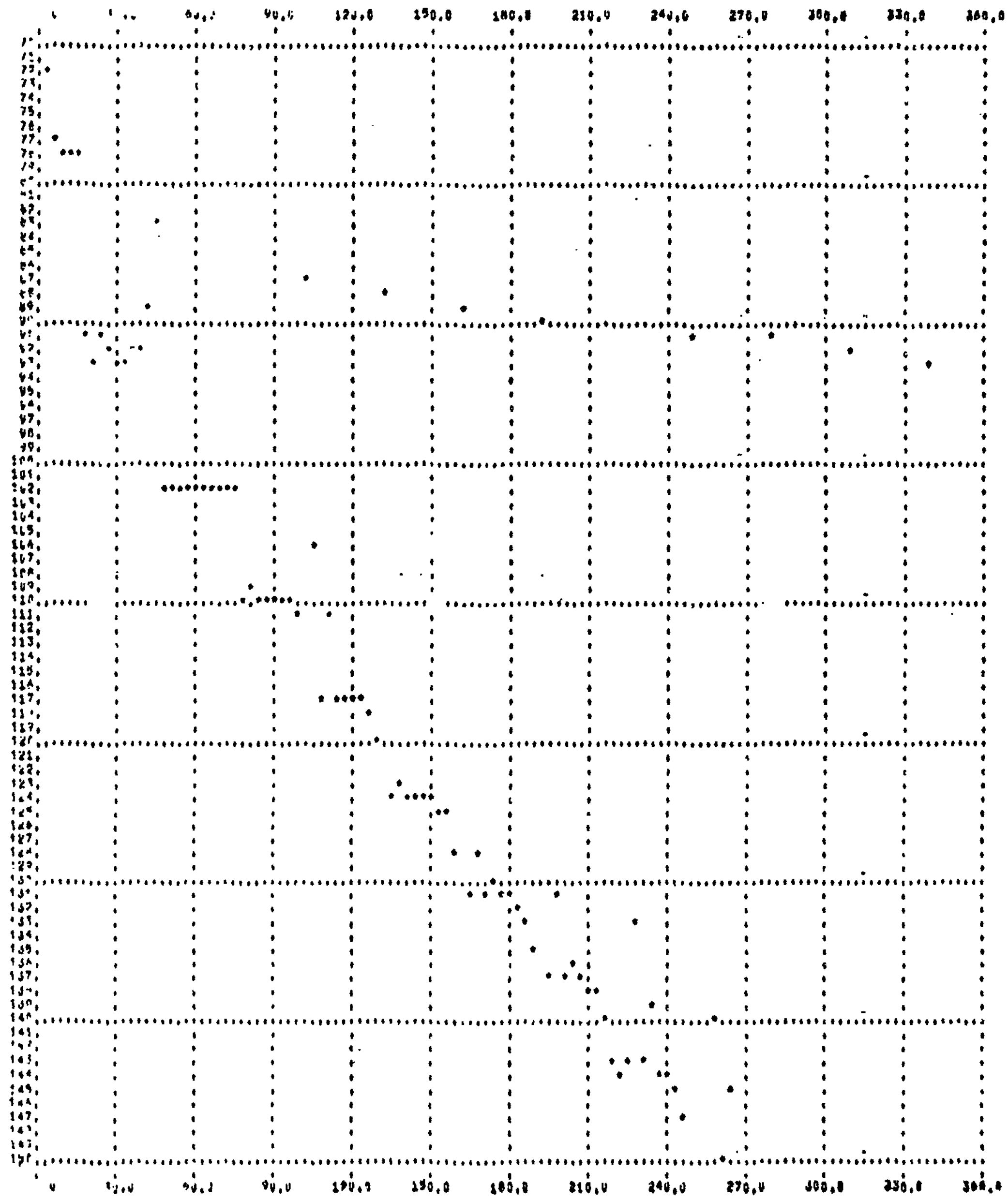

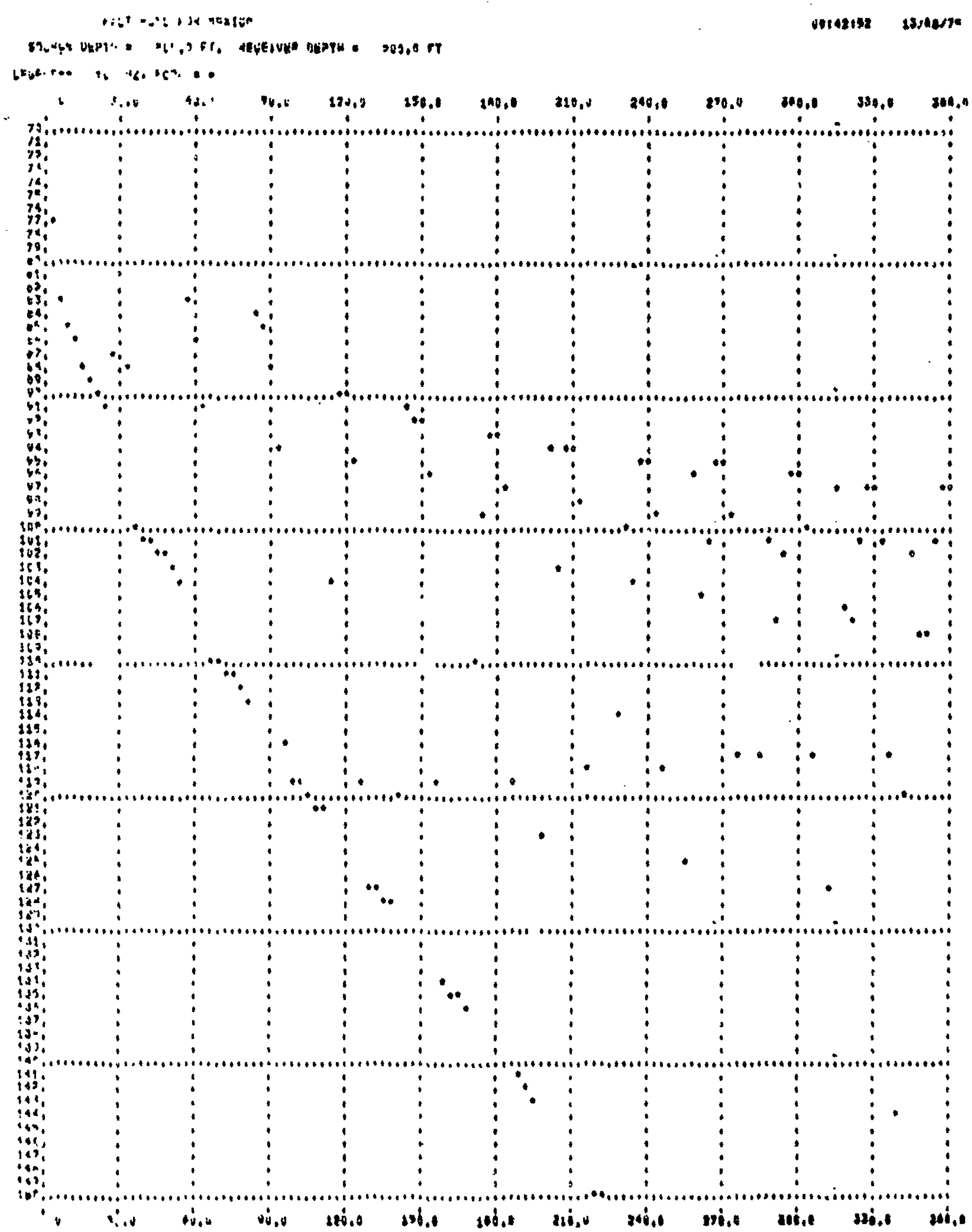

SOURCE DEPTH = ... FT, RECEIVER DEPTH = 3297.0 FT

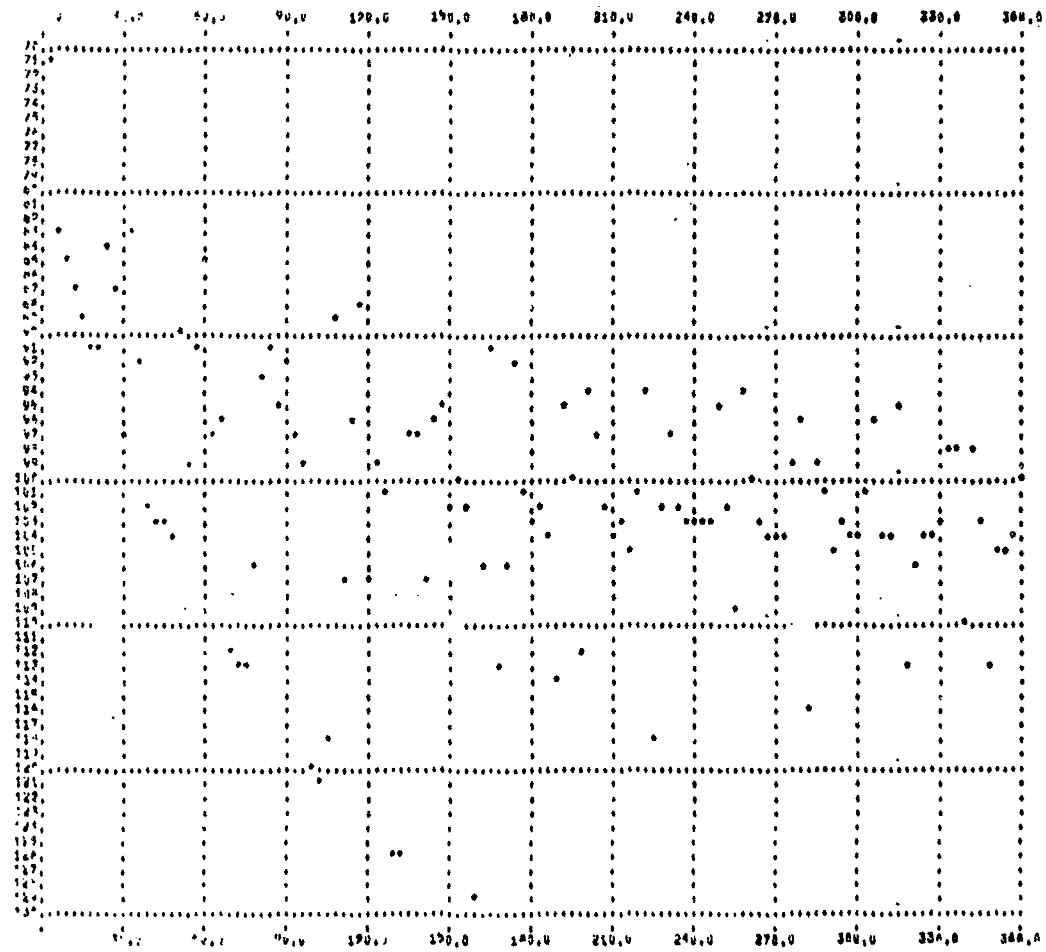

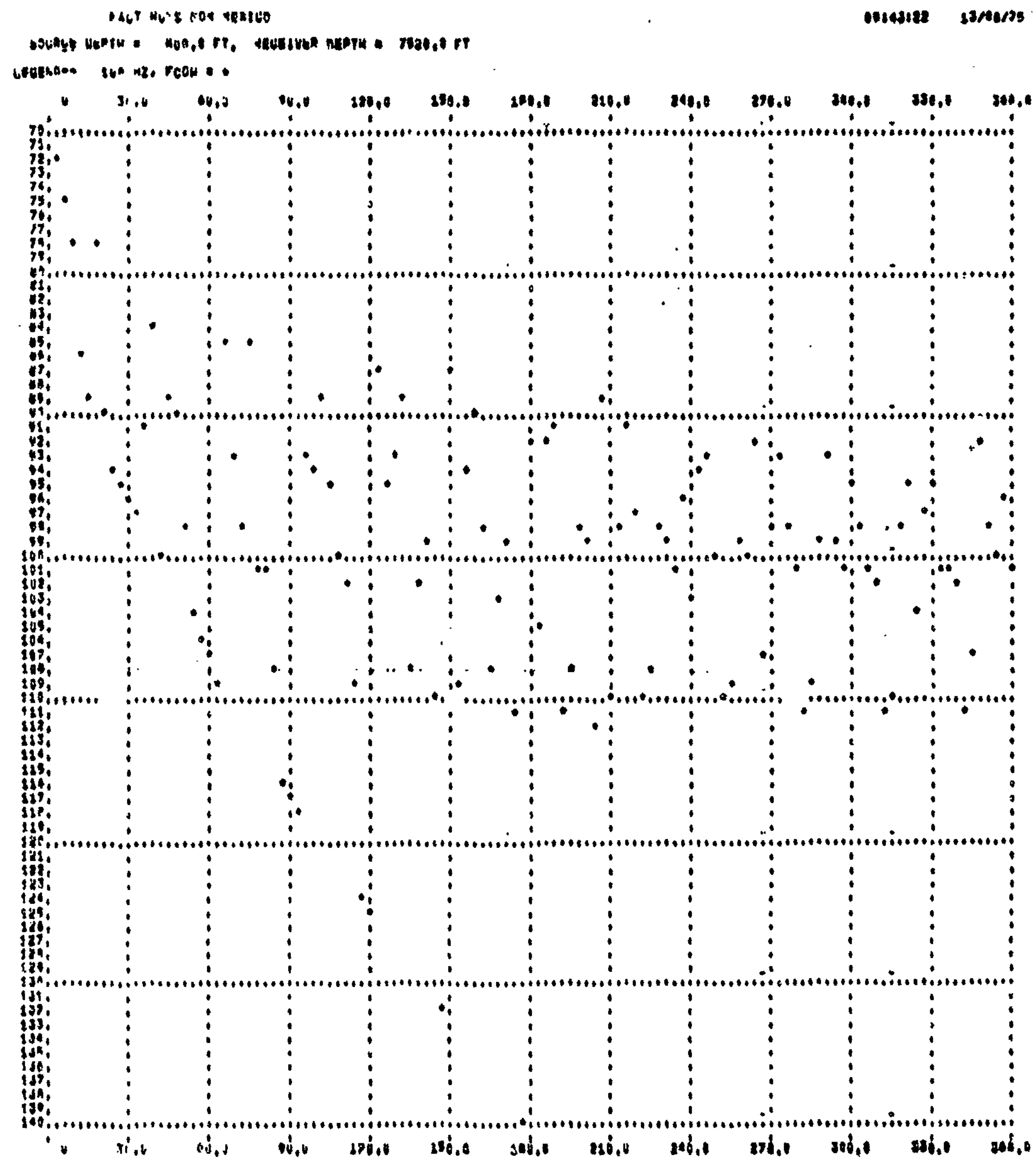

FACT RUNS FOR MEXICO [illegible]

SOURCE DEPTH = [illegible] FT, RECEIVER DEPTH = [illegible] FT

[illegible]

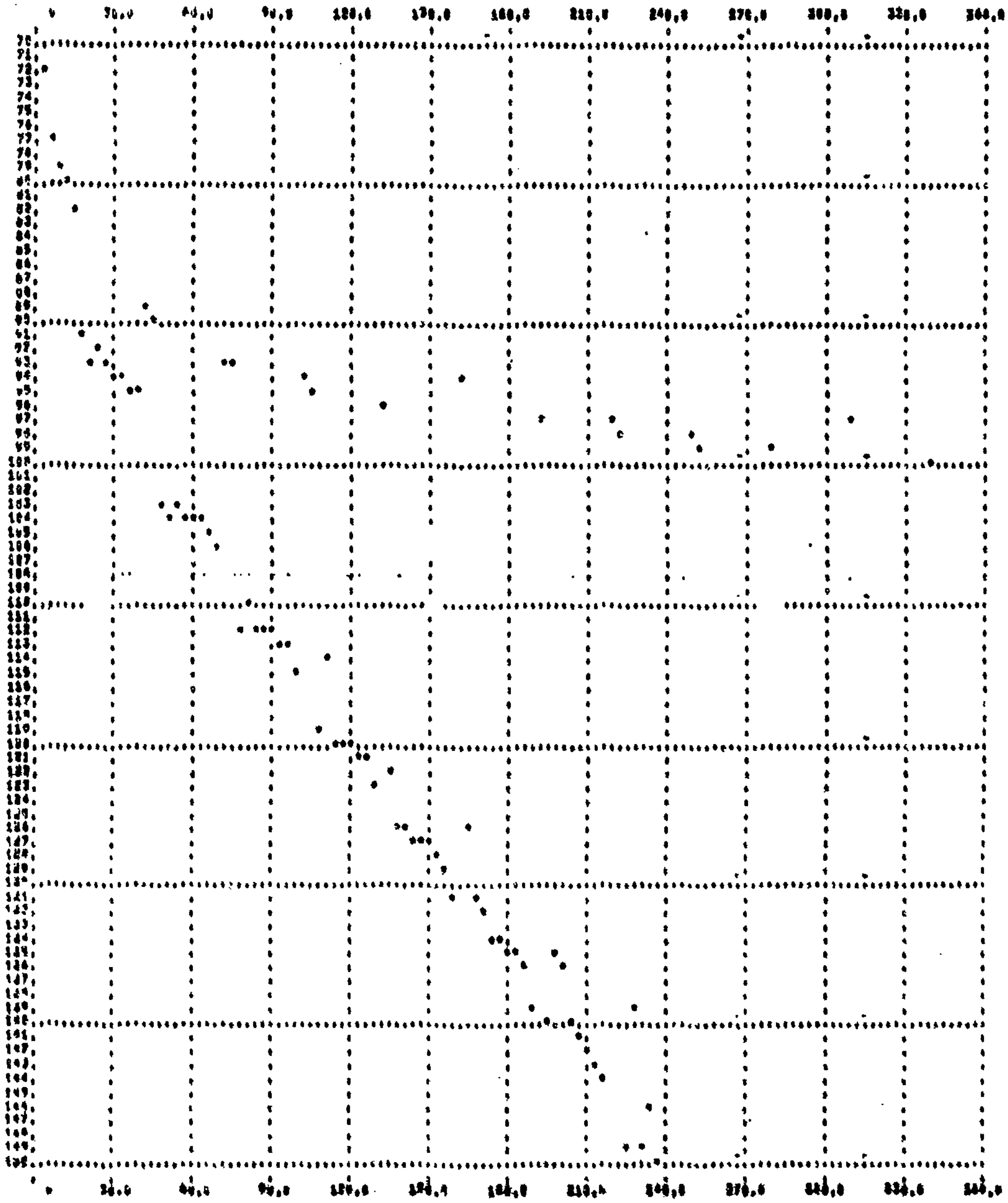

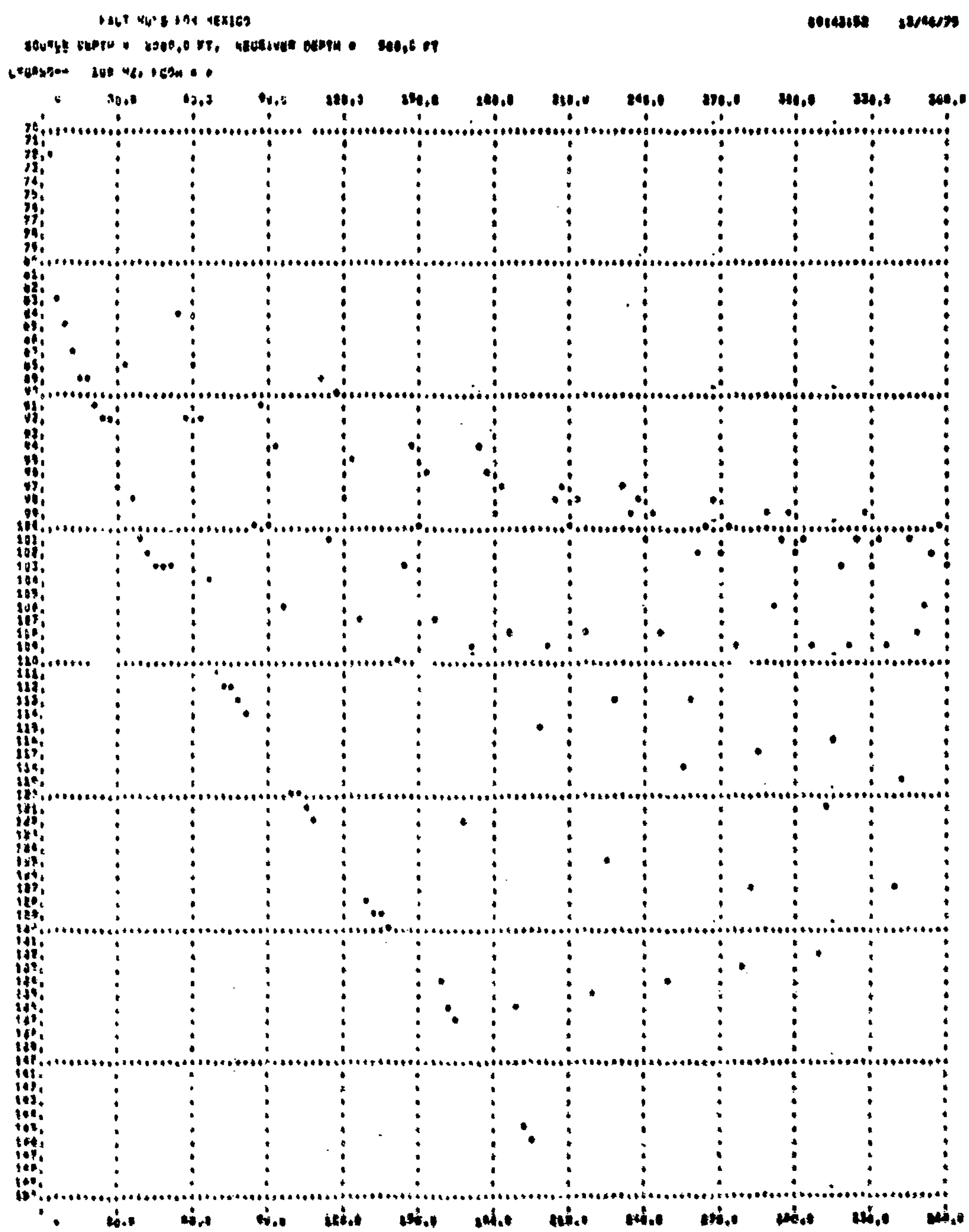

FACT RUNS FOR NEXIUS [illegible]

SOURCE DEPTH = 2088.0 FT, RECEIVER DEPTH = 3807.0 FT

LEGEND-- 128 HZ, FCOM = o

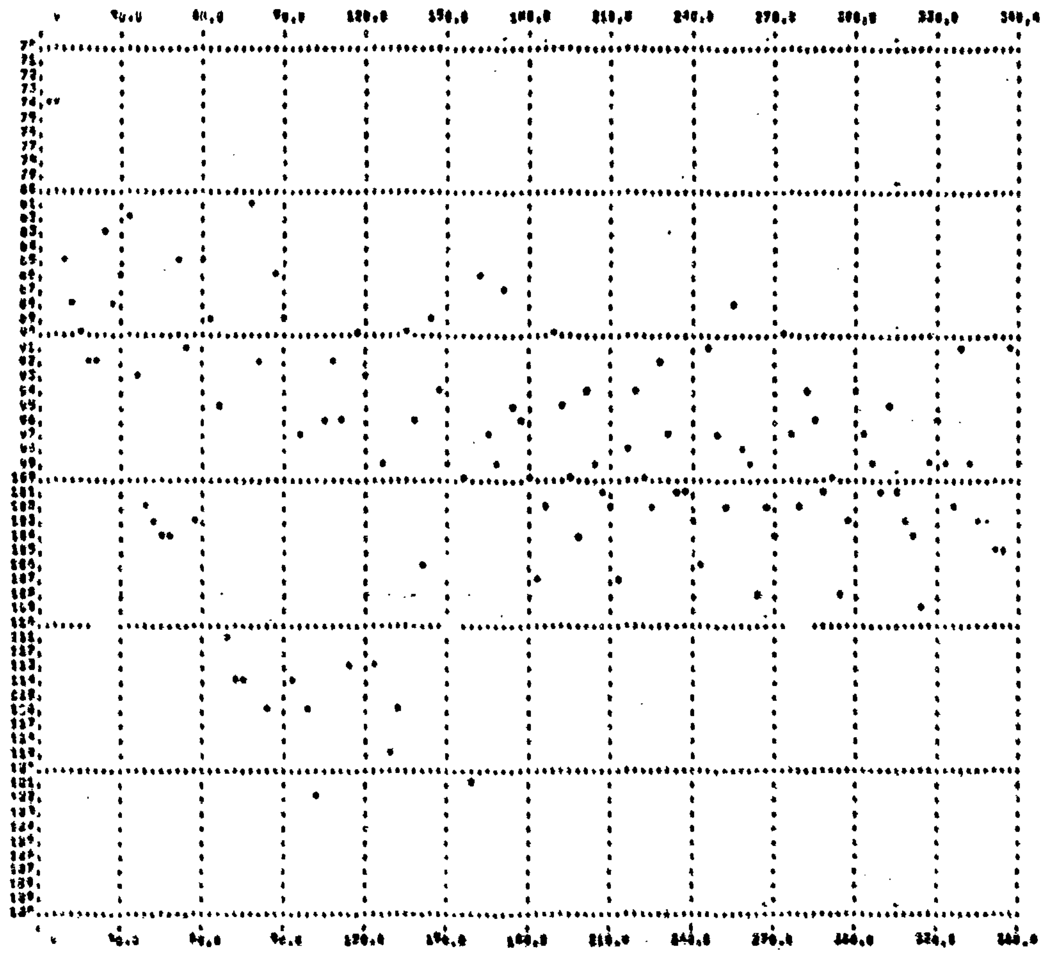

FACT RUNS FOR MEXICO [illegible]

SOURCE DEPTH = [illegible] FT, RECEIVER DEPTH = [illegible] FT

[illegible]

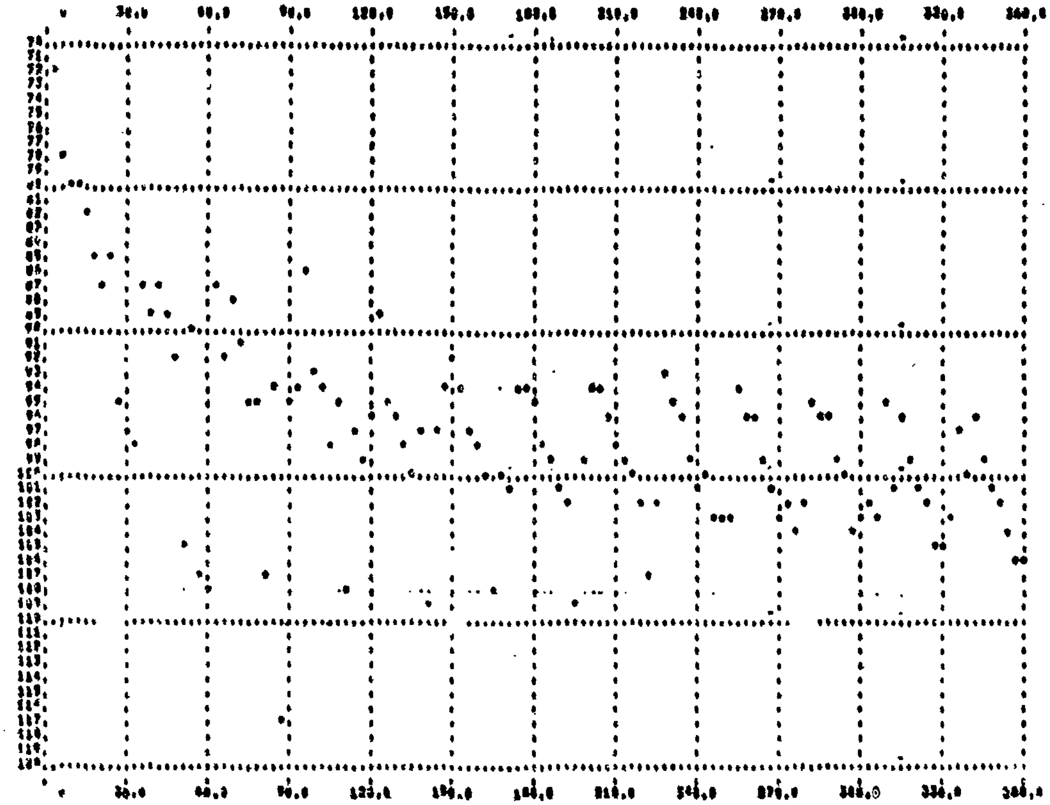

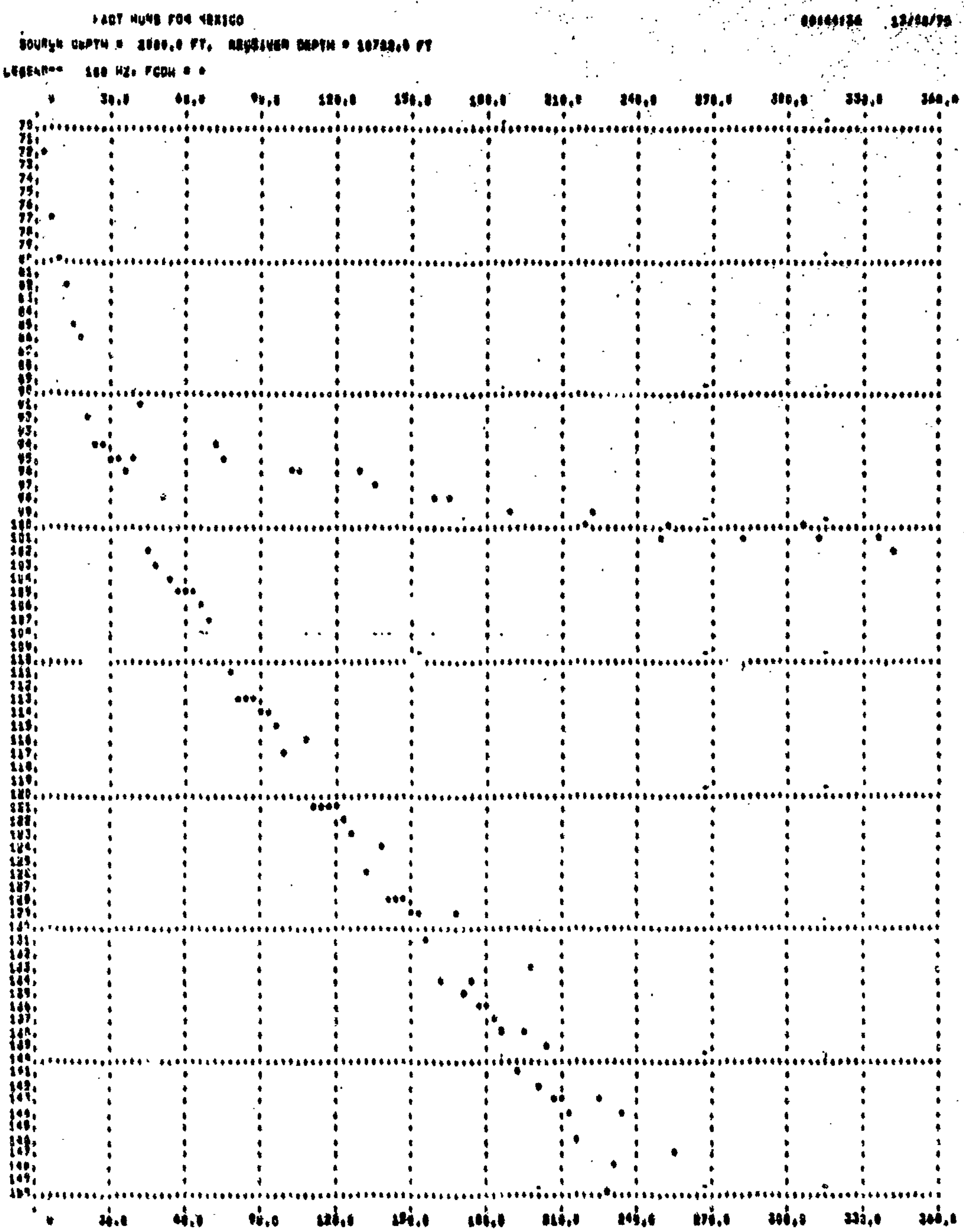

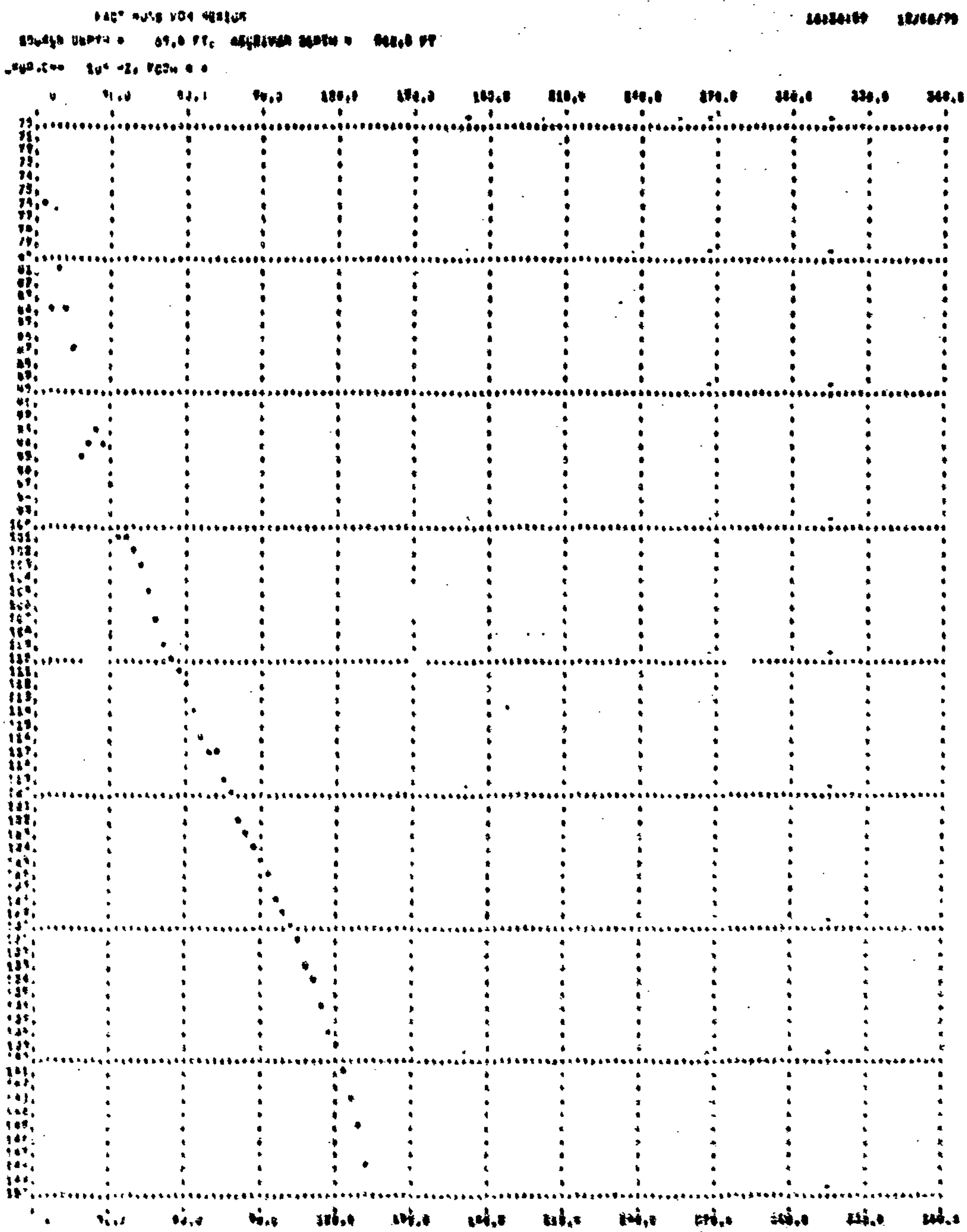

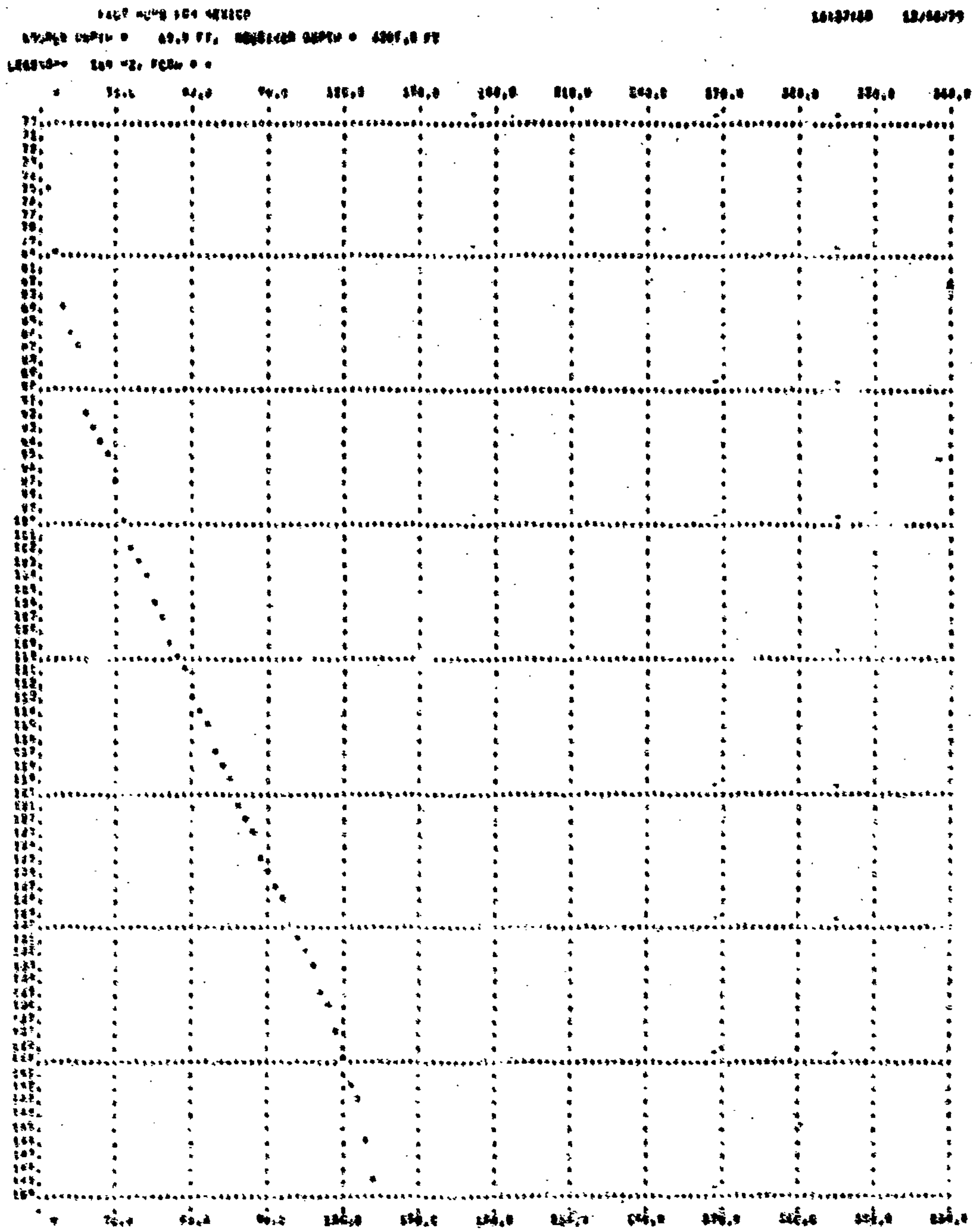

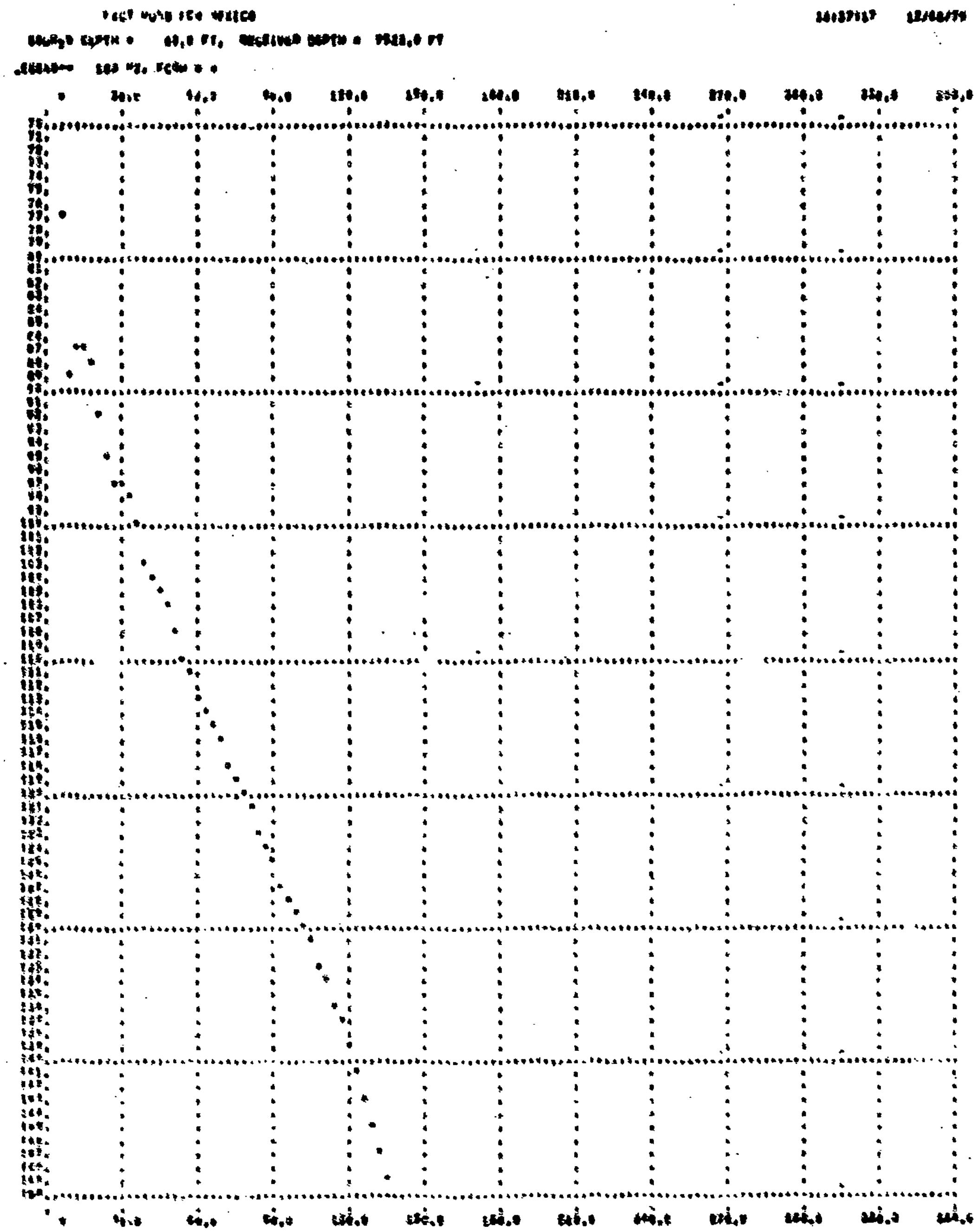

FACT HITS FOR MEXICO 16:37:27 12/08/79

SOURCE DEPTH = 68.0 FT, RECEIVER DEPTH = 10782.0 FT

LEGEND-- 100 HZ, FOO- * *

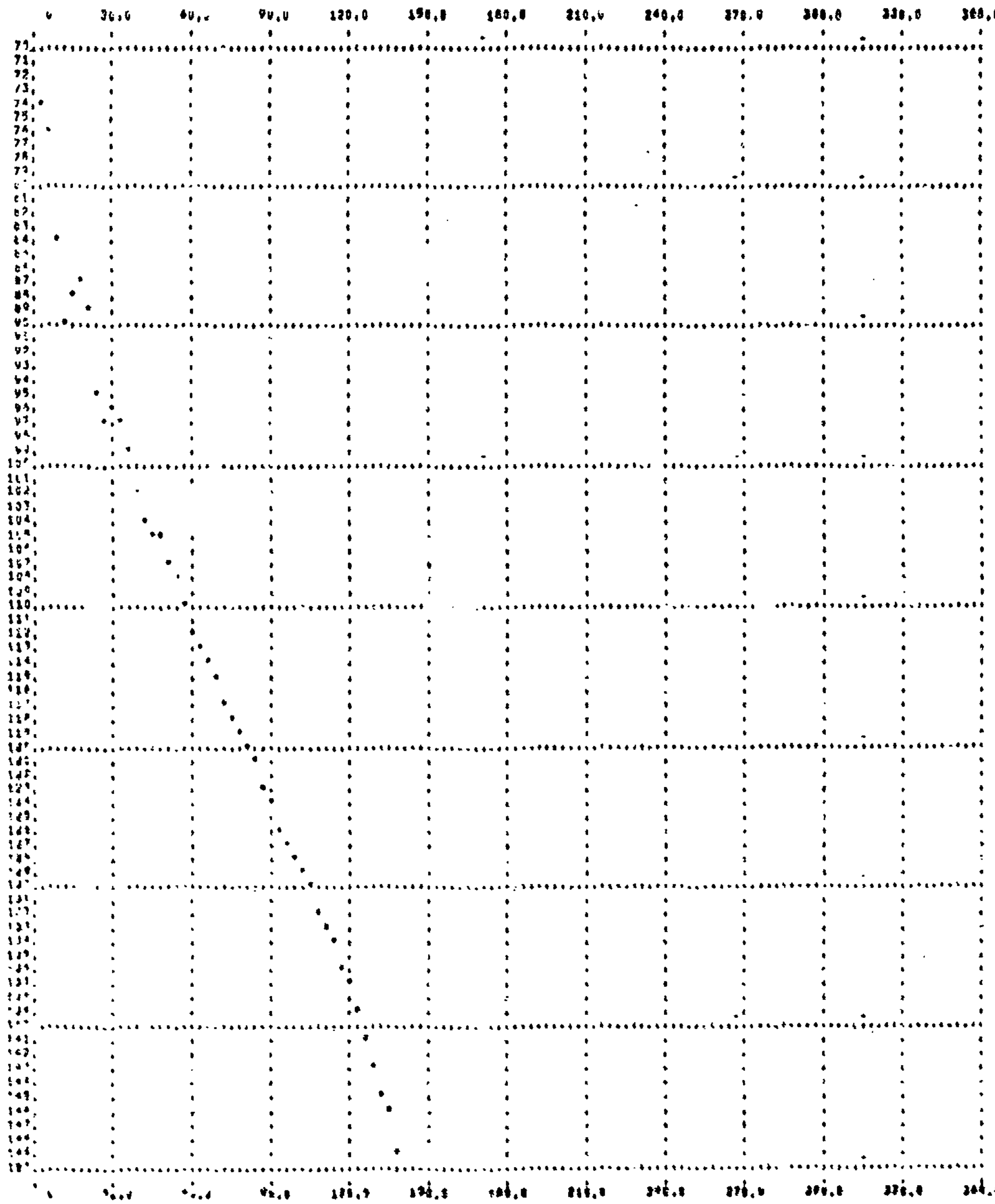

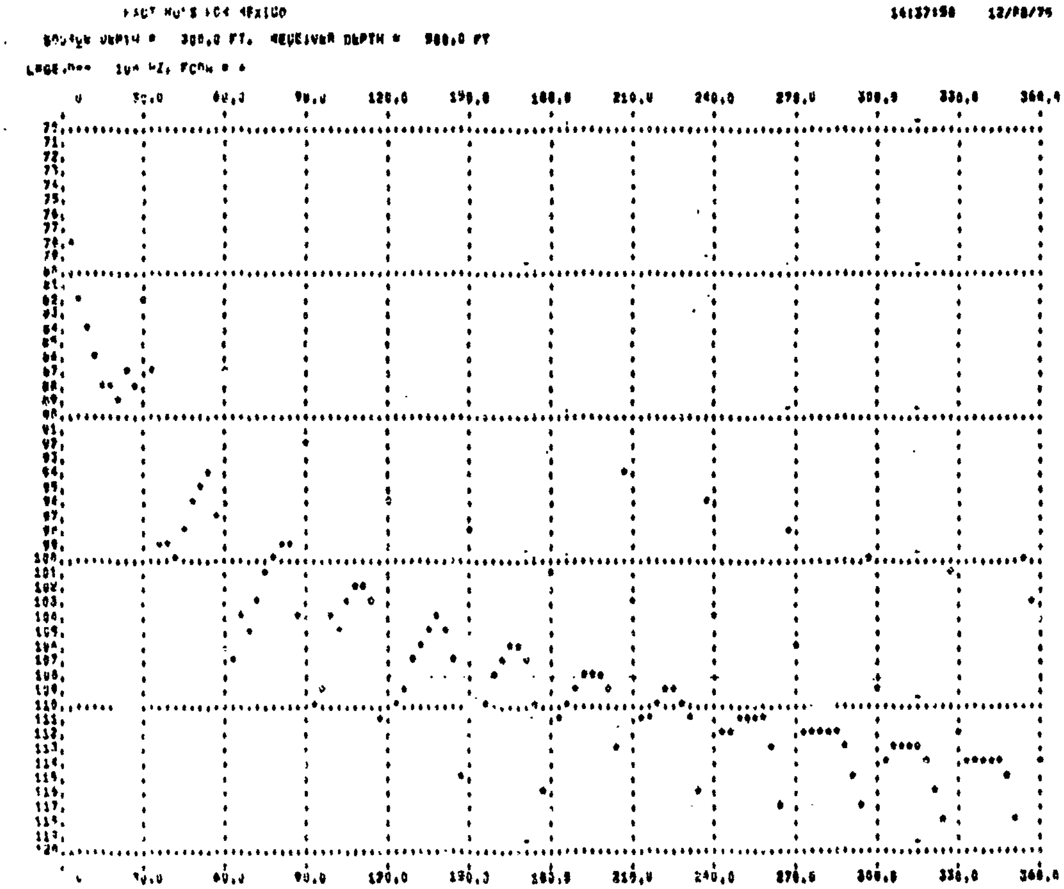
SOURCE DEPTH = 300.0 FT. RECEIVER DEPTH = 900.0 FT
0
30.0
60.0
90.0
120.0
150.0
180.0
210.0
240.0
270.0
300.0
330.0
360.0

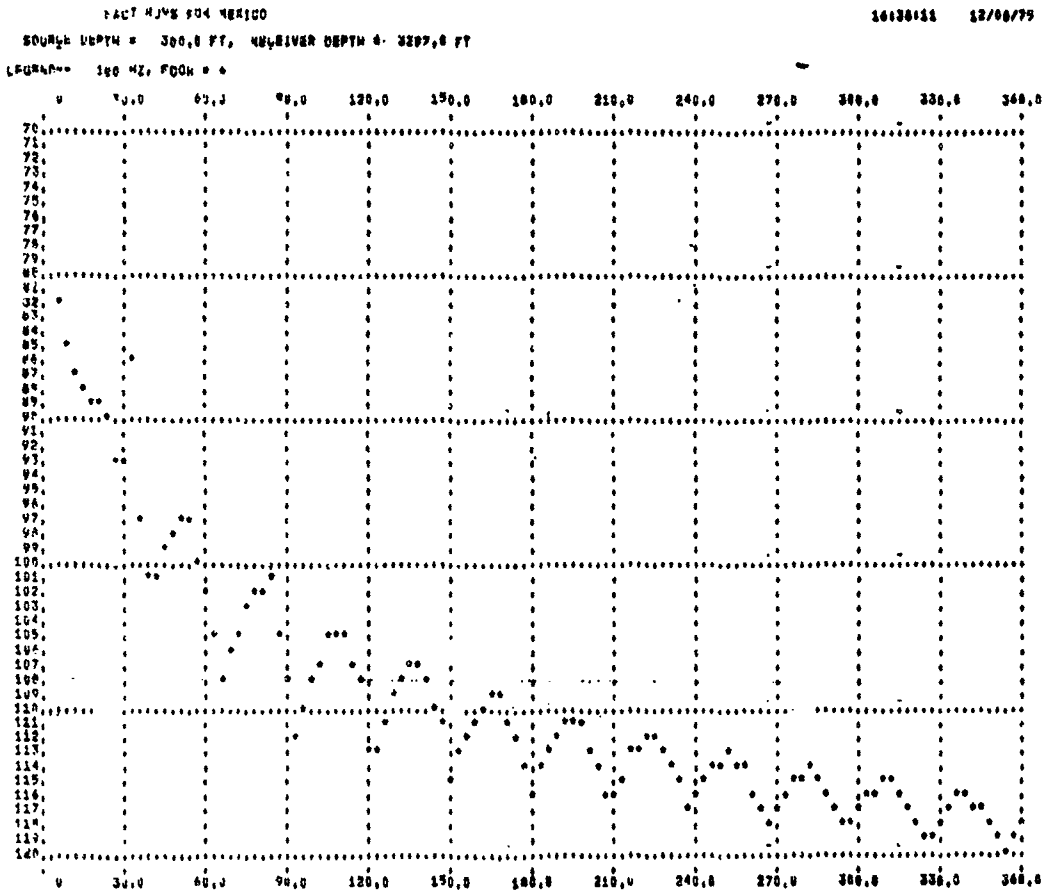
SOURCE DEPTH = 300.0 FT, RECEIVER DEPTH = 3297.0 FT
0
30.0
60.0
90.0
120.0
150.0
180.0
210.0
240.0
270.0
300.0
330.0
360.0

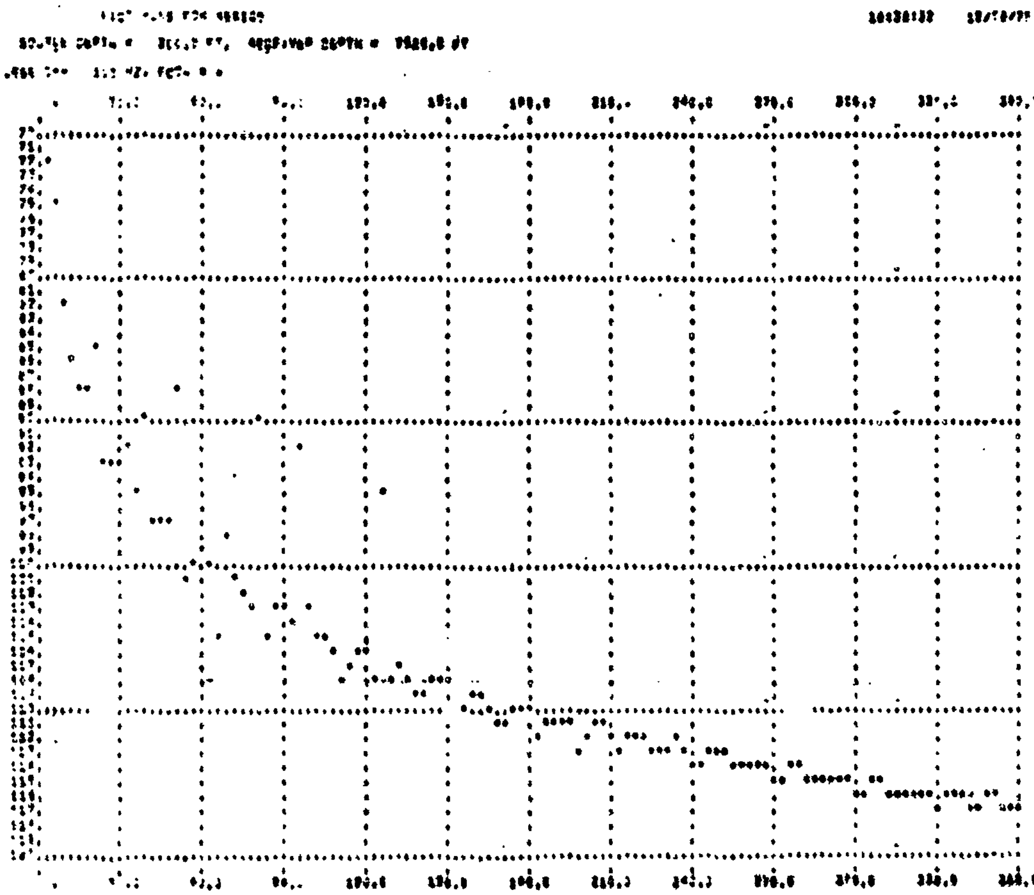

FACT RUNS FOR MEXICO 16120183 12/08/75

SOURCE DEPTH = 300.0 FT, RECEIVER DEPTH = 10782.0 FT

LEGEND** 100 HZ, FOM = *

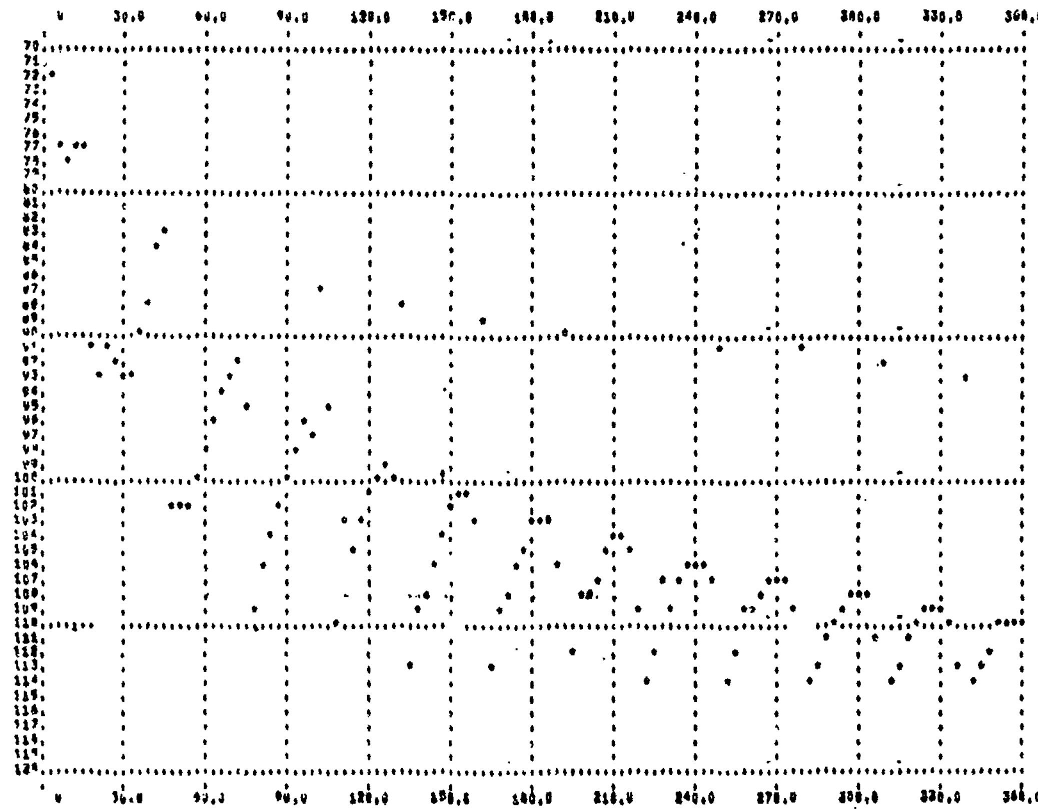

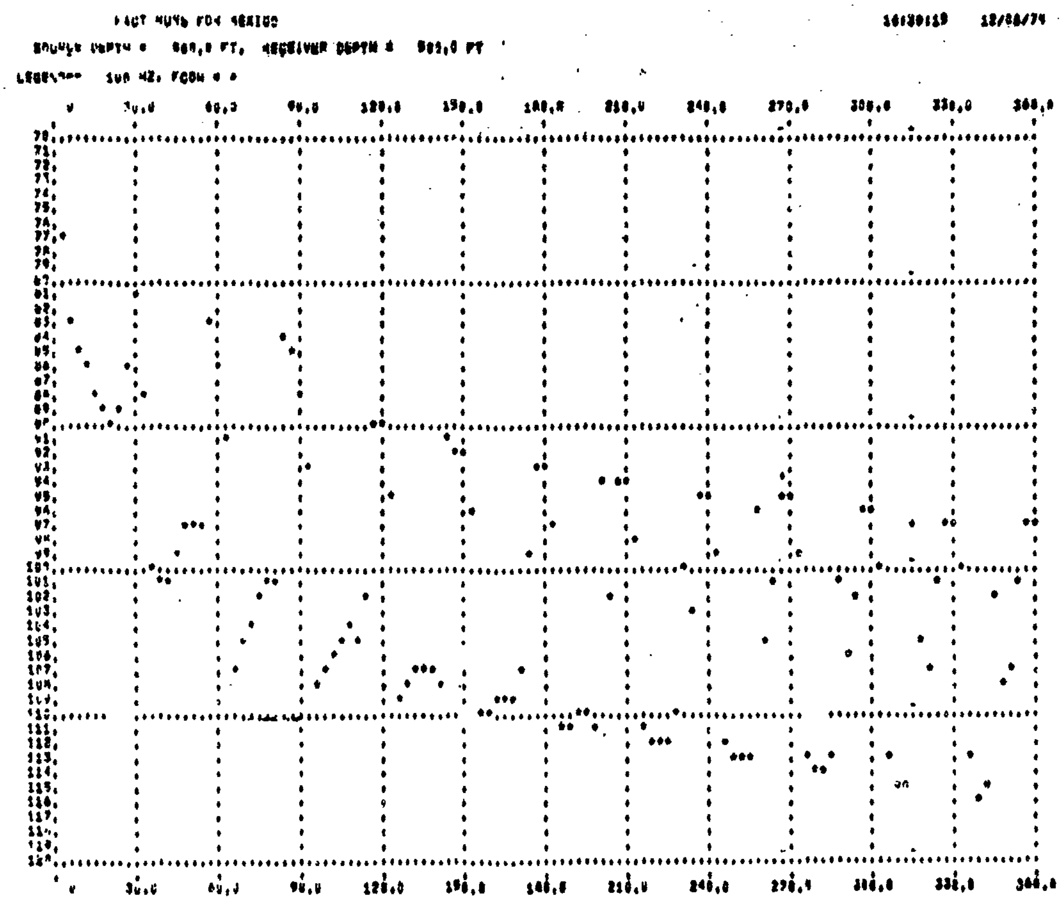

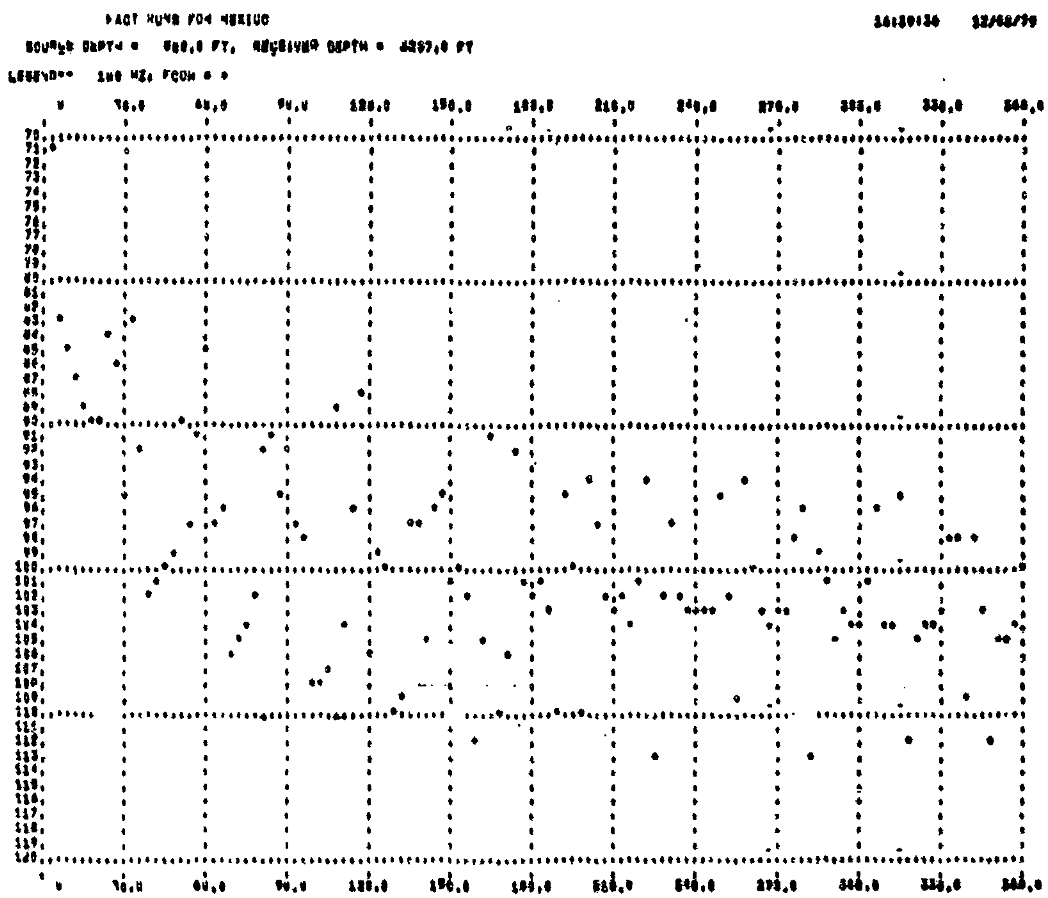

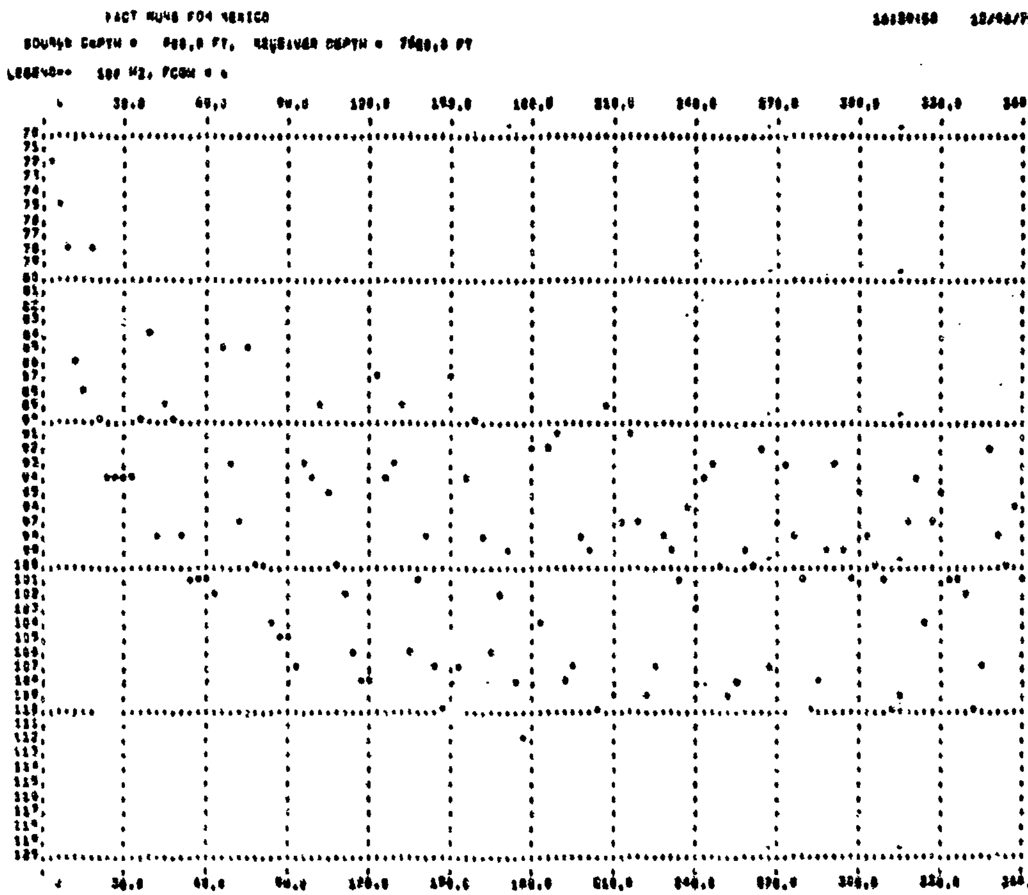
FACT RUNS FOR MEXICO
SOURCE DEPTH =
RECEIVER DEPTH =

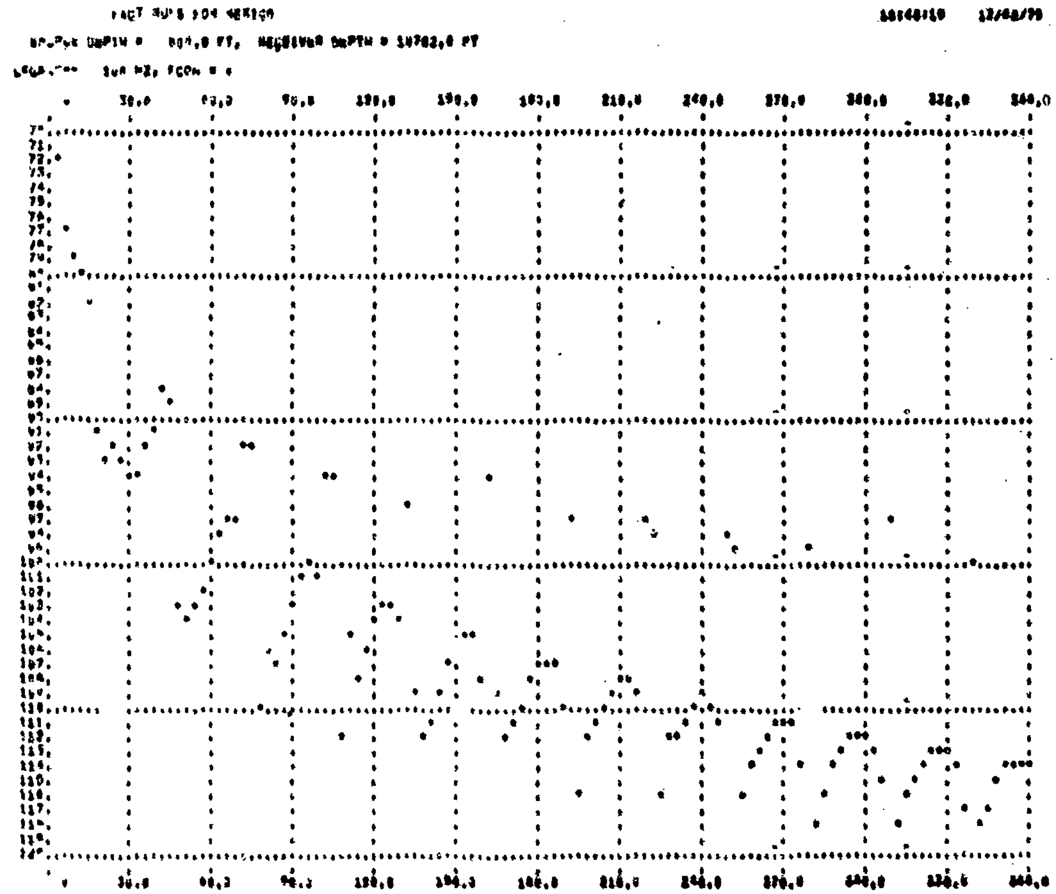

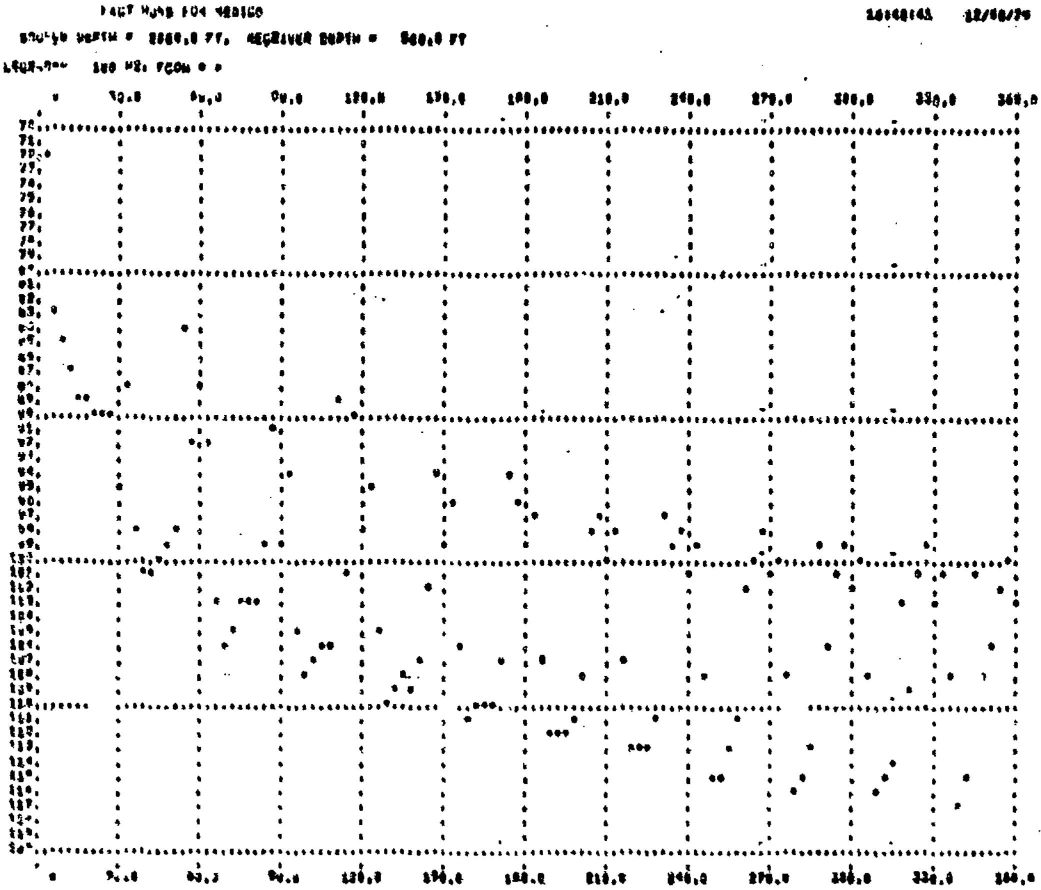

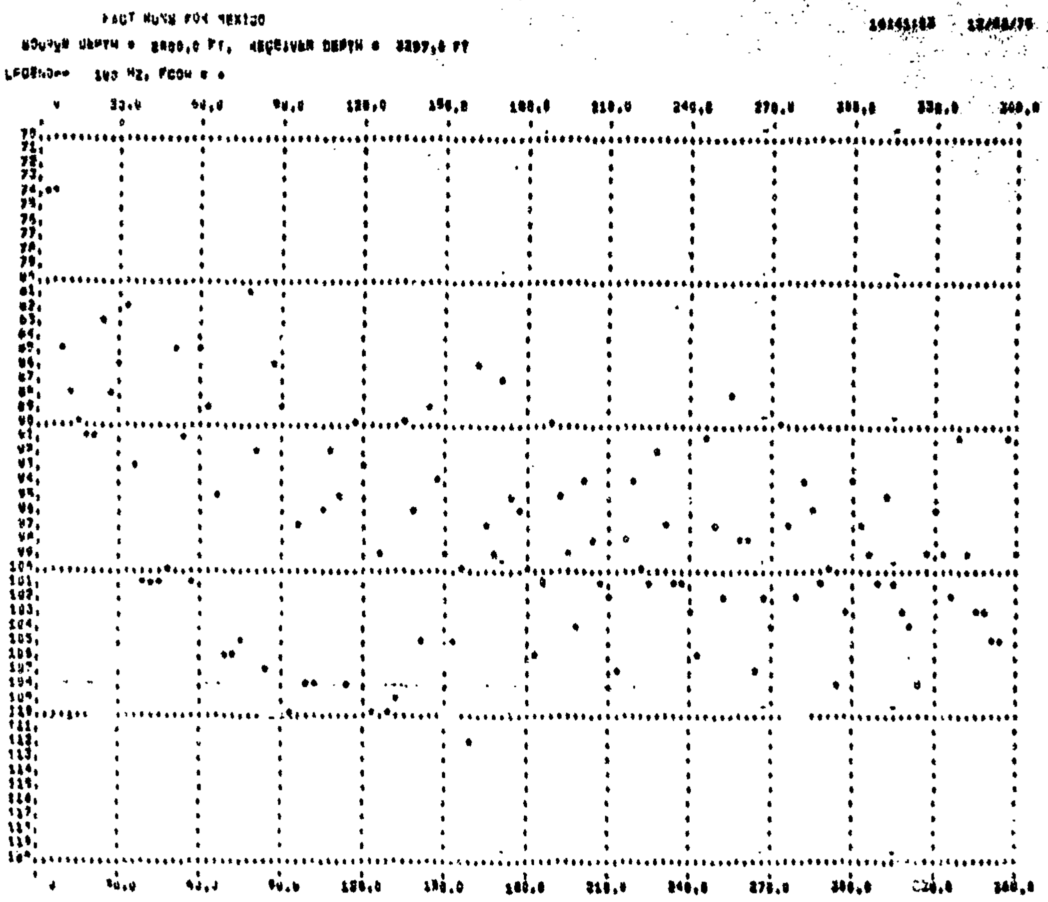
30.0 60.0 90.0 120.0 150.0 180.0 210.0 240.0 270.0 300.0 330.0 360.0

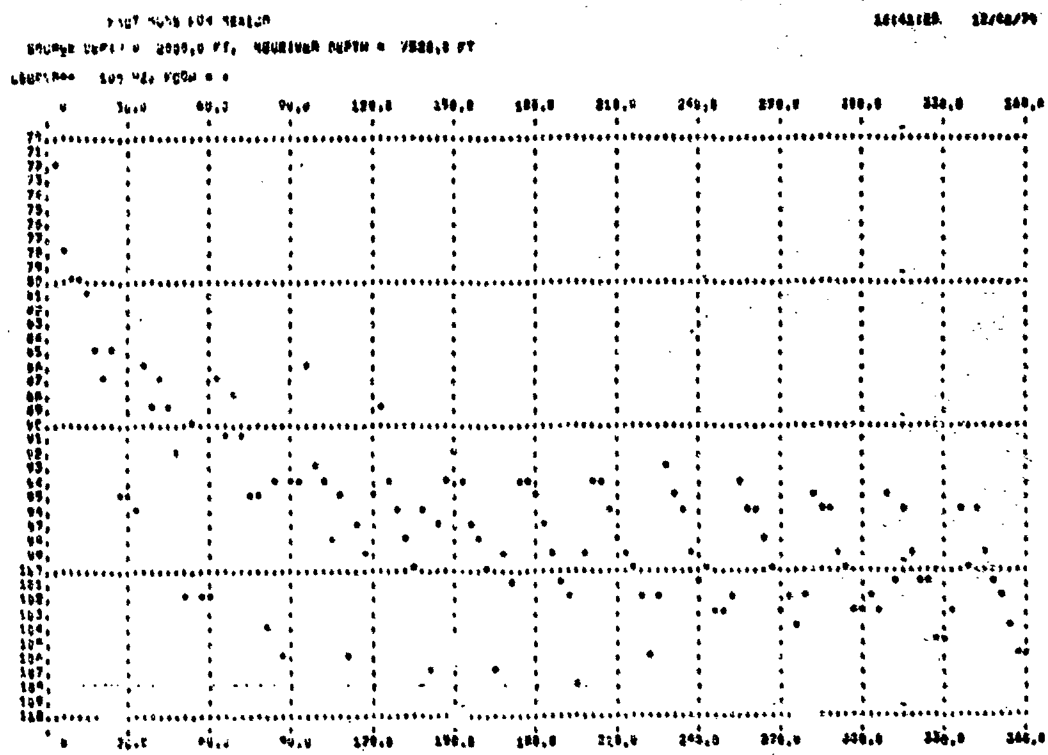

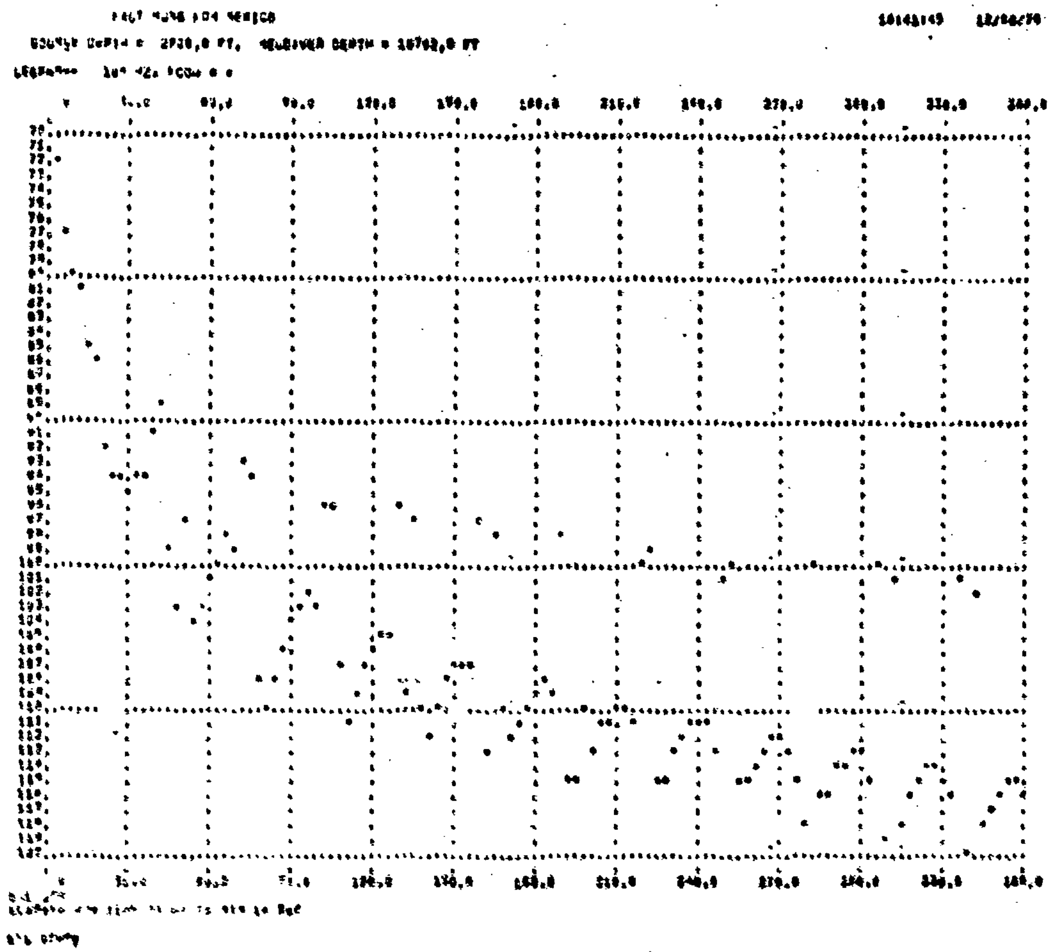

APPENDIX B

EIGENRAY TABULATIONS

This appendix gives tabulations of the predicted behavior of eigenrays for four source depths and four receiver depths and a range of 151.2 nm. For each eigenray the information given is reflecting layer (for this example only the bottom named layer No. 1 is used), source angle, receiver angle, bottom angle, and time required for transmission and number of deep turning points. The SVP shown in Fig. III-2 was used. The computer program EIGENRAY, used to obtain these results, is a layered ocean program which identifies all eigenrays, including bottom penetrating eigenrays, for a given propagation geometry and tabulates the ray parameters which are shown in this appendix.

APPENDIX B

Eigenrays for four receiver depths and four source depths at 151.2 nm range.

Table numbers for source/receiver combinations.

Source Depth ft/m	Receiver Number:	1	2	3	4
	Depth ft/m:	500/152.4	3297/1005	7520/2291.7	10702/3261.7
60/18.3		B1		B2	
300/91.4		B3		B4	
800/243.8		B5		B6	
2000/609.6		B7		B8	

```
RECEIVER RANGE (KM): 151.220
   RECEIVER NO. 1
      NO. DEEP TURNING POINTS:   9
         REFLECTING LAYER NO.: 1
            SRCE ANGLE:   1.1173   RCVR ANGLE: -12.2435   ROT ANGLE:  10.6958   TIME (S):191.381422   SR* RR
            SRCE ANGLE:   1.2449   RCVR ANGLE: -12.2557   ROT ANGLE:  10.7097   TIME (S):191.381446   SR  RR
         REFLECTING LAYER NO.: 1
            SRCE ANGLE:  -0.9248   RCVR ANGLE: -12.2270   ROT ANGLE:  10.4778   TIME (S):191.381615   SR* RR
            SRCE ANGLE:  -1.2422   RCVR ANGLE: -12.2576   ROT ANGLE:  10.7117   TIME (S):191.381882   SR  RR
         REFLECTING LAYER NO.: 1
            SRCE ANGLE:    .7123   RCVR ANGLE:  12.2137   ROT ANGLE:  10.6615   TIME (S):191.402032   SR* RR
            SRCE ANGLE:   1.2907   RCVR ANGLE:  12.2603   ROT ANGLE:  10.7150   TIME (S):191.409473   SR  RR
         REFLECTING LAYER NO.: 1
            SRCE ANGLE:  -0.5739   RCVR ANGLE:  12.2065   ROT ANGLE:  10.4532   TIME (S):191.405077   SR* RR
            SRCE ANGLE:  -1.3203   RCVR ANGLE:  12.2643   ROT ANGLE:  10.7196   TIME (S):191.409864   SR  RR
      NO. DEEP TURNING POINTS:  10
         REFLECTING LAYER NO.: 1
            SRCE ANGLE:   2.7981   RCVR ANGLE: -12.5054   ROT ANGLE:  10.9957   TIME (S):192.417083   SR  RR
         REFLECTING LAYER NO.: 1
            SRCE ANGLE:  -2.8843   RCVR ANGLE: -12.5245   ROT ANGLE:  11.0174   TIME (S):192.418192   SR  RR
         REFLECTING LAYER NO.: 1
            SRCE ANGLE:   3.0978   RCVR ANGLE:  12.5748   ROT ANGLE:  11.0748   TIME (S):192.447481   SR  RR
         REFLECTING LAYER NO.: 1
            SRCE ANGLE:  -3.1745   RCVR ANGLE:  12.5936   ROT ANGLE:  11.0963   TIME (S):192.448640   SR  RR
      NO. DEEP TURNING POINTS:  11
         REFLECTING LAYER NO.: 1
            SRCE ANGLE:   5.9642   RCVR ANGLE: -13.5248   ROT ANGLE:  12.1510   TIME (S):193.498662   SR  RR
         REFLECTING LAYER NO.: 1
            SRCE ANGLE:  -5.9640   RCVR ANGLE: -13.5455   ROT ANGLE:  12.1496   TIME (S):193.501091   SR  RR
         REFLECTING LAYER NO.: 1
            SRCE ANGLE:   6.1030   RCVR ANGLE:  13.6149   ROT ANGLE:  12.2471   TIME (S):193.534835   SR  RR
         REFLECTING LAYER NO.: 1
            SRCE ANGLE:  -6.1453   RCVR ANGLE:  13.6311   ROT ANGLE:  12.2632   TIME (S):193.537347   SR  RR
   RECEIVER NO. 2
      NO. DEEP TURNING POINTS:   9
         REFLECTING LAYER NO.: 1
         REFLECTING LAYER NO.: 1
            SRCE ANGLE:  -1.1347   RCVR ANGLE: -15.2253   ROT ANGLE:  10.6978   TIME (S):191.240381   SR* RR
            SRCE ANGLE:  -1.7644   RCVR ANGLE: -15.2342   ROT ANGLE:  10.7397   TIME (S):191.240329   SR  RR
         REFLECTING LAYER NO.: 1
            SRCE ANGLE:    .3630   RCVR ANGLE:  15.1864   ROT ANGLE:  10.6441   TIME (S):191.550891   SR* RR

            SRCE ANGLE:   1.3492   RCVR ANGLE:  15.2430   ROT ANGLE:  10.7222   TIME (S):191.551916   SR  RR
         REFLECTING LAYER NO.: 1
            SRCE ANGLE:  -0.2493   RCVR ANGLE:  15.1864   ROT ANGLE:  10.6407   TIME (S):191.550093   SR* RR
            SRCE ANGLE:  -1.3900   RCVR ANGLE:  15.2474   ROT ANGLE:  10.7286   TIME (S):191.551437   SR  RR
      NO. DEEP TURNING POINTS:  10
         REFLECTING LAYER NO.: 1
            SRCE ANGLE:   2.4448   RCVR ANGLE: -15.3763   ROT ANGLE:  10.9132   TIME (S):192.273807   SR  RR
         REFLECTING LAYER NO.: 1
            SRCE ANGLE:  -2.5389   RCVR ANGLE: -15.3904   ROT ANGLE:  10.9333   TIME (S):192.274770   SR  RR
         REFLECTING LAYER NO.: 1
            SRCE ANGLE:   3.4407   RCVR ANGLE:  15.5663   ROT ANGLE:  11.1833   TIME (S):192.591905   SR  RR
         REFLECTING LAYER NO.: 1
            SRCE ANGLE:  -3.5465   RCVR ANGLE:  15.5824   ROT ANGLE:  11.2657   TIME (S):192.593312   SR  RR
      NO. DEEP TURNING POINTS:  11
         REFLECTING LAYER NO.: 1
            SRCE ANGLE:   5.5639   RCVR ANGLE: -16.1493   ROT ANGLE:  11.9903   TIME (S):193.347168   SR  RR
         REFLECTING LAYER NO.: 1
            SRCE ANGLE:  -5.6058   RCVR ANGLE: -16.1434   ROT ANGLE:  12.0005   TIME (S):193.349454   SR  RR
         REFLECTING LAYER NO.: 1
            SRCE ANGLE:   6.4787   RCVR ANGLE:  16.4596   ROT ANGLE:  12.4101   TIME (S):193.663278   SR  RR
         REFLECTING LAYER NO.: 1
            SRCE ANGLE:  -6.4427   RCVR ANGLE:  16.4727   ROT ANGLE:  12.4276   TIME (S):193.696924   SR  RR
```

```
RECEIVER NO. 3
   NO. DEEP TURNING POINTS:    9
      REFLECTING LAYER NO.: 1
      REFLECTING LAYER NO.: 1
      REFLECTING LAYER NO.: 1
         SRCE ANGLE:   1.4929   RCVR ANGLE:  13.6260   ROT ANGLE:  10.7410   TIME (S):191.770375   SR  RR
      REFLECTING LAYER NO.: 1
         SRCE ANGLE:  -1.5686   RCVR ANGLE:  13.6334   ROT ANGLE:  10.7505   TIME (S):191.770890   SR  RR
   NO. DEEP TURNING POINTS:   10
      REFLECTING LAYER NO.: 1
         SRCE ANGLE:   2.0164   RCVR ANGLE: -13.6920   ROT ANGLE:  10.8252   TIME (S):192.052990   SR  RR
      REFLECTING LAYER NO.: 1
         SRCE ANGLE:  -2.1048   RCVR ANGLE: -13.7050   ROT ANGLE:  10.8418   TIME (S):192.053772   SR  RR
      REFLECTING LAYER NO.: 1
         SRCE ANGLE:   4.0287   RCVR ANGLE:  14.1212   ROT ANGLE:  11.3670   TIME (S):192.817065   SR  RR
      REFLECTING LAYER NO.: 1
         SRCE ANGLE:  -4.0984   RCVR ANGLE:  14.1386   ROT ANGLE:  11.3888   TIME (S):192.818709   SR  RR
   NO. DEEP TURNING POINTS:   11
      REFLECTING LAYER NO.: 1
         SRCE ANGLE:   5.0[illegible]   RCVR ANGLE: -14.4376   ROT ANGLE:  11.7606   TIME (S):193.115451   SR  RR
      REFLECTING LAYER NO.: 1
         SRCE ANGLE:  -5.0910   RCVR ANGLE: -14.4539   ROT ANGLE:  11.7807   TIME (S):193.117521   SR  RR
      REFLECTING LAYER NO.: 1
         SRCE ANGLE:   6.8930   RCVR ANGLE:  15.1692   ROT ANGLE:  12.6543   TIME (S):193.927302   SR  RR
      REFLECTING LAYER NO.: 1
         SRCE ANGLE:  -6.9242   RCVR ANGLE:  15.1831   ROT ANGLE:  12.6711   TIME (S):193.930142   SR  RR
RECEIVER NO. 4
   NO. DEEP TURNING POINTS:    9
      REFLECTING LAYER NO.: 1
      REFLECTING LAYER NO.: 1
      REFLECTING LAYER NO.: 1
         SRCE ANGLE:   1.6902   RCVR ANGLE:  10.8669   ROT ANGLE:  10.7713   TIME (S):191.907715   SR  RR
      REFLECTING LAYER NO.: 1
         SRCE ANGLE:  -1.7795   RCVR ANGLE:  10.8796   ROT ANGLE:  10.7841   TIME (S):191.908334   SR  RR
   NO. DEEP TURNING POINTS:   10
      REFLECTING LAYER NO.: 1
         SRCE ANGLE:   1.7170   RCVR ANGLE: -10.8697   ROT ANGLE:  10.7740   TIME (S):191.915240   SR  RR
      REFLECTING LAYER NO.: 1
         SRCE ANGLE:  -1.7980   RCVR ANGLE: -10.8826   ROT ANGLE:  10.7871   TIME (S):191.915877   SR  RR
      REFLECTING LAYER NO.: 1
         SRCE ANGLE:   4.5272   RCVR ANGLE:  11.6401   ROT ANGLE:  11.5510   TIME (S):192.961225   SR  RR
      REFLECTING LAYER NO.: 1
         SRCE ANGLE:  -4.5814   RCVR ANGLE:  11.6610   ROT ANGLE:  11.5721   TIME (S):192.963080   SR  RR
   NO. DEEP TURNING POINTS:   11
      REFLECTING LAYER NO.: 1
         SRCE ANGLE:   4.5616   RCVR ANGLE: -11.6533   ROT ANGLE:  11.5643   TIME (S):192.969296   SR  RR
      REFLECTING LAYER NO.: 1
         SRCE ANGLE:  -4.6152   RCVR ANGLE: -11.6742   ROT ANGLE:  11.5854   TIME (S):192.971165   SR  RR
      REFLECTING LAYER NO.: 1
         SRCE ANGLE:   7.2874   RCVR ANGLE:  12.9508   ROT ANGLE:  12.8711   TIME (S):194.084296   SR  RR
      REFLECTING LAYER NO.: 1
         SRCE ANGLE:  -7.3147   RCVR ANGLE:  12.9669   ROT ANGLE:  12.8873   TIME (S):194.087299   SR  RR
```

```
RECEIVER RANGE (KM): 151.200
  RECEIVER NO. 1
    NO. DEEP TURNING POINTS:    6
      REFLECTING LAYER NO.: 1
        SRCE ANGLE:   3.6864   RCVR ANGLE:  -6.4391   ROT ANGLE:   2.3587   TIME (S):189.122298   SR+ RR
      REFLECTING LAYER NO.: 1
        SRCE ANGLE:  -3.7049   RCVR ANGLE:  -6.4580   ROT ANGLE:   2.3875   TIME (S):189.123007   SR+ RR
      REFLECTING LAYER NO.: 1
        SRCE ANGLE:   3.7526   RCVR ANGLE:   6.4775   ROT ANGLE:   2.4611   TIME (S):189.130373   SR+ RR
      REFLECTING LAYER NO.: 1
        SRCE ANGLE:  -3.7717   RCVR ANGLE:   6.4885   ROT ANGLE:   2.4901   TIME (S):189.131110   SR+ RR
    NO. DEEP TURNING POINTS:    7
      REFLECTING LAYER NO.: 1
        SRCE ANGLE:   5.4507   RCVR ANGLE:  -7.5920   ROT ANGLE:   4.6686   TIME (S):189.811197   SR+ RR
      REFLECTING LAYER NO.: 1
        SRCE ANGLE:  -5.4908   RCVR ANGLE:  -7.6144   ROT ANGLE:   4.7050   TIME (S):189.812908   SR+ RR
      REFLECTING LAYER NO.: 1
        SRCE ANGLE:   5.5306   RCVR ANGLE:   7.6495   ROT ANGLE:   4.7619   TIME (S):189.822258   SR+ RR
      REFLECTING LAYER NO.: 1
        SRCE ANGLE:  -5.5714   RCVR ANGLE:   7.6726   ROT ANGLE:   4.7989   TIME (S):189.824031   SR+ RR
    NO. DEEP TURNING POINTS:    8
      REFLECTING LAYER NO.: 1
        SRCE ANGLE:   7.2790   RCVR ANGLE:  -8.9860   ROT ANGLE:   6.7075   TIME (S):190.580118   SR+ RR
      REFLECTING LAYER NO.: 1
        SRCE ANGLE:  -7.3229   RCVR ANGLE:  -9.0215   ROT ANGLE:   6.7551   TIME (S):190.583638   SR+ RR
      REFLECTING LAYER NO.: 1
        SRCE ANGLE:   7.3664   RCVR ANGLE:   9.0569   ROT ANGLE:   6.8025   TIME (S):190.595218   SR+ RR
      REFLECTING LAYER NO.: 1
        SRCE ANGLE:  -7.4114   RCVR ANGLE:   9.0933   ROT ANGLE:   6.8511   TIME (S):190.598850   SR+ RR
  RECEIVER NO. 2
    NO. DEEP TURNING POINTS:    5
      REFLECTING LAYER NO.: 1
      REFLECTING LAYER NO.: 1
      REFLECTING LAYER NO.: 1

        SRCE ANGLE:   1.6352   RCVR ANGLE:  10.6527   ROT ANGLE:*********   TIME (S):188.587812   SR+ RR+
      REFLECTING LAYER NO.: 1
        SRCE ANGLE:  -1.7019   RCVR ANGLE:  10.6759   ROT ANGLE:*********   TIME (S):188.587970   SR+ RR+
    NO. DEEP TURNING POINTS:    6
      REFLECTING LAYER NO.: 1
        SRCE ANGLE:   3.5101   RCVR ANGLE: -11.0941   ROT ANGLE:   2.0874   TIME (S):189.025328   SR+ RR
      REFLECTING LAYER NO.: 1
        SRCE ANGLE:  -3.5358   RCVR ANGLE: -11.0994   ROT ANGLE:   2.1154   TIME (S):189.025972   SR+ RR
      REFLECTING LAYER NO.: 1
        SRCE ANGLE:   3.9369   RCVR ANGLE:  11.2316   ROT ANGLE:   2.7312   TIME (S):189.228257   SR+ RR
      REFLECTING LAYER NO.: 1
        SRCE ANGLE:  -3.9557   RCVR ANGLE:  11.2386   ROT ANGLE:   2.7611   TIME (S):189.229072   SR+ RR
    NO. DEEP TURNING POINTS:    7
      REFLECTING LAYER NO.: 1
        SRCE ANGLE:   5.2608   RCVR ANGLE: -11.7509   ROT ANGLE:   4.4210   TIME (S):189.704549   SR+ RR
      REFLECTING LAYER NO.: 1
        SRCE ANGLE:  -5.2794   RCVR ANGLE: -11.7440   ROT ANGLE:   4.4562   TIME (S):189.708108   SR+ RR
      REFLECTING LAYER NO.: 1
        SRCE ANGLE:   5.7530   RCVR ANGLE:  11.9816   ROT ANGLE:   5.0087   TIME (S):189.928399   SR+ RR
      REFLECTING LAYER NO.: 1
        SRCE ANGLE:  -5.7864   RCVR ANGLE:  11.9975   ROT ANGLE:   5.0471   TIME (S):189.930361   SR+ RR
```

```
RECEIVER NO. 3
   NO. DEEP TURNING POINTS:   5
      REFLECTING LAYER NO.: 1
      REFLECTING LAYER NO.: 1
      REFLECTING LAYER NO.: 1
         SRCE ANGLE:   2.8566   RCVR ANGLE:   8.4416   ROT ANGLE:    .3515   TIME (S):188.738593   SR: RR
      REFLECTING LAYER NO.: 1
         SRCE ANGLE:  -2.8569   RCVR ANGLE:   8.4427   ROT ANGLE:    .3812   TIME (S):188.739823   SR: RR
   NO. DEEP TURNING POINTS:   6
      REFLECTING LAYER NO.: 1
         SRCE ANGLE:   3.3882   RCVR ANGLE:  -8.6061   ROT ANGLE:   1.7078   TIME (S):188.871311   SR: RR
      REFLECTING LAYER NO.: 1
         SRCE ANGLE:  -3.3223   RCVR ANGLE:  -8.6095   ROT ANGLE:   1.7349   TIME (S):188.871879   SR: RR
      REFLECTING LAYER NO.: 1
         SRCE ANGLE:   4.2865   RCVR ANGLE:   8.9854   ROT ANGLE:   3.1101   TIME (S):189.385782   SR: RR
      REFLECTING LAYER NO.: 1
         SRCE ANGLE:  -4.2207   RCVR ANGLE:   8.9962   ROT ANGLE:   3.1414   TIME (S):189.386724   SR: RR
   NO. DEEP TURNING POINTS:   7
      REFLECTING LAYER NO.: 1
         SRCE ANGLE:   4.4597   RCVR ANGLE:  -9.3581   ROT ANGLE:   4.0691   TIME (S):189.542496   SR: RR
      REFLECTING LAYER NO.: 1
         SRCE ANGLE:  -4.3846   RCVR ANGLE:  -9.3725   ROT ANGLE:   4.1024   TIME (S):189.543858   SR: RR


      REFLECTING LAYER NO.: 1
         SRCE ANGLE:   6.8608   RCVR ANGLE:   9.9827   ROT ANGLE:   5.3596   TIME (S):190.098302   SR: RR
      REFLECTING LAYER NO.: 1
         SRCE ANGLE:  -6.8866   RCVR ANGLE:  10.0043   ROT ANGLE:   5.4001   TIME (S):190.100511   SR: RR
RECEIVER NO. 4
   NO. DEEP TURNING POINTS:   5
      REFLECTING LAYER NO.: 1
      REFLECTING LAYER NO.: 1
      REFLECTING LAYER NO.: 1
         SRCE ANGLE:   3.0881   RCVR ANGLE:   1.7645   ROT ANGLE:   1.8895   TIME (S):188.803587   SR: RR
      REFLECTING LAYER NO.: 1
         SRCE ANGLE:  -3.0172   RCVR ANGLE:   1.7811   ROT ANGLE:   1.0383   TIME (S):188.834059   SR: RR
   NO. DEEP TURNING POINTS:   6
      REFLECTING LAYER NO.: 1
         SRCE ANGLE:   3.0568   RCVR ANGLE:  -1.8447   ROT ANGLE:   1.1440   TIME (S):188.884619   SR: RR
      REFLECTING LAYER NO.: 1
         SRCE ANGLE:  -3.8669   RCVR ANGLE:  -1.8416   ROT ANGLE:   1.1710   TIME (S):188.885103   SR: RR
      REFLECTING LAYER NO.: 1
         SRCE ANGLE:   4.5468   RCVR ANGLE:   3.8636   ROT ANGLE:   3.5827   TIME (S):189.461271   SR: RR
      REFLECTING LAYER NO.: 1
         SRCE ANGLE:  -4.5091   RCVR ANGLE:   3.8035   ROT ANGLE:   3.6149   TIME (S):189.462480   SR: RR
   NO. DEEP TURNING POINTS:   7
      REFLECTING LAYER NO.: 1
         SRCE ANGLE:   4.6058   RCVR ANGLE:  -3.8093   ROT ANGLE:   3.6319   TIME (S):189.463895   SR: RR
      REFLECTING LAYER NO.: 1
         SRCE ANGLE:  -4.6360   RCVR ANGLE:  -3.9392   ROT ANGLE:   3.6641   TIME (S):189.465046   SR: RR
      REFLECTING LAYER NO.: 1
         SRCE ANGLE:   6.4036   RCVR ANGLE:   5.9215   ROT ANGLE:   5.7426   TIME (S):190.189126   SR: RR
      REFLECTING LAYER NO.: 1
         SRCE ANGLE:  -6.4303   RCVR ANGLE:   5.9623   ROT ANGLE:   5.7866   TIME (S):190.191458   SR: RR
```

```
RECEIVER RANGE (NM): 151.280
  RECEIVER NO. 1
    NO. DEEP TURNING POINTS:    6
      REFLECTING LAYER NO.: 1
        SRCE ANGLE:   7.6338   RCVR ANGLE:  -6.4119   ROT ANGLE:    2.7822   TIME (S):189.111097   SR* RR
      REFLECTING LAYER NO.: 1
        SRCE ANGLE:  -7.6867   RCVR ANGLE:  -6.4784   ROT ANGLE:    2.4636   TIME (S):189.134280   SR* RR
      REFLECTING LAYER NO.: 1
        SRCE ANGLE:   7.6621   RCVR ANGLE:   6.4491   ROT ANGLE:    2.3852   TIME (S):189.119103   SR* RR
      REFLECTING LAYER NO.: 1
        SRCE ANGLE:  -7.7108   RCVR ANGLE:   6.5178   ROT ANGLE:    2.5656   TIME (S):189.142454   SR* RR
    NO. DEEP TURNING POINTS:    7
      REFLECTING LAYER NO.: 1
        SRCE ANGLE:   8.6118   RCVR ANGLE:  -7.5530   ROT ANGLE:    4.6048   TIME (S):189.797912   SR* RR
      REFLECTING LAYER NO.: 1
        SRCE ANGLE:  -8.6988   RCVR ANGLE:  -7.6530   ROT ANGLE:    4.7674   TIME (S):189.826302   SR* RR
      REFLECTING LAYER NO.: 1
        SRCE ANGLE:   8.6611   RCVR ANGLE:   7.6110   ROT ANGLE:    4.6995   TIME (S):189.808870   SR* RR
      REFLECTING LAYER NO.: 1
        SRCE ANGLE:  -8.7404   RCVR ANGLE:   7.7115   ROT ANGLE:    4.8611   TIME (S):189.837529   SR* RR
    NO. DEEP TURNING POINTS:    8
      REFLECTING LAYER NO.: 1
        SRCE ANGLE:   9.8528   RCVR ANGLE:  -8.9456   ROT ANGLE:    6.6534   TIME (S):190.564356   SR* RR
      REFLECTING LAYER NO.: 1
        SRCE ANGLE:  -9.9581   RCVR ANGLE:  -9.0620   ROT ANGLE:    6.8092   TIME (S):190.599534   SR* RR
      REFLECTING LAYER NO.: 1
        SRCE ANGLE:   9.9148   RCVR ANGLE:   9.0165   ROT ANGLE:    6.7484   TIME (S):190.579332   SR* RR
      REFLECTING LAYER NO.: 1
        SRCE ANGLE: -10.0297   RCVR ANGLE:   9.1341   ROT ANGLE:    6.9053   TIME (S):190.614871   SR* RR
  RECEIVER NO. 2
    NO. DEEP TURNING POINTS:    5
      REFLECTING LAYER NO.: 1
      REFLECTING LAYER NO.: 1
      REFLECTING LAYER NO.: 1
      REFLECTING LAYER NO.: 1
        SRCE ANGLE:  [illegible].5636   RCVR ANGLE:   8.8712   ROT ANGLE:*********   TIME (S):188.607932   SR* RR*
        SRCE ANGLE:  -[illegible].7087   RCVR ANGLE:   8.9288   ROT ANGLE:*********   TIME (S):188.607979   SR* RR*
        SRCE ANGLE:  -6.3680   RCVR ANGLE:  10.3021   ROT ANGLE:*********   TIME (S):188.596157   SR* RR*
        SRCE ANGLE:  -7.2835   RCVR ANGLE:  10.8985   ROT ANGLE:     .0367   TIME (S):198.598803   SR* RR
    NO. DEEP TURNING POINTS:    6
      REFLECTING LAYER NO.: 1
        SRCE ANGLE:   7.5562   RCVR ANGLE: -11.0808   ROT ANGLE:    2.0099   TIME (S):189.014299   SR* RR
      REFLECTING LAYER NO.: 1
        SRCE ANGLE:  -7.8046   RCVR ANGLE: -11.1141   ROT ANGLE:    2.1925   TIME (S):189.037065   SR* RR
      REFLECTING LAYER NO.: 1
        SRCE ANGLE:   7.7583   RCVR ANGLE:  11.2137   ROT ANGLE:    2.6543   TIME (S):189.216792   SR* RR
      REFLECTING LAYER NO.: 1
        SRCE ANGLE:  -7.8131   RCVR ANGLE:  11.2560   ROT ANGLE:    2.8355   TIME (S):189.240616   SR* RR
    NO. DEEP TURNING POINTS:    7
      REFLECTING LAYER NO.: 1
        SRCE ANGLE:   8.4854   RCVR ANGLE: -11.7275   ROT ANGLE:    4.3575   TIME (S):189.693531   SR* RR
      REFLECTING LAYER NO.: 1
        SRCE ANGLE:  -8.5653   RCVR ANGLE: -11.7870   ROT ANGLE:    4.5195   TIME (S):189.721230   SR* RR
      REFLECTING LAYER NO.: 1
        SRCE ANGLE:   8.7973   RCVR ANGLE:  11.9563   ROT ANGLE:    4.9472   TIME (S):189.914732   SR* RR
      REFLECTING LAYER NO.: 1
        SRCE ANGLE:  -8.8884   RCVR ANGLE:  12.0231   ROT ANGLE:    5.1084   TIME (S):189.944121   SR* RR
```

```
RECEIVER NO. 3
  NO. DEEP TURNING POINTS:   5
    REFLECTING LAYER NO.: 1
    REFLECTING LAYER NO.: 1
    REFLECTING LAYER NO.: 1
      SRCE ANGLE:   7.1627   RCVR ANGLE:   4.7715   ROT ANGLE:**********   TIME (S):188.719650   SRO RRO
      SRCE ANGLE:   3.9883   RCVR ANGLE:   5.8226   ROT ANGLE:**********   TIME (S):188.722871   SRO RRO
      SRCE ANGLE:   5.4715   RCVR ANGLE:   6.9130   ROT ANGLE:**********   TIME (S):188.728160   SRO RRO
      SRCE ANGLE:   7.2882   RCVR ANGLE:   8.4381   ROT ANGLE:     .7573   TIME (S):188.728188   SRO RR
    REFLECTING LAYER NO.: 1
      SRCE ANGLE:  -6.6669   RCVR ANGLE:   4.3510   ROT ANGLE:**********   TIME (S):188.719808   SRO RRO
      SRCE ANGLE:  -7.2980   RCVR ANGLE:   8.4475   ROT ANGLE:     .4752   TIME (S):188.749443   SRO RR
  NO. DEEP TURNING POINTS:   6
    REFLECTING LAYER NO.: 1
      SRCE ANGLE:   [illegible]

      SRCE ANGLE:   7.4896   RCVR ANGLE:  -8.5898   ROT ANGLE:    1.6203   TIME (S):188.860490   SRO RR
    REFLECTING LAYER NO.: 1
      SRCE ANGLE:  -7.5046   RCVR ANGLE:  -8.6255   ROT ANGLE:    1.8130   TIME (S):188.882756   SRO RR
    REFLECTING LAYER NO.: 1
      SRCE ANGLE:   7.8808   RCVR ANGLE:   8.9605   ROT ANGLE:    3.0967   TIME (S):189.374017   SRO RR
    REFLECTING LAYER NO.: 1
      SRCE ANGLE:  -7.9577   RCVR ANGLE:   9.0718   ROT ANGLE:    3.2143   TIME (S):189.398577   SRO RR
  NO. DEEP TURNING POINTS:   7
    REFLECTING LAYER NO.: 1
      SRCE ANGLE:   8.3045   RCVR ANGLE:  -9.3304   ROT ANGLE:    4.0045   TIME (S):189.529842   SRO RR
    REFLECTING LAYER NO.: 1
      SRCE ANGLE:  -8.3886   RCVR ANGLE:  -9.4007   ROT ANGLE:    4.1669   TIME (S):189.556610   SRO RR
    REFLECTING LAYER NO.: 1
      SRCE ANGLE:   8.9989   RCVR ANGLE:   9.9586   ROT ANGLE:    5.2093   TIME (S):190.084229   SRO RR
    REFLECTING LAYER NO.: 1
      SRCE ANGLE:  -9.0967   RCVR ANGLE:  10.0307   ROT ANGLE:    5.4404   TIME (S):190.114706   SRO RR
RECEIVER NO. 4
  NO. DEEP TURNING POINTS:   5
    REFLECTING LAYER NO.: 1
    REFLECTING LAYER NO.: 1
    REFLECTING LAYER NO.: 1
      SRCE ANGLE:   7.3671   RCVR ANGLE:   1.7150   ROT ANGLE:     .9703   TIME (S):188.793068   SRO RR
    REFLECTING LAYER NO.: 1
      SRCE ANGLE:  -7.3884   RCVR ANGLE:   1.8361   ROT ANGLE:    1.1248   TIME (S):188.814633   SRO RR
  NO. DEEP TURNING POINTS:   6
    REFLECTING LAYER NO.: 1
      SRCE ANGLE:   7.3980   RCVR ANGLE:  -1.7048   ROT ANGLE:    1.0617   TIME (S):188.794035   SRO RR
    REFLECTING LAYER NO.: 1
      SRCE ANGLE:  -7.7880   RCVR ANGLE:  -1.9149   ROT ANGLE:    1.2592   TIME (S):188.819725   SRO RR
    REFLECTING LAYER NO.: 1
      SRCE ANGLE:   8.0896   RCVR ANGLE:   3.7097   ROT ANGLE:    3.5137   TIME (S):189.440088   SRO RR
    REFLECTING LAYER NO.: 1
      SRCE ANGLE:  -8.1575   RCVR ANGLE:   3.9574   ROT ANGLE:    3.6836   TIME (S):189.474677   SRO RR
  NO. DEEP TURNING POINTS:   7
    REFLECTING LAYER NO.: 1
      SRCE ANGLE:   8.1044   RCVR ANGLE:  -3.8462   ROT ANGLE:    3.5439   TIME (S):189.451466   SRO RR
    REFLECTING LAYER NO.: 1
      SRCE ANGLE:  -8.1709   RCVR ANGLE:  -4.0029   ROT ANGLE:    3.7318   TIME (S):189.477160   SRO RR
    REFLECTING LAYER NO.: 1
      SRCE ANGLE:   9.2208   RCVR ANGLE:   5.8454   ROT ANGLE:    5.6866   TIME (S):190.176507   SRO RR
    REFLECTING LAYER NO.: 1
      SRCE ANGLE:  -9.3274   RCVR ANGLE:   6.0185   ROT ANGLE:    5.8625   TIME (S):190.204316   SRO RR
```

COPY AVAILABLE TO DDC DOES NOT PERMIT FULLY LEGIBLE PRODUCTION

```
RECEIVER RANGE (KM): 101.782
  RECEIVER NO. 1
    NO. DEEP TURNING POINTS:   6
      REFLECTING LAYER NO.: 1
      REFLECTING LAYER NO.: 1
      REFLECTING LAYER NO.: 1
      REFLECTING LAYER NO.: 1
        SRCE ANGLE:  -9.8701   RCVR ANGLE:   5.4363   ROT ANGLE:*********   TIME (S):188.542712   SR RR*
        SRCE ANGLE:  -9.9283   RCVR ANGLE:   5.5147   ROT ANGLE:*********   TIME (S):188.542730   SR RR*
    NO. DEEP TURNING POINTS:   6
      REFLECTING LAYER NO.: 1
        SRCE ANGLE:  10.4107   RCVR ANGLE:  -6.3696   ROT ANGLE:   2.1601   TIME (S):189.071848   SR RR
      REFLECTING LAYER NO.: 1
        SRCE ANGLE: -10.5264   RCVR ANGLE:  -6.5754   ROT ANGLE:   2.5850   TIME (S):189.173857   SR RR
      REFLECTING LAYER NO.: 1
        SRCE ANGLE:  10.4410   RCVR ANGLE:   6.4052   ROT ANGLE:   2.2634   TIME (S):189.079744   SR RR
      REFLECTING LAYER NO.: 1

        SRCE ANGLE: -10.5708   RCVR ANGLE:   6.5662   ROT ANGLE:   2.6867   TIME (S):189.182150   SR RR
    NO. DEEP TURNING POINTS:   7
      REFLECTING LAYER NO.: 1
        SRCE ANGLE:  11.1127   RCVR ANGLE:  -7.4870   ROT ANGLE:   4.4950   TIME (S):189.755212   SR RR
      REFLECTING LAYER NO.: 1
        SRCE ANGLE:  11.2910   RCVR ANGLE:  -7.7220   ROT ANGLE:   4.8779   TIME (S):189.869532   SR RR
      REFLECTING LAYER NO.: 1
        SRCE ANGLE:  11.1707   RCVR ANGLE:   7.5432   ROT ANGLE:   4.5885   TIME (S):189.765991   SR RR
      REFLECTING LAYER NO.: 1
        SRCE ANGLE: -11.3314   RCVR ANGLE:   7.7816   ROT ANGLE:   4.9716   TIME (S):189.880967   SR RR
  RECEIVER NO. 2
    NO. DEEP TURNING POINTS:   5
      REFLECTING LAYER NO.: 1
      REFLECTING LAYER NO.: 1
      REFLECTING LAYER NO.: 1
      REFLECTING LAYER NO.: 1
        SRCE ANGLE:  -7.7104   RCVR ANGLE:   8.6290   ROT ANGLE:*********   TIME (S):188.633793   SR RR*
        SRCE ANGLE:  -8.5068   RCVR ANGLE:   8.9765   ROT ANGLE:*********   TIME (S):188.635069   SR RR*
        SRCE ANGLE:  -9.7719   RCVR ANGLE:   9.8951   ROT ANGLE:*********   TIME (S):188.630786   SR RR*
        SRCE ANGLE: -10.1940   RCVR ANGLE:  10.8980   ROT ANGLE:    .1782   TIME (S):188.636092   SR RR
    NO. DEEP TURNING POINTS:   6
      REFLECTING LAYER NO.: 1
        SRCE ANGLE:  10.3648   RCVR ANGLE: -11.0587   ROT ANGLE:   1.8876   TIME (S):188.975311   SR RR
      REFLECTING LAYER NO.: 1
        SRCE ANGLE: -10.4528   RCVR ANGLE: -11.1385   ROT ANGLE:   2.3141   TIME (S):189.076368   SR RR
      REFLECTING LAYER NO.: 1
        SRCE ANGLE:  10.5895   RCVR ANGLE:  11.1858   ROT ANGLE:   2.5348   TIME (S):189.177132   SR RR
      REFLECTING LAYER NO.: 1
        SRCE ANGLE: -10.6140   RCVR ANGLE:  11.2876   ROT ANGLE:   2.9562   TIME (S):189.280648   SR RR
    NO. DEEP TURNING POINTS:   7
      REFLECTING LAYER NO.: 1
        SRCE ANGLE:  11.0756   RCVR ANGLE: -11.6871   ROT ANGLE:   4.2462   TIME (S):189.651293   SR RR
      REFLECTING LAYER NO.: 1
        SRCE ANGLE: -11.1974   RCVR ANGLE: -11.8383   ROT ANGLE:   4.6304   TIME (S):189.763977   SR RR
      REFLECTING LAYER NO.: 1
        SRCE ANGLE:  11.2735   RCVR ANGLE:  11.9116   ROT ANGLE:   4.8767   TIME (S):189.871365   SR RR
      REFLECTING LAYER NO.: 1
        SRCE ANGLE: -11.4467   RCVR ANGLE:  12.0697   ROT ANGLE:   5.2185   TIME (S):189.988048   SR RR
```

COPY AVAILABLE TO DDC DOES NOT PERMIT FULLY LEGIBLE PRODUCTION

```
RECEIVER NO. 3
   NO. DEEP TURNING POINTS:    5
      REFLECTING LAYER NO.: 1
      REFLECTING LAYER NO.: 1
      REFLECTING LAYER NO.: 1

         SRCE ANGLE:   7.9991   RCVR ANGLE:    5.4162   BOT ANGLE:*********   TIME (S):188.694560   SRC RR*
         SRCE ANGLE:   8.2644   RCVR ANGLE:    5.4590   BOT ANGLE:*********   TIME (S):188.694790   SRC RR*
         SRCE ANGLE:   9.4767   RCVR ANGLE:    7.4414   BOT ANGLE:*********   TIME (S):188.686095   SRC RR*
         SRCE ANGLE:  10.1964   RCVR ANGLE:    8.4350   BOT ANGLE:    .1157   TIME (S):188.690872   SRC RR
      REFLECTING LAYER NO.: 1
         SRCE ANGLE:  -4.5447   RCVR ANGLE:    3.1760   BOT ANGLE:*********   TIME (S):188.730249   SRC RR*
         SRCE ANGLE: -10.2197   RCVR ANGLE:    8.4565   BOT ANGLE:    .4161   TIME (S):188.787615   SRC RR
   NO. DEEP TURNING POINTS:    6
      REFLECTING LAYER NO.: 1
         SRCE ANGLE:   4.9980   RCVR ANGLE:   -3.2456   BOT ANGLE:*********   TIME (S):188.712226   SRC RR*
         SRCE ANGLE:  10.3860   RCVR ANGLE:   -8.5469   BOT ANGLE:   1.5871   TIME (S):188.821812   SRC RR
      REFLECTING LAYER NO.: 1
         SRCE ANGLE:  -5.7730   RCVR ANGLE:   -8.5180   BOT ANGLE:*********   TIME (S):188.748910   SRC RR*
         SRCE ANGLE: -10.3784   RCVR ANGLE:   -8.6516   BOT ANGLE:   1.9346   TIME (S):188.921875   SRC RR
      REFLECTING LAYER NO.: 1
         SRCE ANGLE:  10.5988   RCVR ANGLE:    6.9284   BOT ANGLE:   2.9155   TIME (S):189.333878   SRC RR
      REFLECTING LAYER NO.: 1
         SRCE ANGLE: -10.7215   RCVR ANGLE:    9.8654   BOT ANGLE:   3.3346   TIME (S):189.439129   SRC RR
   NO. DEEP TURNING POINTS:    7
      REFLECTING LAYER NO.: 1
         SRCE ANGLE:  10.9960   RCVR ANGLE:   -4.2834   BOT ANGLE:   3.8030   TIME (S):189.489220   SRC RR
      REFLECTING LAYER NO.: 1
         SRCE ANGLE: -11.0477   RCVR ANGLE:   -9.4581   BOT ANGLE:   4.2780   TIME (S):189.598784   SRC RR
      REFLECTING LAYER NO.: 1
         SRCE ANGLE:  11.4775   RCVR ANGLE:    9.8924   BOT ANGLE:   5.1882   TIME (S):190.048131   SRC RR
      REFLECTING LAYER NO.: 1
         SRCE ANGLE: -11.6835   RCVR ANGLE:   10.0061   BOT ANGLE:   5.5780   TIME (S):190.150388   SRC RR
RECEIVER NO. 4
   NO. DEEP TURNING POINTS:    5
      REFLECTING LAYER NO.: 1
      REFLECTING LAYER NO.: 1
      REFLECTING LAYER NO.: 1
         SRCE ANGLE:  13.2261   RCVR ANGLE:    1.6440   BOT ANGLE:    .7861   TIME (S):188.754777   SRC RR
      REFLECTING LAYER NO.: 1
         SRCE ANGLE: -10.2792   RCVR ANGLE:    1.9192   BOT ANGLE:   1.2487   TIME (S):188.853069   SRC RR
   NO. DEEP TURNING POINTS:    6
      REFLECTING LAYER NO.: 1
         SRCE ANGLE:  10.2374   RCVR ANGLE:   -1.7237   BOT ANGLE:    .9365   TIME (S):188.755788   SRC RR
      REFLECTING LAYER NO.: 1
         SRCE ANGLE: -10.3632   RCVR ANGLE:   -1.9096   BOT ANGLE:   1.3780   TIME (S):188.854733   SRC RR
      REFLECTING LAYER NO.: 1
         SRCE ANGLE:  10.7467   RCVR ANGLE:    3.6627   BOT ANGLE:   3.3071   TIME (S):189.409767   SRC RR
      REFLECTING LAYER NO.: 1

         SRCE ANGLE: -10.8733   RCVR ANGLE:    4.8456   BOT ANGLE:   3.7995   TIME (S):189.519964   SRC RR
   NO. DEEP TURNING POINTS:    7
      REFLECTING LAYER NO.: 1
         SRCE ANGLE:  10.7579   RCVR ANGLE:   -1.7397   BOT ANGLE:   3.4487   TIME (S):189.410768   SRC RR
      REFLECTING LAYER NO.: 1
         SRCE ANGLE: -10.8374   RCVR ANGLE:   -6.1491   BOT ANGLE:   3.8445   TIME (S):189.518714   SRC RR
      REFLECTING LAYER NO.: 1
         SRCE ANGLE:  11.0776   RCVR ANGLE:    5.7414   BOT ANGLE:   4.5774   TIME (S):190.120451   SRC RR
      REFLECTING LAYER NO.: 1
         SRCE ANGLE: -11.1846   RCVR ANGLE:    6.1227   BOT ANGLE:   5.0494   TIME (S):190.251857   SRC RR
```

APPENDIX C

ORGANIZATIONS

ORGANIZATIONS

PERSONNEL

MAJOR EQUIPMENTS

(to be added later)

APPENDIX D

OPERATIONAL DETAILS

DETAILED OPERATIONAL PLANS

ACOUSTIC SOURCE FREQUENCIES

SCHEDULING

RADIO FREQUENCIES, ETC.

(to be added later)

APPENDIX E

SUS PROCESSOR DESCRIPTION

The analog data recordings are time compressed in playback and converted to digital format along with associated timing and system information. Three data channels or hydrophones are converted simultaneously. The data are filtered in playback for antialiasing and antistrumming (low frequency receiver effects). The sampling rate, which is synchronized by a tone on the data tape to minimize analog record/playback variations, is determined by the frequency range of analysis. The broadband digitized signals are not archived after the processing is completed.

The heart of the automatic SUS processor is a software system with an adaptive algorithm that determines the threshold for detection based on estimates of the ambient noise and the envelope of the SUS signal. Coincident detection is required across multichannels to minimize the false alarm rate. For example, Fig. E-1 shows the arrival of a shot received on the hydrophone data channels. Source information from the exercise operations is input to the processor, which utilizes a simple propagation model to calculate an expected event arrival time window.

The SUS signal duration is independently determined on each data channel since varying propagation paths can exist between the source and receiving hydrophones. An adaptive filter based on the signal energy relative to the ambient noise energy is used to determine the shot signal termination. Information from each detected SUS is used to update the filter parameters for each following event.

Once the event is detected and the signal duration is determined, an FFT algorithm is used to determine the high resolution spectrum of the signal plus noise. The resolution in the spectral estimation is

CHANNEL 1

CHANNEL 2

CHANNEL 3

FIGURE E-1

SUS ARRIVAL ON THREE HYDROPHONE CHANNELS
(Signal envelope versus time)

based on the sampling rate chosen and a 4096 point transform. The spectrum of the ambient noise immediately preceding each SUS is determined in a like manner.

The structure of the received SUS frequency spectrum is determined by the multipath arrival structure and the SUS source character. For example, Fig. E-2 shows the spectrum of two different SUS arrivals including the noise spectrum preceding each arrival. The spectra are remarkably different because of the source depth difference, which determines the SUS bubble pulse frequency.

The general flow of the shot processing is summarized in Fig. E-3, and the parameters of the processor are outlined in Fig. E-4.

Processor Outputs

For each SUS signal detected the following information is output to digital tape and is used in the analysis of the acoustics of the environment:

1) SUS event time to 0.01 sec.
2) SUS duration to 0.01 sec.
3) High resolution spectra of signal plus noise.
4) High resolution spectra of the ambient noise sample associated with each SUS.
5) SUS signal energy, ambient noise energy, and signal-to-noise estimates in 1 and 1/3 octave frequency bands.
6) Propagation loss and signal-to-noise estimates versus range and/or time.

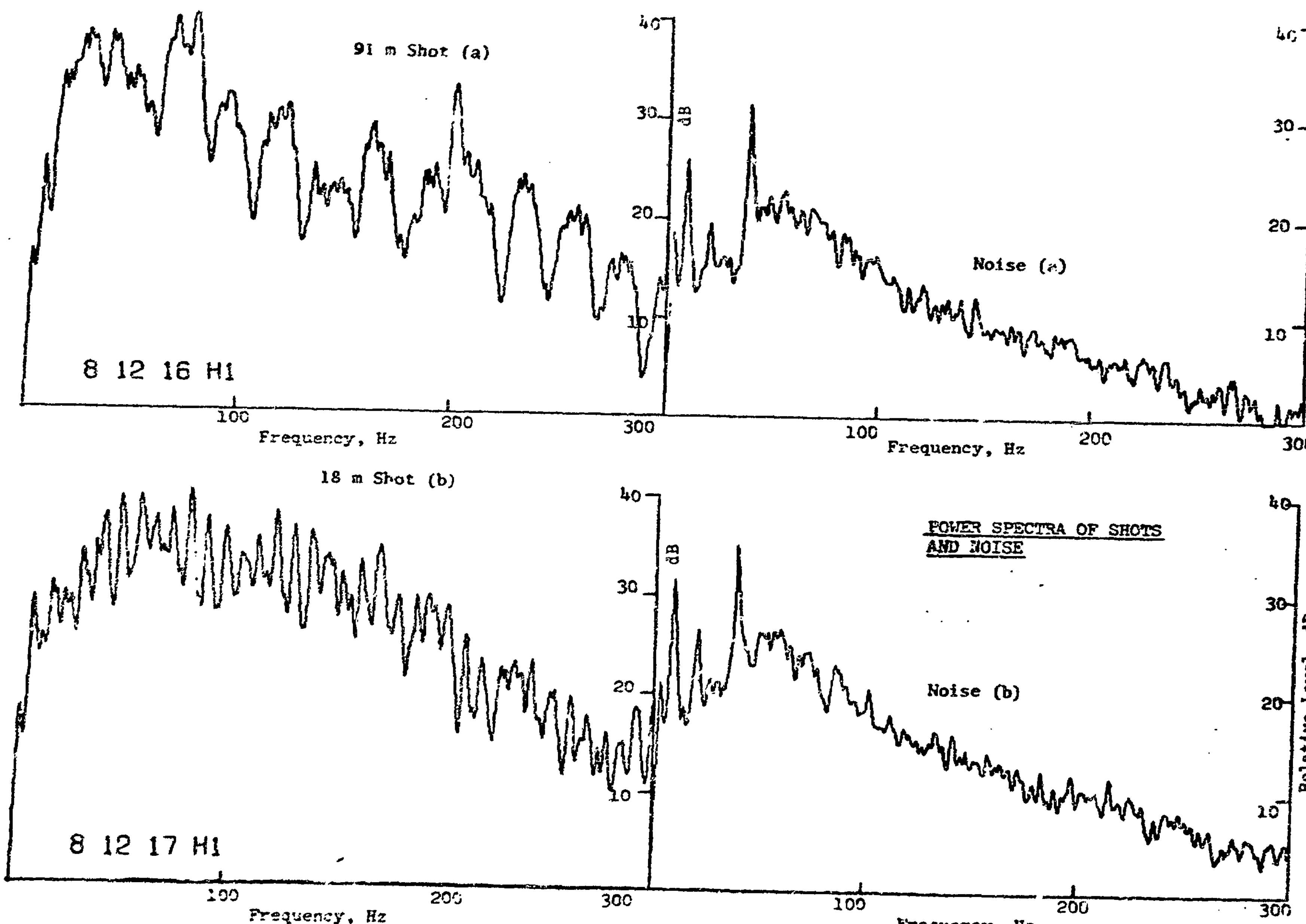
91 m Shot (a)
8 12 16 H1
Noise (a)
18 m Shot (b)
8 12 17 H1
Noise (b)
POWER SPECTRA OF SHOTS AND NOISE
dB
Relative Level, dB
Frequency, Hz
100
200
300
10
20
30
40

FIGURE E-2

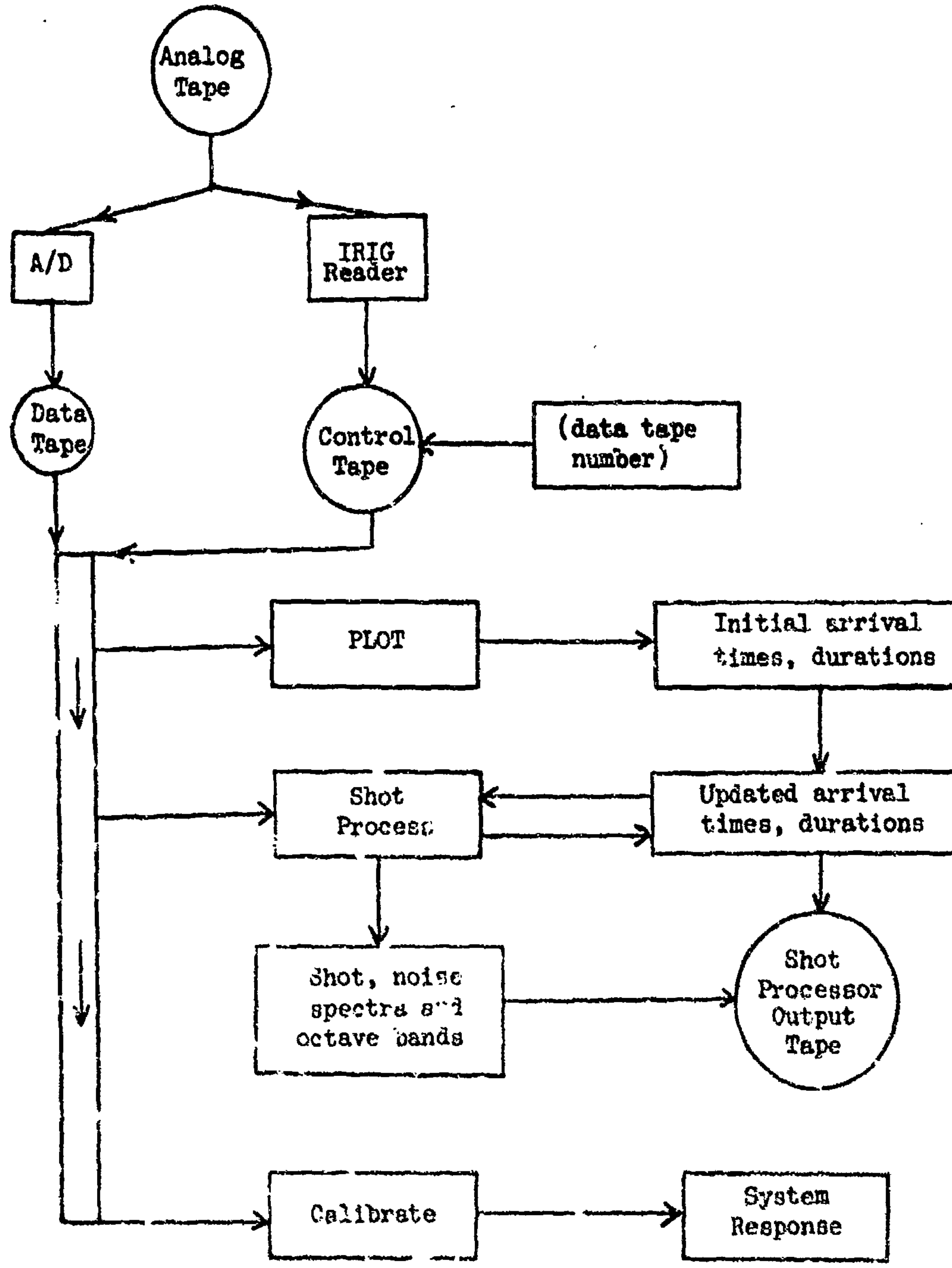

FIGURE E-3

GENERAL FLOW OF SHOT PROCESSING

DATA SOURCE: ANALOG TAPE

PROCESSING TECHNIQUE: ANALOG TO DIGITAL CONVERSION OF CONTINUOUS RECORD INTERMEDIATE STORAGE ON DIGITAL TAPE AUTOMATIC COMPUTER EVENT DETECTION ADAPTIVE SIGNAL DURATION DETERMINE FFT ENERGY ANALYSIS. RANDOM ACCESS DISK FOR SIGNAL SORTING

SIMULTANEOUS PROCESSING OF THREE HYDROPHONE CHANNELS

PLAYBACK SPEEDUP: 20/1

PROCESSING SPEED: 10 TO 15 sec FOR HYDROPHONE SHOT INCLUDING NOISE (EXERCISE DEPENDENT)

RESOLUTION: EVENTS TO 0.01 sec, FREQUENCY TO 0.15 Hz

AVAILABLE OUTPUTS:

- SIGNAL ARRIVAL TIMES
- SIGNAL DURATION
- POWER SPECTRA FOR SIGNAL AND NOISE
- OCTAVE BAND ENERGIES
- PROPAGATION LOSS
- SIGNAL-TO-NOISE RATIOS

FIGURE E-4

ARL/UT SUS PROCESSING SYSTEM

APPENDIX F

AN/CW PROCESSOR DESCRIPTION

The AN/CW processor is a hardware/software configuration designed to perform a narrowband analysis over a variable frequency range handling large volumes of data. The system is divided into five tasks: A/D conversion, spectral estimation, band estimation, editing, and display. Parameters such as bandwidth, frequency range and resolution, and integration or averaging time can be readily adopted to suit different applications.

For the A/D task, the analog data recordings are time compressed in playback and converted to digital format. The equipment configuration is shown in Fig. F-1. One hydrophone channel is digitized on each processing, run along with the corresponding timing and receiving system information. Programmable amplifiers, controlled by the digital computer, are used to maximize the dynamic range utilization of the A/D converter. The sampling signal is phased locked to a reference on the data tape to minimize errors due to record/playback fluctuations.

During one A/D pass the computer flags any sample whose amplitude exceeds the range of the A/D converter. The computer also determines the peak and average amplitude of the data for each minute. This information is used to determine the desired amplifier setting for the data in the following minute. Time synchronization checks are maintained by the computer throughout an A/D run.

The second task of the processor is to compute and calibrate a narrowband spectra from contiguous time increments throughout the data period analyzed. Currently an 8192 point FFT is used to provide a frequency resolution of 0.07 Hz for the frequency range of 10 to 300 Hz.

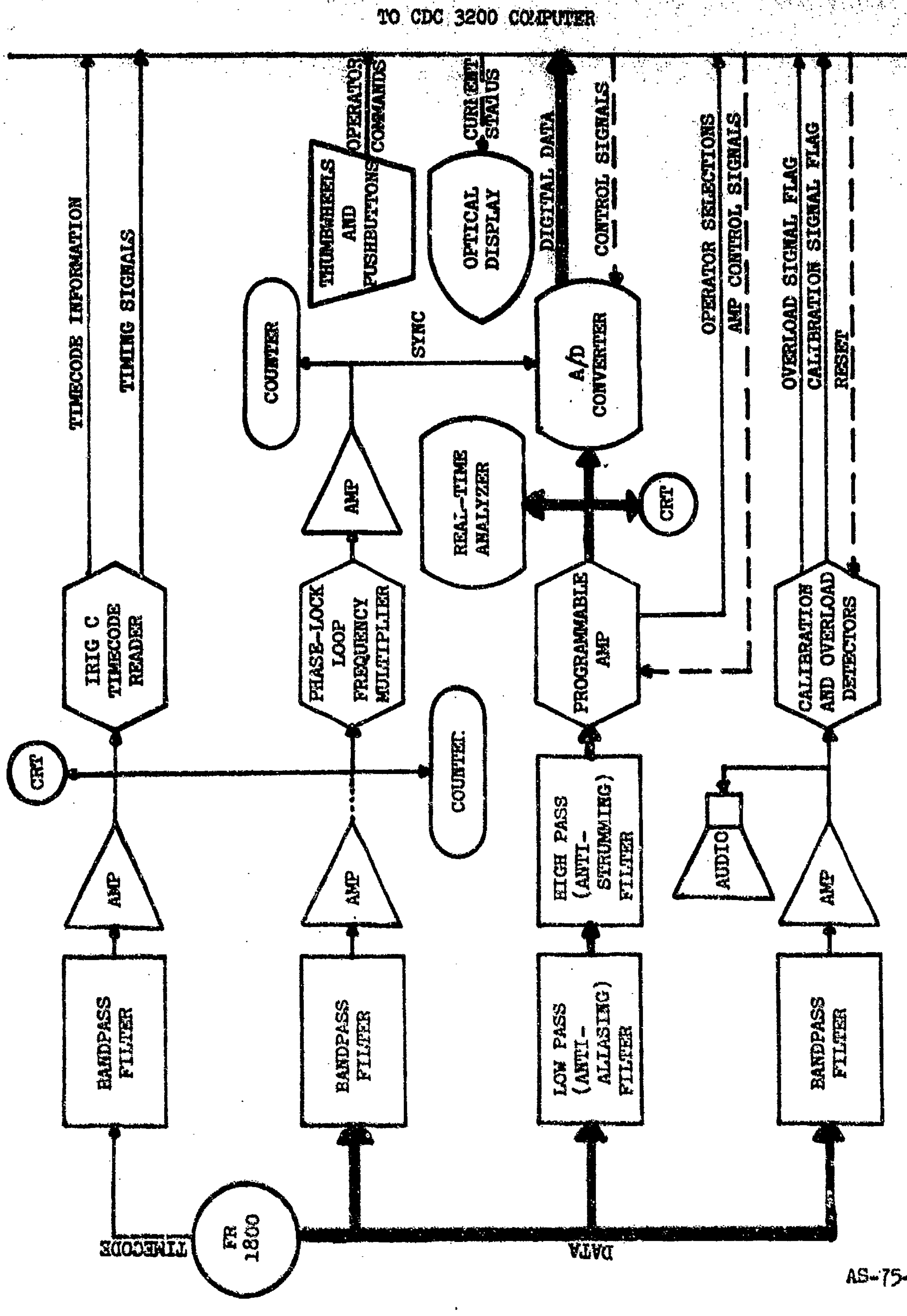

FIGURE F-1

AS-75-2319

The ambient noise spectra can be time averaged over a selected period and output as narrowband and/or octave band time series. Various statistical algorithms are available to furnish the information required to perform an acoustical analysis of the data.

The CW analysis is achieved by using the calibrated narrowband spectra to estimate the signal power in a given frequency band. The spectra are first averaged for a specified period. From these averages, two types of band estimates are obtained. For each CW signal, a narrow (±1 Hz) band centered about the source frequency is searched for its spectral peak line. The power in a narrower band (0.22 Hz) centered about this peak is then determined. Peak tracking is used to compensate for any doppler shift and variation in source frequency that might occur. The second type of band estimate determines the ambient noise power in a wider band (4 Hz) associated with each source frequency. An algorithm is used to minimize the effects of extraneous shipping lines and short-term nonstationarities that often contaminate data of this type.

The third task performed by the AN/CW processor automatically edits the reduced data for artifacts and contamination from these sources:

1. environmental effects such as biological and seismic noise,

2. exercise effects such as conflicting sources (SUS), source level fluctuations, source timing, and shipping noise, and

3. receiver and recording system effects.

The techniques and algorithms used in the editing phase are software implemented with the exception of some SUS detection accomplished during the A/D phase. These algorithms consist of calibrations, data quality indicators, information from exercise operations, and adaptive filters for octave and narrowband noise estimators, peak tracking, and correction of receiver system artifacts.

The data display consists of graphics and tabulations specified and required in the final analysis performed. Figure F-2 summarizes the CW/AN processing.

Processor Outputs

The following outputs of the AN/CW processor are available for analysis:

1. ambient noise spectra in narrow and/or octave bands,

2. CW signal power, noise power, and signal-to-noise estimates in narrow frequency bands, and

3. propagation loss (PL), noise power estimates, and signal-to-noise estimates versus range and/or time.

Examples of PL and signal excess (S+N/N) in the deep ocean are shown in Figs. F-3 and F-4. These show the PL along the same track for an inbound source and then an outbound source. The figures illustrate the repeatability of the PL as a function of range and equally interesting is that they show rather large variations in the noise background. Noise variations like this are difficult to interpret when viewed through a narrowband processor and ARL has found that a valuable aid in interpretation is a time versus frequency plot of the total available spectrum. For example, the noise increase in Fig. F-3 is identified as a moving broadband source in the three-dimensional plot shown in Fig. F-5. Another view of Fig. F-5 is Fig. F-6, which is a better illustration of the quantitative rise in the noise level.

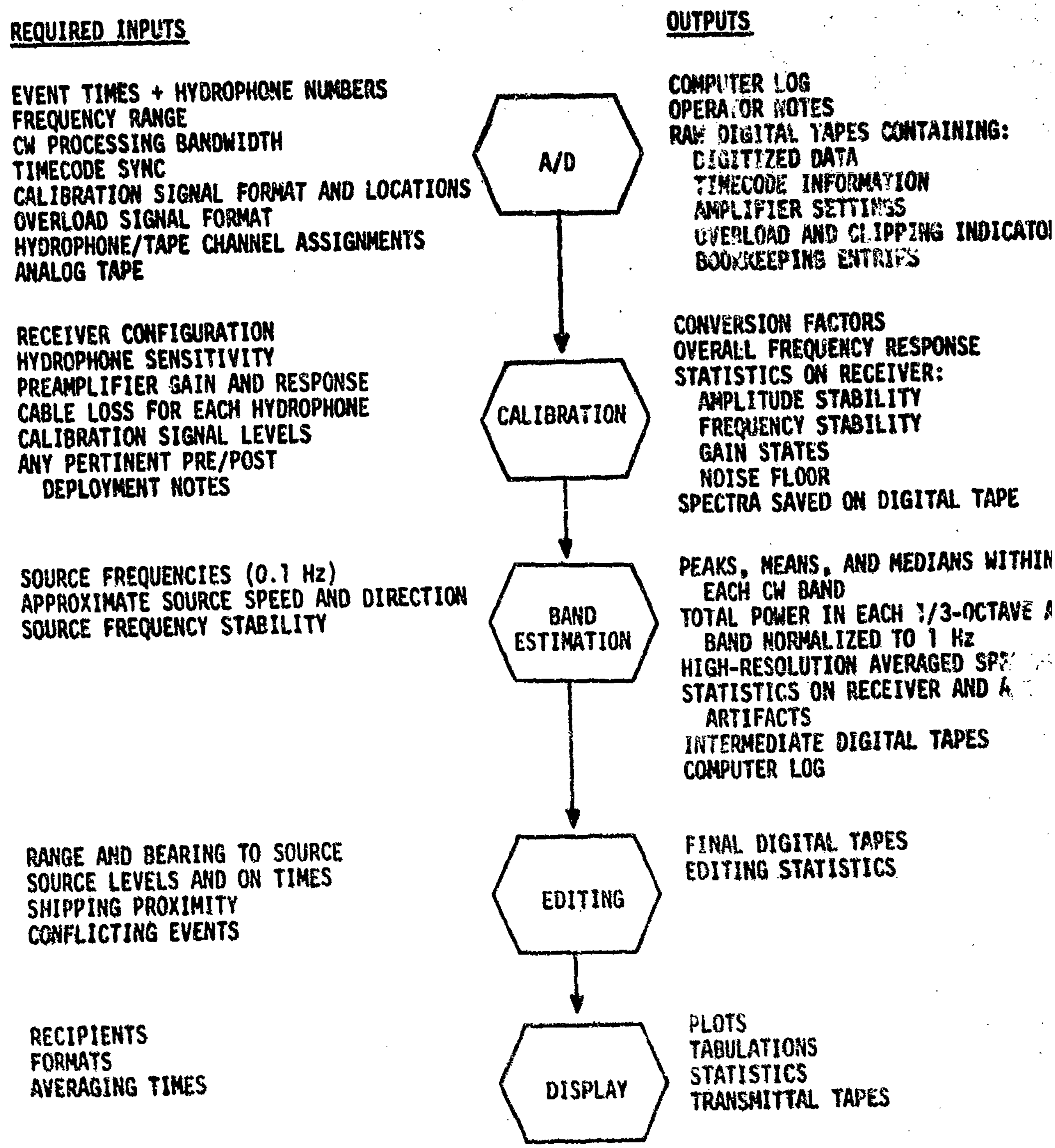

FIGURE F-2

ARL/UT CW/AN PROCESSOR

AS-75-2324

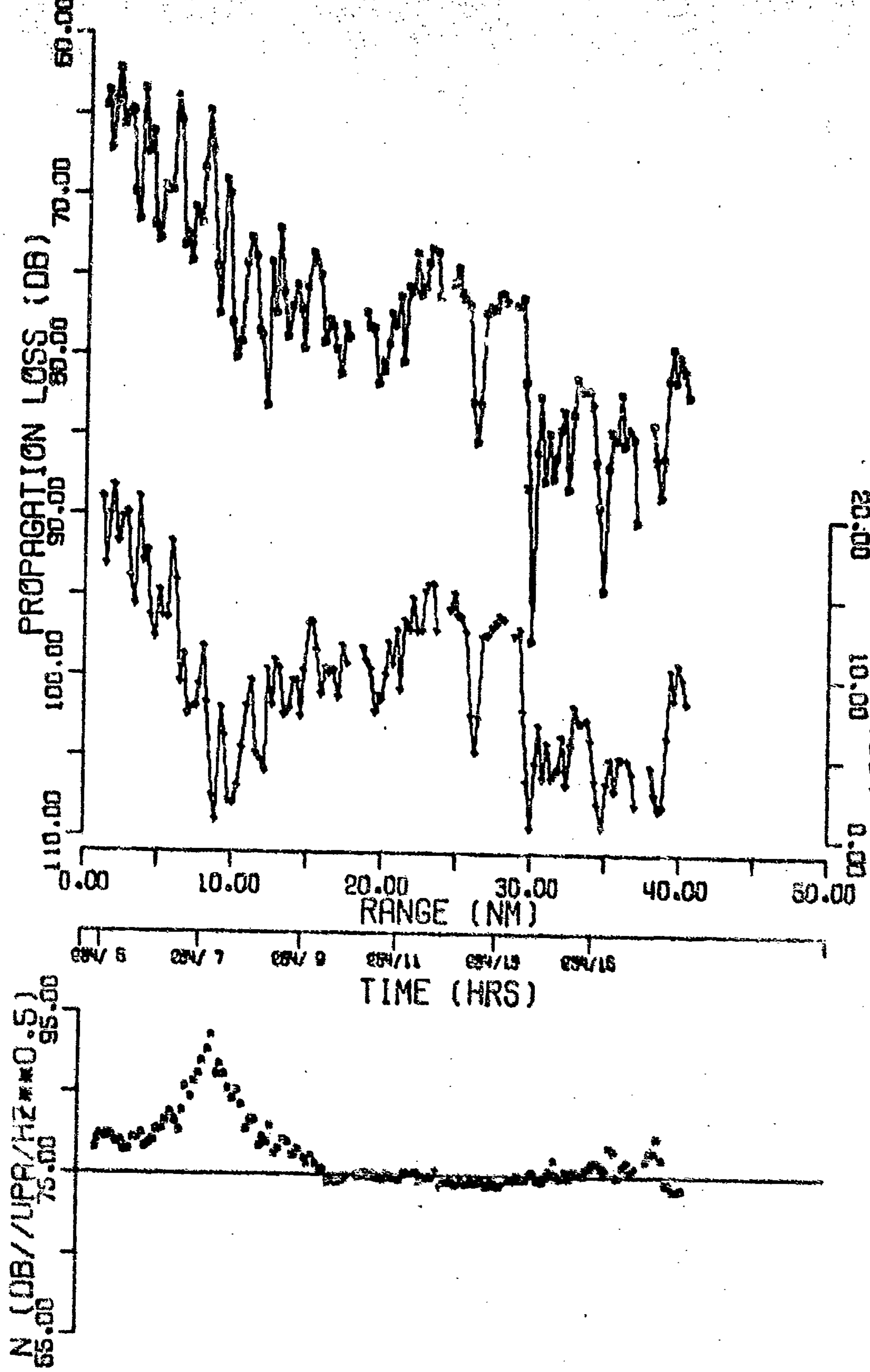

FIGURE F-3

ACODAC SYSTEM 1 HYDROPHONE 6 5328 M BOTTOM
CHAIN TRACK G-F SOURCE J15-3 70 Hz 91 M 157 dB

AS-75-2320

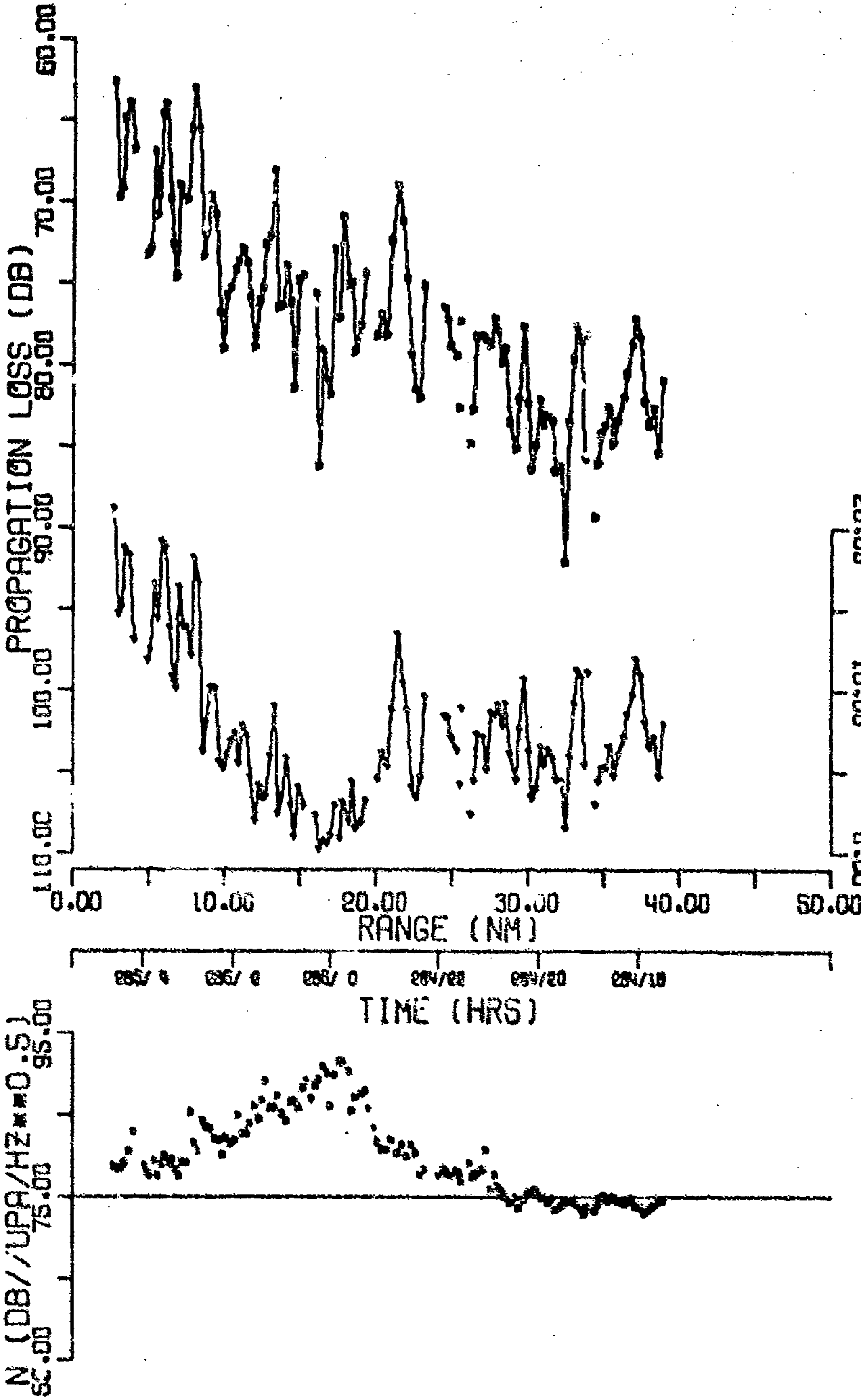

FIGURE F-4

ACODAC SYSTEM 1 HYDROPHONE 6 5328 M BOTTOM
CHAIN TRACK F-G SOURCE J15-3 70 Hz 91 M 156 dB

AS-75-2321

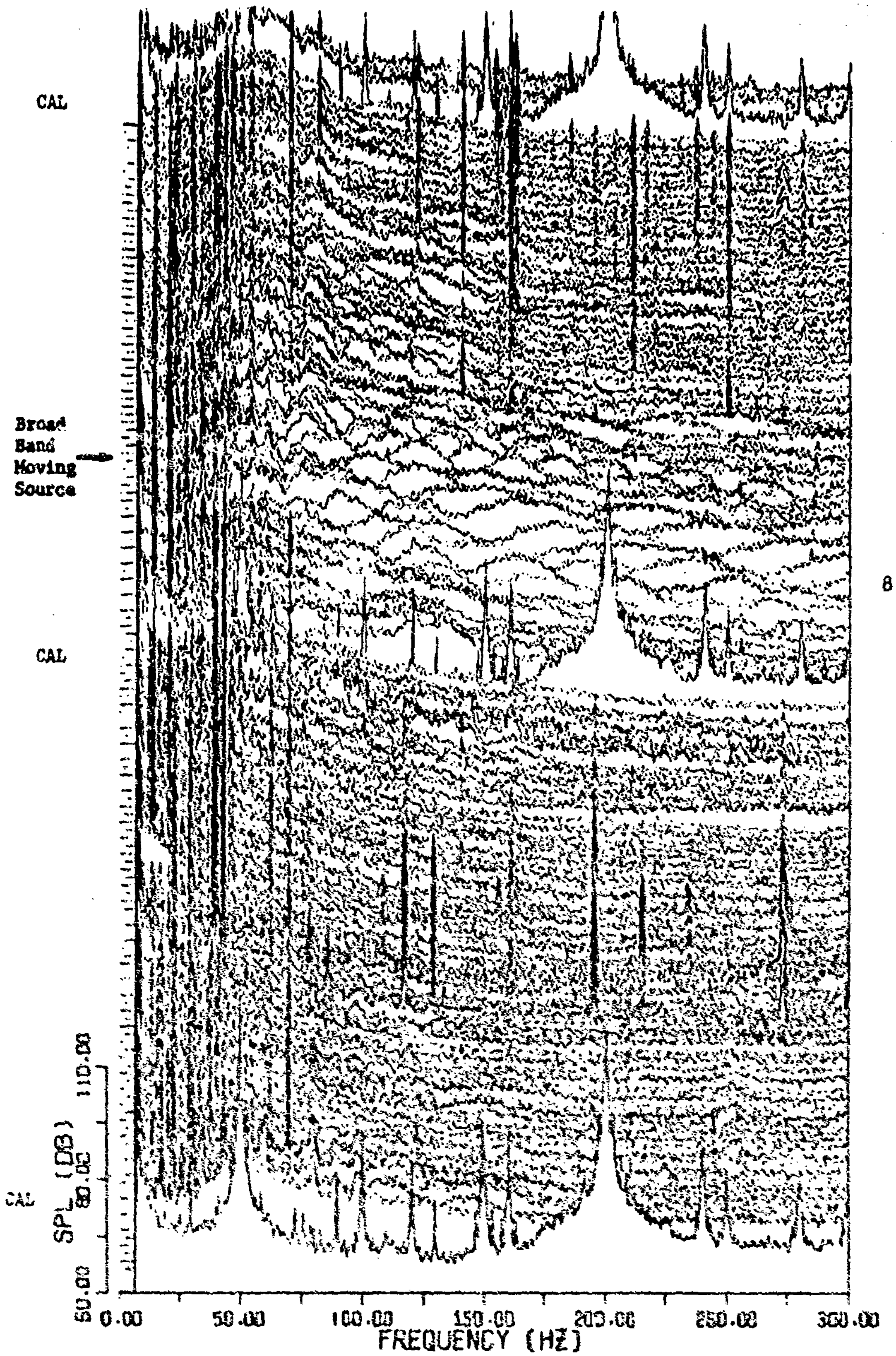

FIGURE F-5

5328m BOTTOM
11/16/00 - 12/04/30 J-15 F TO G VIBROSEIS G TO E

AS-75-2322

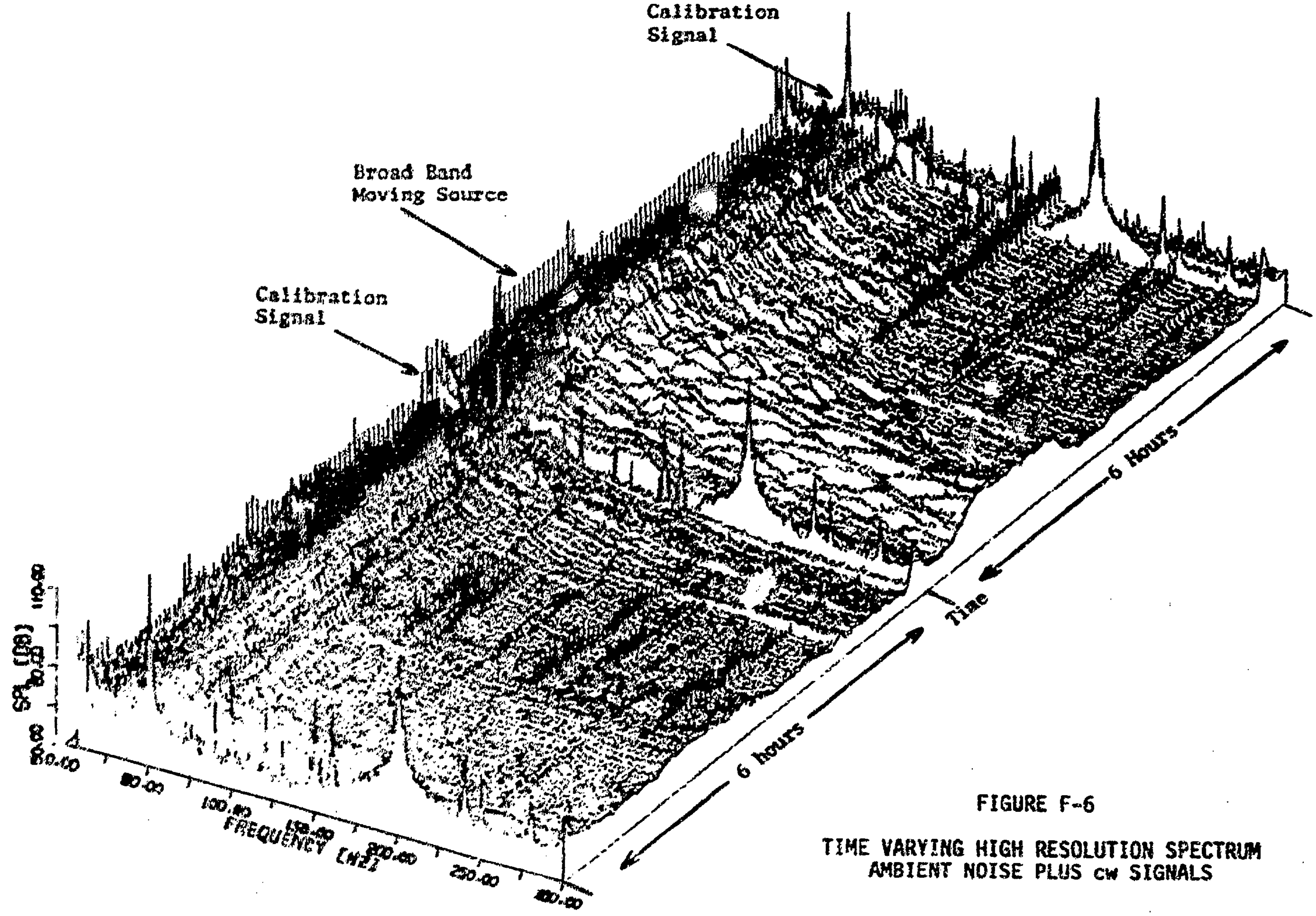

FIGURE F-6

TIME VARYING HIGH RESOLUTION SPECTRUM
AMBIENT NOISE PLUS cw SIGNALS

APPENDIX G

6 January 1975

MEMORANDUM

From: Chairman, Technical Advisory Group, Bottom Interaction Experiment
To: Manager, Long Range Acoustic Propagation Project

Subj: Report and Recommendations of Technical Advisory Group

Ref: (a) ONR Code 102-OSC:REM:ke ltr of 8 August 1975
(b) "Acoustic Bottom Interaction Experiment Description," Loyd D. Hampton, Applied Research Laboratories, 13 August 1975 (Preliminary Copy)
(c) NAVOCEANO Code 6130:RSW:jaa memo of 1 December 1975
(d) "Acoustic Bottom Interaction Experiment Description," Loyd D. Hampton, ARL-TR-75-41, . November 1975

Encl: (1) Attendance at First Meeting of Technical Advisory Group for the Bottom Interaction Experiment (28 August 1975)
(2) Attendance at Second Meeting of Technical Advisiory Group for the Bottom Interaction Experiment (11 December 1975)

1. Reference (a) established an ad hoc Technical Advisory Group (TAG) for the LRAPP-sponsored ocean acoustics exercise in the eastern Pacific Ocean in an acoustic bottom limited environment (Bottom Interaction Experiment). The first meeting of the TAG was held in Austin, Texas, on 28 August 1975 to review the preliminary experiment description contained in reference (b). Enclosure (1) lists the participants at the first meeting. At that meeting the location for the proposed experiment was changed to an area having a smoother bottom. In addition, a number of suggestions were made concerning the experiment objectives, plan, and details contained in reference (b). As a result of the discussions and suggestions made at the first TAG meeting, together with comments received from those who could not attend, the preliminary experiment description was revised by the Chief Scientist, Dr. Loyd Hampton.

2. The second meeting of the TAG was held in accordance with reference (c) on 11 December 1975 in Washington, DC. Enclosure (2) lists the TAG members and others who attended this meeting. Although the Bottom Interaction Experiment has been postponed due to funding deferrals and the loss of required ACODAC systems in another LRAPP exercise, the meeting was held to review the revised experiment description to ensure that a technically sound plan is available for use whenever the experiment is rescheduled. The TAG was informed by the LRAPP staff that the earliest possible period for the conduct of the experiment would be FY 7T and that decisions concerning the fate of the experiment had not yet been made.

6 January 1976

Subj: Report and Recommendations of Technical Advisory Group

3. The TAG notes that the experiment was originally planned in accordance with an overall sequence of LRAPP exercises scheduled for FY 76, which placed certain geographic, financial, and resource constraints on it. In view of the postponement of the experiment these constraints no longer exist in the same way and they may unnecessarily limit the conduct of the proposed experiment; however, at my direction the revised experiment description was reviewed largely in the context of the original constraints.

4. The TAG considers the Bottom Interaction Experiment Description to be well conceived and thought out. In particular, the TAG commends the Chief Scientist for his application of acoustic models in the experiment design. The TAG endorses the revised experiment plan within the limits of the original constraints. The TAG does suggest, however, that selected aspects of the plan should be reviewed further if the experiment is to be conducted at some time. In particular, it is recommended that the following parts of the plan be reviewed:

a. Experiment Location: The area selected is generally well-suited for a bottom interaction experiment and offers some advantages in that it permits a number of related transmission phenomena to be investigated, together with propagation in a bottom limited region. In addition, some bottom loss and geophysical data already exist for the area, although it should be noted that the region is geophysically complex, possibly making interpretation of the resulting data difficult. The area chosen has logistic advantages of proximity to the continental U.S., as well as consistency with the overall geographic and time sequence of the originally planned FY 76 LRAPP exercises. Should the experiment be conducted in the future it may be desirable to move the experiment to a geophysically less complicated region, to a region of higher geographic priority, and/or to a region where more detailed geophysical information is available, such as an area containing deep sea drilling sites. Moving the experiment to another location may, but not necessarily, improve the results on their application to future systems or geographic interests.

b. Use of Near-Bottom Hydrophones: The experiment as currently planned utilizes a set of near-bottom hydrophones on the ACODACs. The use of these near-bottom hydrophones may be of some advantage for certain system applications; however, their use in interpreting the data, particularly for determining bottom loss, may be limited by the lack of sufficient time separation between direct and bottom reflected signals. The desirability of using these near-bottom hydrophones in the ACODAC configuration should be reviewed in the context of system related versus experiment objectives. At this time the TAG does not recommend a particular deep hydrophone configuration.

c. <u>CW Projector</u>: There does not appear to be sufficient justification at this time for including a CW projector in the experiment. It appears that the experiment objectives can be satisfied without the use of the projector and it should be dropped from the experiment unless further justified.

5. In view of existing financial constraints for experiment planning and the postponement of the experiment, and in order to maintain the integrity of the experiment design the TAG does not suggest the Chief Scientist modify the experiment plan at this time to incorporate the above recommendations. The TAG recommended to the Chief Scientist that, with some minor changes, reference (d) should be forwarded to the Manager, LRAPP, for final review, and then printed in limited numbers for future reference and use.

6. In light of proposed future LRAPP-sponsored exercises, the TAG strongly recommends that the Bottom Interaction Experiment be conducted prior to the conduct of similar measurements in the Indian Ocean. Planning such as went into the development of the Bottom Interaction Experiment and the results from such an experiment should be used in developing an Indian Ocean exercise plan. The experience and results gained from a preliminary bottom interaction experiment should be invaluable for the conduct of future measurements in bottom limited regions.

6 January 1976

Subj: Report and Recommendations of Technical Advisory Group

7. Finally, the TAG recommends that consideration be given to expanding the sponsorship of the proposed Bottom Interaction Experiment to include the interests of NAVELECSYSCOM and ONR. Combined sponsorship would increase the resources available to support such an experiment. Judiciou planning could satisfy the mutual interests of the 6.1, 6.2 and 6.3 communities and provide a cost effective means of conducting a significant experiment.

ROBERT S. WINOKUR

Copy to:
J. T. Gottwald, Tracor, TAG Member
J. S. Hanna, AESD, TAG Member
M. G. Lewis, NAVELEX, TAG Member
M. S. Weinstein, USI, TAG Member
L. D. Hampton, ARL/UT, Chief Scientist
R. E. Morrison, LRAPP

Attendance at First Meeting of Technical Advisory Group
for the Bottom Interaction Experiment (28 August 1975)

R. S. Winokur, NAVOCEANO, TAG Chairman
M. S. Weinstein, USI, TAG Member
A. F. Wittenborn, Tracor, representing J. T. Gottwald, TAG Member
L. D. Hampton, ARL/UT, Chief Scientist
G. E. Ellis, ARL/UT
A. L. Anderson, ARL/UT
A. A. Kirst, T.I.
R. E. Morrison, LRAPP
R. N. Lane, LRAPP

Attendance at Second Meeting of Technical Advisory Group
for the Bottom Interaction Experiment (11 December 1975)

R. S. Winokur, NAVOCEANO, TAG Chairman
J. T. Gottwald, Tracor, TAG Member
J. S. Hanna, AESD, TAG Member
M. G. Lewis, NAVELEX, TAG Member
M. S. Weinstein, USI, TAG Member
A. L. Anderson, ARL/UT
H. F. Bezdek, ONR, Code 486
L. D. Hampton, ARL/UT, Chief Scientist
R. N. Lane, LRAPP
R. E. Morrison, LRAPP
J. Reese, PME-124

2 January 1976

DISTRIBUTION LIST FOR
ARL-TR-75-41
UNDER CONTRACT N00014-75-C-0429
UNCLASSIFIED

Chief of Naval Operations
Department of the Navy
Washington, DC 20350
Attn: OP-955F (1)

Chief of Naval Research
Department of the Navy
Arlington, VA 22217
Attn: Code 102IP (1)
Code 102N (2)
Code 102-OS (1)
Code 483 (1)
Code 486 (1)
Code 212 (1)

Naval Sea Systems Command
Department of the Navy
Washington, DC 20362
Attn: Code 06H1 (1)
Code 034 (1)

Office of Naval Research (1)
Branch Office Chicago
536 S. Clark Street
Chicago, IL 60605

Commander (1)
Naval Oceanographic Office
Department of the Navy
Washington, DC 20373
Attn: Code 6130 (1)
Code 6160 (1)

Director (1)
Naval Research Laboratory
Department of the Navy
Washington, DC 20372
Attn: Code 2627 (1)
Code 8160 (1)
Code 8167 (1)
Code 8168 (1)

Project Manager
Antisubmarine Warfare Systems Project
Department of the Navy
Washington, DC 20360
Attn: ASW-11 (1)

Officer-in-Charge (1)
New London Laboratory
Naval Underwater Systems Center
New London, CT 06320
Attn: Code TA (1)
Code TA112 (1)

Commanding Officer
Naval Electronic Systems Command
Department of the Navy
Washington, DC 20362
Attn: ELEX 320 (1)
PME-124 (1)
PME-124T (1)
PME-124TA (1)
PME-124-30 (1)

Commanding Officer (1)
Naval Ocean Research and Development Activity
Bay St. Louis, MI 39520
Attn: Code 22 (5)

Commander (1)
Naval Undersea Center
San Diego, CA 94625
Attn: Code 4007 (3)

Commander (1)
Naval Air Development Center
Warminster, PA 18974
Attn: Code 205 (2)

Commanding Officer and Director (12)
Defense Services Administration
Defense Documentation Center
Cameron Station, Building 5
5010 Duke Street
Alexandria, VA 22314

Office of Naval Research (1)
Resident Representative
Room 582, Federal Building
Austin, TX 78701

Dist. List for ARL-TR-75-41 under Contract N00014-75-C-0429 (cont'd)

Texas Instruments
13500 N. Central Expressway
P. O. Box 5474 M.S. 262
Dallas, TX 75222
Attn: Mr. A. Kirst (1)

Tracor, Incorporated
6500 Tracor Lane
Austin, TX 78721
Attn: Dr. G. Wittenborn (1)
Mr. J. T. Gottwald (1)

Underwater Systems, Inc.
World Bldg.
8121 Georgia Avenue
Silver Spring, MD 20910
Attn: Dr. M. S. Weinstein (1)

Woods Hole Oceanographic Institute
Woods Hole, MA 02543
Attn: Dr. E. E. Hays (1)

Director
Marine Physical Laboratory
Scripps Institution of Oceanography
University of California
San Diego, CA 92152
Attn: Dr. G. B. Morris (1)

University of Miami
Rosenstiel School of Marine and
Atmospheric Science
10 Rickenbacker Causeway
Miami, FL 33149
Attn: Dr. S. C. Daubin (1)

DEPARTMENT OF THE NAVY
OFFICE OF NAVAL RESEARCH
875 NORTH RANDOLPH STREET
SUITE 1425
ARLINGTON VA 22203-1995

IN REPLY REFER TO:

5510/1
Ser 321OA/011/06
31 Jan 06

MEMORANDUM FOR DISTRIBUTION LIST

Subj: DECLASSIFICATION OF LONG RANGE ACOUSTIC PROPAGATION PROJECT (LRAPP) DOCUMENTS

Ref: (a) SECNAVINST 5510.36

Encl: (1) List of DECLASSIFIED LRAPP Documents

1. In accordance with reference (a), a declassification review has been conducted on a number of classified LRAPP documents.

2. The LRAPP documents listed in enclosure (1) have been downgraded to UNCLASSIFIED and have been approved for public release. These documents should be remarked as follows:

   Classification changed to UNCLASSIFIED by authority of the Chief of Naval Operations (N772) letter N772A/6U875630, 20 January 2006.

   DISTRIBUTION STATEMENT A: Approved for Public Release; Distribution is unlimited.

3. Questions may be directed to the undersigned on (703) 696-4619, DSN 426-4619.

BRIAN LINK
By direction

Subj: DECLASSIFICATION OF LONG RANGE ACOUSTIC PROPAGATION PROJECT (LRAPP) DOCUMENTS

DISTRIBUTION LIST:

NAVOCEANO (Code N121LC – Jaime Ratliff)
NRL Washington (Code 5596.3 – Mary Templeman)
PEO LMW Det San Diego (PMS 181)
DTIC-OCQ (Larry Downing)
ARL, U of Texas
Blue Sea Corporation (Dr.Roy Gaul)
ONR 32B (CAPT Paul Stewart)
ONR 321OA (Dr. Ellen Livingston)
APL, U of Washington
APL, Johns Hopkins University
ARL, Penn State University
MPL of Scripps Institution of Oceanography
WHOI
NAVSEA
NAVAIR
NUWC
SAIC

Declassified LRAPP Documents

Report Number	Personal Author	Title	Publication Source (Originator)	Pub. Date	Current Availability	Class.
55	Weinstein, M. S., et al.	SUS QUALITY ASSESSMENT, SQUARE DEAL	Undersea Systems, Inc.	750207	ADA007559; ND	U
BKD2380	Unavailable	WESTLANT 74 PHASE 1 DATA SUMMARY (U)	B-K Dyanmics, Inc.	750301	NS; ND	U
TM-SA23-C44-75	Wilcox, J. D.	MOTION MODEL VALIDATION FROM LRAPP ATLANTIC TEST BED DATA	Naval Underwater Systems Center	750317	ND	U
RAFF7412; 74-482	Scheu, J. E.	SQUARE DEAL SHIPPING DENSITIES (U)	Raff Associates, Inc.	750401	ADC003198; NS; ND	U
PSI TR-004018	Barnes, A. E., et al.	ON THE ESTIMATION OF SHIPPING DENSITIES FROM OBSERVED DATA	Planning Systems Inc.	750401	ND AD 096 582	U
NUSC TD No.4937	LaPlante, R. F., et al.	THE MOORED ACOUSTIC BUOY SYSTEM (MABS)	Naval Underwater Systems Center	750404	ADB003783; ND	U
USI 460-1-75	Weinstein, M. S., et al.	SUS SIGNAL DATA PROCESSING (U) INVESTIGATIONS CONDUCTED UNDER THE DIAGNOSTIC PLAN FOR CHURCH ANCHOR AND SQUARE DEAL SHOT DATA (U)	Underwater Systems, Inc.	750414	ADC002353; ND	U
Unavailable	Ellis, G. E.	SUMMARY OF ENVIRONMENTAL ACOUSTIC DATA PROCESSING	University of Texas, Applied Research Laboratories	750618	ADA011836	U
Unavailable	Edelblute, D. J.	OCEANOGRAPHIC MEASUREMENT SYSTEM TEST AT SANTA CRUZ ACOUSTIC RANGE FACILITY (SCARF)	Lockheed Missiles and Space Co., Inc.	751015	ADB007190	U
Unavailable	Unavailable	SUS SOURCE LEVEL COMMITTEE REPORT	Underwater Systems, Inc.	751105	ADA019469	U
Unavailable	Hampton, L. D.	ACOUSTIC BOTTOM INTERACTION EXPERIMENT DESCRIPTION	University of Texas, Applied Research Laboratories	760102	ADA021330	U
PSI-TR-036030	Turk, L. A., et al.	CHURCH ANCHOR: AREA ASSESSMENT FOR TOWED ARRAYS (U)	Planning Systems Inc.	760301	ND	U
NUC TP 419	Wagstaff, R. A., et al.	HORIZONTAL DIRECTIONALITY OF AMBIENT SEA NOISE IN THE NORTH PACIFIC OCEAN (U)	Naval Undersea Center	760501	ADC007023; NS; ND	U
NRL-MR-3316	Young, A. M., et al.	AN ACOUSTIC MONITORING SYSTEMS FOR THE VIBROSEIS LOW-FREQUENCY UNDERWATER ACOUSTIC SOURCE	Naval Research Laboratory	760601	ADA028239; ND	U
ARL-TR-75-32	Ellis, G. E.	SUMMARY OF ENVIRONMENTAL ACOUSTIC DATA PROCESSING	University of Texas, Applied Research Laboratories	760705	ADA028084; ND	U
Unavailable	Unavailable	SUMMARY OF ENVIRONMENTAL ACOUSTIC DATA PROCESSING	University of Texas, Computer Science Division	761013	ADA032562	U
TTA83676285	Unavailable	ANALYSIS PLAN FOR NARROWBAND/ NARROWBEAM AMBIENT NOISE (U)	Tetra Tech, Inc.	761112	ADC008275; NS; ND	U
USI 564-1-77	Wallace, W. E., et al.	REPORT OF CW WORKSHOP. NORDA, BAY ST. LOUIS, MISS., 28-29 SEPT 1976	Underwater Systems, Inc.	770124	ND	U